Est. 1841 | YORK ST JOHN UNIVERSITY

Redfearn, Isabella Daisy (2026) Inhibiting transforming growth factor-β in pancreatic cancer to encourage vascular normalisation and improve therapeutic response. Masters thesis, York St John University.

Downloaded from: https://ray.yorksj.ac.uk/id/eprint/16248/

Research at York St John (RaY) is an institutional repository. It supports the principles of open access by making the research outputs of the University available in digital form. Copyright of the items stored in RaY reside with the authors and/or other copyright owners. Users may access full text items free of charge, and may download a copy for private study or non-commercial research. For further reuse terms, see licence terms governing individual outputs. Institutional Repository Policy Statement

RaY

Research at the University of York St John

For more information please contact RaY at ray@yorksj.ac.uk

Inhibiting transforming growth factor-β in pancreatic cancer to encourage vascular normalisation and improve therapeutic response

Isabella Daisy Redfearn

Submitted in accordance with the requirements for the degree of Master of Science by Research

York St John University

School of Health Sciences

September 2026

The candidate confirms that the work submitted is their own and that appropriate credit has been given where reference has been made to the work of others.

This copy has been supplied with the understanding that it is copyright material. Any reuse must comply with the Copyright, Designs and Patents Act 1988 and any licence under which this copy is released.

© 2026 York St John University and Isabella Daisy Redfearn

The right of Isabella Daisy Redfearn to be identified as Author of this work has been asserted by them in accordance with the Copyright, Designs and Patents Act 1988.

Declaration on the Use of Generative AI

In accordance with York St John University's policy on generative artificial intelligence, I hereby declare that:

1. I have used generative AI tools only as a supportive resource—for example, to improve readability or assist with basic grammar and style—recognising that these tools serve to support, and not replace, my own original thinking and critical analysis.

2. Any information, text fragments, or ideas generated by AI have been critically evaluated, edited, and integrated by me. No AI-produced content has been used verbatim in the final thesis, and no substantial sections were generated by AI and submitted as original work.

3. Any uses of AI are explicitly acknowledged in relevant sections throughout the thesis.

4. I have documented any use of AI and retained relevant records (e.g., text-based transcripts) to ensure transparency in alignment with the university's standards on academic integrity.

5. I have not entered any confidential, personally identifiable, proprietary, or copyrighted content into any AI service, consistent with data-protection and copyright requirements.

6. I recognise my responsibility to evaluate AI outputs for accuracy, bias, and relevance, and to ensure that final content of my research reflects my own scholarly judgment.

7. My submission adheres fully to York St John University's Research Misconduct Policy and the Code of Practice for Research Degrees, and I confirm that no use of generative AI could reasonably be considered to constitute plagiarism, false authorship, or misrepresentation as outlined in university guidance.

Acknowledgements

This year and the writing and submission of this thesis has been extremely challenging and rewarding, and I would like to thank those who helped me make it possible.

Firstly, I would like to thank my supervisor, Dr Adam Odell, for guiding me during this entire process and putting up with my endless questioning. I am also deeply grateful to my secondary supervisor Dr Katharine Herbert and the rest of the Biomedical Science department for their support this year. I would like to specifically thank the laboratory technicians Ashleigh Elliot and Amy Wells, who work extremely hard to create an accepting and positive working environment and provide never-ending support to the post-graduate researchers.

I want to thank my lab partner Neave Crawford, who I've been lucky enough to do this entire process alongside and I would not have made it through this process without her friendship. I would also like to thank the other PGRs, including Amy Wells and Lewis Reed, I am looking forward to a Dusk 2-for-1 cocktail and cheesy garlic bread when this is done with you.

I am immensely grateful to my partner Rose Thewsey for providing endless emotional support and pep talks during the last year. Finally, I couldn't have done this without my mum and dad and would like to thank them for their endless support throughout this year.

Abstract

Pancreatic ductal adenocarcinoma (PDAC) is the fifth most common cause of cancer death in the UK. The most effective treatment is surgery, followed by adjuvant chemotherapy, however this treatment option is only available to 10-20% of patients, and the standard-of-care chemotherapy, gemcitabine, has a 5-year overall survival rate of 31.4%. The PDAC tumour microenvironment is one of the main contributors to poor treatment response, and it is made up of a dense desmoplastic stroma, caused by cancer-associated fibroblasts, stromal cells that cause fibrosis and produce collagen, contributing to a stiff extracellular matrix. This dense stroma creates a hypoxic environment, with limited and non-functional blood vessels, exhibiting disorganised lining and leaky structures that impedes drug delivery, increases drug resistance and promotes metastasis. TGF-β is an anti-inflammatory cytokine that has many roles in cancer development including angiogenesis, the formation of new blood vessels. Inhibiting TGF-β has previously been used in other cancers to normalise tumour vasculature, reduce the hypoxic environment, enhance immune cell infiltration and improve drug delivery, however this effect has not been investigated in PDAC. This study investigates the effect of inhibiting TGF-β on cells and tumour vasculature in pancreatic cancer. PDAC cell lines were used to determine the effect of a TGF-β receptor inhibitor, LY2109671 on cell viability, with inhibition decreasing viability in a dose-dependent manner. Changes in protein and mRNA expression were investigated with TGF-β increasing expression levels of the latent TGF-β, an effect that was inhibited by LY2109671. Fibroblast, and endothelial cells also demonstrated LY2109671 inhibition of TGF-β-induced protein and mRNA expression of TGF-β, COL1A1 and bFGF. Finally, LY2109671 was able to reverse the TGF-β-induced suppression of vessel formation in fibroblast and endothelial co-cultures. The results of this study highlight a potential treatment option to be used alongside standard-of-care chemotherapy to improve treatment response in PDAC patients.

Table of Contents

Acknowledgements 4

Abstract 5
Table of Contents 5
Abbreviations 7
List of Figures 9
List of Tables 10
1. Introduction 11
1.1 Pancreatic Cancer Overview 11
1.2 Pancreatic Cancer Treatment 14
1.3 The Tumour Microenvironment 15
1.4 Angiogenesis 17
1.5 Transforming Growth Factor-β 19
1.6 Aims & Objectives 24
2. Methods 25
2.1 Cell Culture 25
2.2 Test Compounds 25
2.3 MTT Viability Assays 26
2.4 SDS-PAGE 26
2.5 Western Blotting 27
2.6 qPCR 27
2.7 Co-cpulture angiogenesis assays 28
2.8 HUVEC Immunofluorescence 29
2.9 Statistical analysis 30
3. Inhibiting TGF-β signalling in PDAC cell lines 31
3.1. Three TGF-β inhibitors LY2109671, Dexamethasone, and SB431542 affected cell viability and the phosphorylation of SMAD2/3 in PDAC cell lines. 31
3.2. LY2109671 affects the protein and mRNA expression of TGF-β and VEGF-A in PDAC cell lines. 38
4. Inhibiting TGF-β signalling in fibroblast cell lines 42
4.1. Human Dermal Fibroblasts 42
4.2. Pancreatic Cancer Associated Fibroblasts 46
5. Inhibiting TGF-β signalling affects HUVEC morphology and the formation of blood vessels in co-cultures 50
5.1. The effect of TGF-β signalling on HUVECs 50
5.2 HDF Angiogenesis Assays 56
5.3 CAF Angiogenesis Assays 62
6. Discussion 64

6.1 TGF-βR inhibitors LY2109671 and SB431542 reduce PDAC cell line viability and reduce the phosphorylation of SMAD2/3 64
6.2 TGF-β suppression reduces TGF-β protein and mRNA expression in PDAC cell lines 66
6.3 TGF-β suppression prevents expression of ECM proteins and TGF-β in fibroblastic cell lines..... 69
6.4 TGF-β suppression effect on endothelial cells..... 73
6.5 LY2109671 supported the formation of vessels in HDF and CAF co-cultures 74
7. General Conclusion..... 78
8. Bibliography..... 79

Abbreviations

Abbreviation	Definition

5-FU	5-fluorouracil
ADEX	Aberrantly differentiated endocrine exocrine
bFGF	Basic fibroblast growth factor
BSA	Bovine serum albumin
CAF	Cancer-associated fibroblast
DMEM	Dulbecco's Modified Eagles Media
DMSO	Dimethyl sulfoxide
ECGM	Endothelial cell growth medium
ECM	Extracellular matrix
EMT	Epithelial-mesenchymal transition
ERK	Extracellular signal regulated kinase
FBS	Foetal bovine serum
HDF	Human dermal fibroblast
HUVEC	Human umbilical vein endothelial cells
iCAF	Inflammatory CAF
IFP	Interstitial fluid pressure
LTBP	Latent TGF-β binding proteins
MAPK	MAP kinase
MTT	3-(4,5-Dimethylthiazol-2-yl)-2,5-Diphenltetrazolium Bromide
MVD	Microvessel density
MyCAF	Myofibroblastic CAF
OS	Overall survival
P/S	Penicillin/streptomycin
PanINs	Pancreatic intraepithelial neoplasias
PBS	Phosphate buffered saline
PC	Pancreatic cancer
PDAC	Pancreatic ductal adenocarcinoma
PI3K	Phosphatidylinositol-3-kinase
PP1	Protein phosphatase 1
RPMI 1640	Roswell Park Memorial Institute 1640
TAF	Tumour angiogenesis factor
TGF-β	Transforming growth factor-β
TGF-βR	Transforming growth factor-β receptor
TME	Tumour microenvironment
VEGF-A	Vascular endothelial growth factor-A
α-SMA	Alpha smooth muscle actin

List of Figures

Figure 1.1. The pathogenesis and progression of pancreatic cancer

Figure 1.2. The canonical TGF-β pathway

Figure 3.1. TGF-β inhibitors LY2109761, dexamethasone and SB431542 decrease cell viability in PDAC cell lines in dose-dependent manners

Figure 3.2. TGF-β inhibitors LY2109671 and SB431542 decrease cell viability and prevent the phosphorylation of SMAD2/3 at 5μM

Figure 3.3. LY2109671 prevents the phosphorylation of SMAD2/3 after TGF-β stimulation in Panc1 and BxPc3 cells

Figure 3.4. LY2109671 inhibits TGF-β protein expression in PDAC cell lines

Figure 3.5. LY2109671 inhibits TGF-β induced gene expression in Panc1 and BxPc3 cells

Figure 4.1. LY2109671 prevents the TGF-β induced increase in COL1A1 protein expression in HDF

Figure 4.2. LY2109671 inhibits the TGF-β induced increase in bFGF mRNA expression

Figure 4.3. LY2109671 prevents the TGF-β induced increase of TGF-β and COL1A1 protein expression

Figure 4.4. TGF-β significantly increased mRNA expression of VEGF-A, bFGF, and α-SMA in CAFs that was reversed by LY2109671

Figure 5.1. LY2109671 inhibits the TGF-β induced increase in detected protein expression in HUVECs

Figure 5.2. 48-hour LY2109671 treatment changes the morphology of HUVECs after treatment but has no impact on CD31 expression

Figure 5.3. 72-hour LY2109671 treatment changes the morphology of HUVECs after treatment but has no impact on CD31 expression

Figure 5.4. Co-cultures of fibroblasts and HUVECs can produce vessels or blood islands

Figure 5.5. LY2109671 prevents the effect of TGF-β on total vessel length and the number of branch points in HDF and HUVEC co-cultures

Figure 5.6. PDAC cell conditioned media had no effect on vessel formation in HDF and HUVEC co-cultures

Figure 5.7. LY2109671 reverses the effect of TGF-β on total vessel length and the number of branch points in CAF and HUVEC co-cultures

List of Tables

Table 2.1. Primer Sequences used in qPCR

1. Introduction

1.1 Pancreatic Cancer Overview

Pancreatic cancer (PC) is the fifth most common cause of cancer death in the UK, with over 60% of cases being diagnosed at late stages due to vague symptoms and the lack of sensitive and specific biomarkers (Kleeff et al. 2016; Cancer Research UK 2024). Pancreatic ductal adenocarcinoma (PDAC) is the most common type of PC, accounting for 95% of all cases. As most patients are diagnosed at later stages, the cancer can be more aggressive or already metastatic at the time of detection, limiting their treatment options (Wood, L.D. et al. 2022; Levi et al. 2025). The most effective current treatment is surgery followed by adjuvant chemotherapy; however, only 10-20% of patients are eligible for surgery, leaving chemotherapy as the main treatment option (Liao, W.-C. et al. 2013; Mizrahi et al. 2020). Standard-of-care chemotherapy gemcitabine has a 5-year overall survival (OS) of 31.4% and a relapse-free survival of 18.3 months (Conroy et al. 2022; Palmer et al. 2024). Other chemotherapies commonly used in the treatment of PDAC, such as FOLFIRINOX, a combination of four drugs that inhibits DNA and RNA synthesis, report similar results for OS and relapse rates. However, this alternative treatment can have more severe side effects that many patients are unable to tolerate, highlighting the need for alternative treatment options for PDAC patients.

The majority of PDACs develop after the formation of precursor lesions, known as pancreatic intraepithelial neoplasia (PanIN) (Figure 1.1). Many PanINs occur due to mutations in pancreatic ductal epithelial cells and can be characterised into low-, moderate-, or high-grade lesions, with high-grade lesions most likely to develop into PDAC (Basturk et al. 2015). Low-grade PanINs typically form through mutations in the oncogene *KRAS*, and after acquiring additional mutations, typically in tumour suppressor genes, they can develop into invasive PDAC (Makohon-Moore et al. 2018).

The most common mutation causing PanINs is *KRAS*, seen in approximately 90% of patients (Aguirre, A.J. et al. 2018; Mullen et al. 2025). KRAS is a small GTPase that helps control signalling pathways, including the RAF/MEK/ERK MAP Kinase (MAPK) pathway and the phosphatidylinositol-3-kinase (PI3K)/AKT pathway (Drizyte-Miller et al. 2025). In non-cancerous cells, these pathways are vital in numerous cellular processes, including differentiation, proliferation, apoptosis, and metabolic and cell cycle regulation; however, during cancer

development, they become dysregulated and continuously activated, often due to mutations in the *KRAS* gene (Guo, Y. et al. 2020; Fadhal 2023). These pathways support KRAS-driven oncogenesis, and KRAS is deemed a potential target for treatment due to the number of patients presenting with this mutation (Pihlak et al. 2018).

Higher-grade PanINs can develop from low-grade PanINs after accumulating further genetic mutations. Loss of the tumour suppressor *CDKN2A* is typically the second major mutation seen within PanIN progression, with *TP53* and *SMAD4* mutations characterising the highest-grade lesions (Connor, A.A. and Gallinger 2022). *CDKN2A*, *TP53,* and *SMAD4* are tumour suppressor genes typically activated in response to cellular stress, including, cell cycle arrest, DNA repair, or apoptosis. Mutations within these genes are found in 30%, 75% and 32% of PDAC cases, respectively (Raphael et al. 2017; Mullen et al. 2025).

TP53 encodes the p53 protein, a transcription factor and tumour suppressor involved in responding to cellular stress and protecting DNA integrity. It is involved in cell cycle arrest, DNA repair, and apoptosis, along with many other pathways (Hernández Borrero and El-Deiry 2021). *TP53* mutations in PDAC patients are typically missense, and these mutations can affect ECM deposition, influence CAF behaviour and create an immunosuppressive microenvironment, causing patients with this mutation to have a lower survival rate (Addadi et al. 2010; Maddalena et al. 2021).

Another key tumour suppressor protein commonly mutated in PDAC is SMAD4. In the early stages of cancer, SMAD4 acts as a tumour suppressor, due to its role in the transforming growth factor-β (TGF-β) signalling pathway. This pathway controls cell proliferation, angiogenesis, and invasion. It also can induce cell cycle arrest at the G1/S checkpoint and control the expression of pro-apoptotic genes, including BIK, BCL-X_L and GADD45b (Jang, C.-W. et al. 2002; Yoo et al. 2003; Shi, W. et al. 2004; Spender et al. 2009). Inactivation of SMAD4 is due to homozygous deletion or mutations with the loss of the wild-type allele (Racu et al. 2022). This results in abnormal signalling cascades within the TGF-β pathway, preventing cell cycle arrest and apoptosis, and promoting tumour progression and metastasis (Yao, H. et al. 2024).

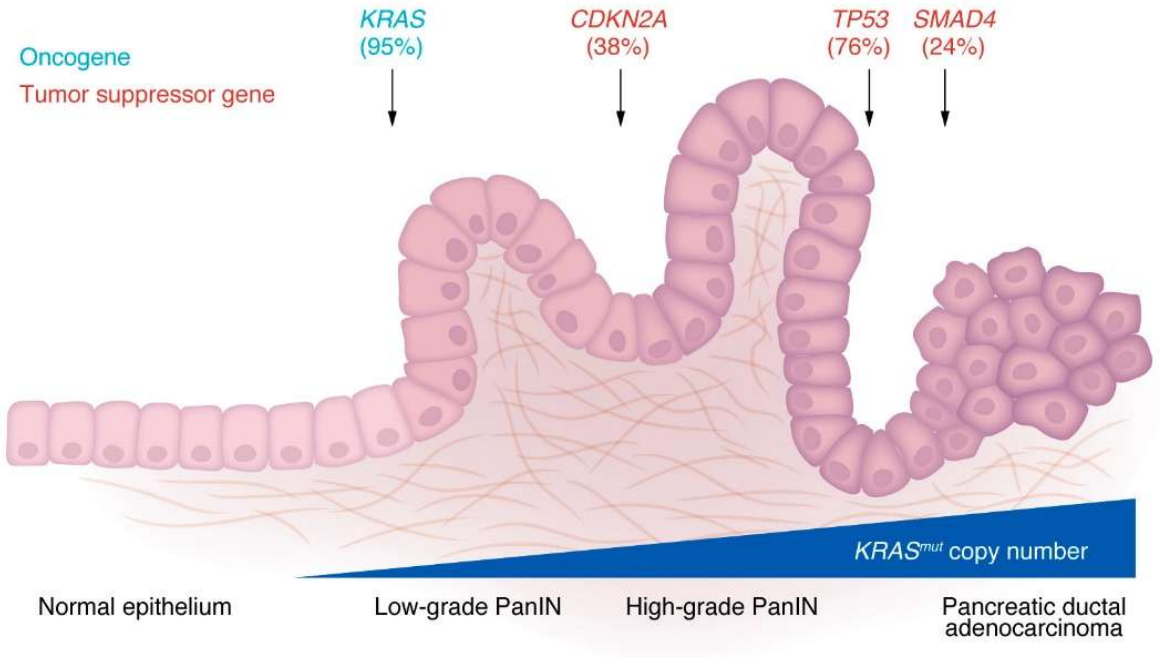


Figure 1.1 – The pathogenesis and progression of Pancreatic Cancer. PanINs are initially caused by *KRAS* activating mutations, with higher graded PanINs commonly occurring with mutations within tumour suppressor genes *TP53*, *CDKN2A* and *SMAD4*. As more mutations occur, invasive PDAC develops. (Image taken from Connor, A.A. and Gallinger 2022 and Drizyte-Miller et al. 2025)

1.2 Pancreatic Cancer Treatment

Treatment for PDAC can be complex, as many patients are diagnosed at later stages of the disease, due to a lack of specific symptoms and biomarkers, and most patients present with metastases at diagnosis (Strobel et al. 2019). These factors mean that only 10-20% of patients are eligible for surgical resection, with patients unable to undergo surgery having chemotherapy as the standard of care (Sarfaty et al. 2023).

Gemcitabine was approved for the treatment of PDAC in 1996 and is still one of the most common chemotherapies used clinically. Gemcitabine enters tumour cells through transporters before it is phosphorylated to its active metabolite, gemcitabine triphosphate. Gemcitabine triphosphate is incorporated into DNA as a false nucleoside, causing the inhibition of DNA polymerases and including cellular apoptosis (Hamed et al. 2013; Jia, Y. and Xie, J. 2015).

Regardless of gemcitabine's use as a monotherapy, it is more commonly used in combination with other drugs to increase its therapeutic response. One combination drug is nab-paclitaxel, in which paclitaxel is bound to nanoparticle albumin. This structure allows more effective delivery of paclitaxel into targeted cancer cells. Once paclitaxel has entered a cancer cell, it interferes with microtubule formation, causing cell death (Verweij et al. 1994; Ma, W.W. and Hidalgo 2013). Combination treatment with gemcitabine and nab-paclitaxel increased OS in PDAC patients from 8.5 months with monotherapy to 13.87 months with combination therapy (Von Hoff et al. 2013; Prejac et al. 2022).

Another treatment alternative for PDAC patients is FOLFIRINOX, a combination of 5-fluorouracil (5-FU), leucovorin, irinotecan and oxaliplatin. These four drugs work together to inhibit thymidylate synthase and topoisomerase 1, creating cross-links between DNA strands, preventing DNA and RNA replication, causing cell death (Longley et al. 2003; Quinn et al. 2015). Treatment with FOLFIRINOX improved 5-year OS to 43.2% compared to gemcitabine monotherapy OS of 31.4% (Conroy et al. 2022). Despite the higher OS rates seen, the treatment plan is more toxic in patients and causes more harmful adverse effects, such as neutropenia and diarrhoea, so FOLFIRINOX usage is limited to patients with a higher tolerance for these side effects (Janssen, Q.P. et al. 2025; Ohba et al. 2025). As many patients are diagnosed in later stages of life, with comorbidities, using this harsher chemotherapy for a minimal increase in life expectancy is not deemed worth the more severe side effects.

Treatment in pancreatic cancer patients is further hindered due to the tumour's characteristic dense desmoplastic stroma. This dense stromal environment often acts as a barrier, preventing efficient intratumoral penetration of chemotherapy and contributing to drug resistance (Chakkera et al. 2024). Consequently, there is an urgent need for further investigation into new treatment alternatives for pancreatic cancer due to the standard-of-care chemotherapies gemcitabine, nab-paclitaxel, and FOLFIRINOX all having low OS rates or harsh adverse effects. Additionally, the dense stromal environment hinders treatment effectiveness, meaning further strategies targeting this aspect of the TME are needed to improve current standard-of-care treatments.

1.3 The Tumour Microenvironment

The PDAC TME can greatly impact chemotherapy response and is seen as one of the main factors contributing to poor treatment response. In PDAC, the TME is characterised by a dense desmoplastic stroma. This stroma creates a hypovascular environment composed of a stiff extracellular matrix (ECM), cancer cells, cancer-associated fibroblasts (CAFs), immune cells, blood vessels, and lymphatic vessels (Ferrara et al. 2021). Fibroblast proliferation causes increased fibrosis and releases large amounts of collagen and hyaluronan, creating the dense stroma and stiff ECM. This creates a hypoxic environment that impedes drug delivery, increases drug resistance, and promotes metastasis (Masugi 2022; Olaoba et al. 2024).

PDAC tumours can be classified into subtypes that are identified through differences in structural variation, and differentiational and mutational differences. These subtypes include squamous, pancreatic progenitor, immunogenic, and aberrantly differentiated endocrine exocrine (ADEX) (Bailey, P. et al. 2016). The squamous subtype was characterised by gene networks involved in inflammation, metabolic reprogramming, and TGF-β signalling, with *TP53* mutations commonly seen. The desmoplastic subtype is a variant of the squamous subtype, characterised by high α-SMA expression and other stromal components (Puleo et al. 2018). Gene mutations regulating fatty acid oxidation, steroid hormone biosynthesis, and drug metabolism were key in pancreatic progenitor subtypes, with inactivating TGF-β receptor mutations also common. The ADEX subtype was classified by transcriptional network upregulation that mediated the characterisation of both exocrine and endocrine tissues. Finally,

the immunogenic subtype is characterised by significant immune infiltration (Collisson, E.A. et al. 2011, 2019; Bailey, P. et al. 2016; Puleo et al. 2018). These subtypes are linked to varying patient OS and these structural differences in tumours can result in differing patient responses to chemotherapy (Guenther et al. 2025). This highlights the need for more specific, novel treatments for each subtype to improve patient responses and OS rates (Collisson, E.A. et al. 2019; Xu, R. et al. 2024).

CAFs are a key feature of PDAC tumours and are produced from many activated fibroblast and endothelial cell populations (Zeisberg, E.M. et al. 2007; Miyazaki, Y. et al. 2020; Iwamoto et al. 2021). CAFs play an integral role within the TME, controlling the production of cytokines, collagen, and hyaluronan (McCarthy et al. 2018). The cytokines and proteins produced by CAFs increase solid stress and cause fibrosis within the tumour. This affects vasculature structure and formation, leading to high interstitial fluid pressure, promoting tumour metastasis and chemoresistance, and increasing hypoxia (Chauhan et al. 2013; Zhang, T. et al. 2022). The two main types of CAFs found within the PDAC TME are myofibroblastic (myCAF) and inflammatory (iCAF). Within a tumour, myCAF differentiation is mediated by TGF-β signalling, and they express high levels of α-SMA and control stroma remodelling (Öhlund et al. 2017). In contrast, iCAFs contribute to the immunosuppressive environment and express low levels of α-SMA and high levels of Il-6, an inflammatory molecule that supports cancer progression, invasion and immune suppression (Brichkina et al. 2023). myCAFs are the predominant mediators of the dense desmoplastic stroma, producing VEGF-A and influencing angiogenesis within the TME, making them a key target for normalising vasculature (De Francesco et al. 2013; Tang, D. et al. 2016; Biffi et al. 2019).

The dense stroma affects blood vessel structure and formation, with tumour blood vessels exhibiting abnormal growth. Within blood vessels in normal tissue, endothelial cells usually form a continuous inner lining around the lumen, which is attached to a basement membrane containing pericytes (Pugsley and Tabrizchi 2000). Tumour blood vessels lack this continuous layer of endothelial cells, with the cells branching, overlapped and disorganised (Hashizume et al. 2000). Furthermore, the basement membrane will bind loosely to the disordered and weakly connected endothelial cells, causing increased vessel leakiness and leading to high intratumoral hypoxia (Natarajan, V. et al. 2022). These features create gaps in the lining of tumour blood vessels, contributing to a leaky structure and increased intratumoral pressure. This causes the

escape of tumour cells, the formation of metastases and the prevention of efficient drug delivery.

The leaky, inefficient structure of the tumour blood vessels is further exacerbated by the high interstitial fluid pressure (IFP) within the tumour. One reason for high IFP is the dense stroma collapsing lymphatic vessels, preventing effective drainage of excess fluid leaking out of the blood vessels (Chauhan et al. 2014; Fink, D.M., Steele and Hollingsworth 2016). One main consequence of high IFP is the prevention of drug delivery to cancer cells (Libutti et al. 2018) . High IFP, coupled with the physical barrier generated by the dense desmoplastic stroma and high collagen levels, impedes chemotherapy delivery from the bloodstream into the tumour (DuFort et al. 2016; Song, X. et al. 2023). Targeting components that contribute to the dense environment, such as collagen, has been shown to lower the IFP, significantly increasing OS and significantly decreasing metastatic tumour burden in mouse models (Provenzano et al. 2012). A clear strategy to improve chemotherapy efficiency for PDAC patients should target the dense desmoplastic stroma and tumour blood vessels to reverse the immunosuppressive environment, reduce hypoxia, and allow more efficient drug delivery.

1.4 Angiogenesis

Angiogenesis is the formation of new blood vessels from existing capillaries to create a complete vascular network, and it is controlled by pro-angiogenic and anti-angiogenic factors (Larionova et al. 2021). Angiogenesis is essential in embryonic development, wound healing and the menstrual cycle, but is also a pathway frequently affected in many diseases. It has been characterised as one of the hallmarks of cancer and is a required process for tumour growth, development, and metastasis (Hanahan and Weinberg 2000).

Angiogenesis is controlled by pro-angiogenic factors and occurs through basement membrane degradation and the activation, proliferation, and migration of endothelial cells to form new vasculature (Liu, X. et al. 2025). In rapid tumour growth, where tumour cells require more oxygen and nutrients, the balance between pro-angiogenic and anti-angiogenic factors becomes dysregulated, causing the “angiogenic switch” (Baeriswyl and Christofori 2009; Liu, Z.-L. et al. 2023a). This “switch” tilts the balance towards pro-angiogenesis caused by increased tumour hypoxia and release of tumour angiogenesis factors (TAFs). Key TAFs include the dominant

angiogenesis regulator, vascular endothelial growth factor-A (VEGF-A), which stimulates existing, nearby blood vessels to undergo angiogenesis (Yanagisawa et al. 2021). Vessels formed from TAF release display intensive sprouting with deformed membranes and lumen structures, reducing nutrient exchange and efficient drug delivery while further contributing to the tumour's hypoxic environment (Jain, R.K. et al. 2014).

PDAC tumours have a very low microvessel density (MVD), which is the ratio of tumour vessels to tumour volume. Despite high VEGF production, the vasculature struggles to form because of the dense desmoplastic stroma and high IFP (An, Y.-F. et al. 2023). Many studies have demonstrated that a high MVD and high VEGF-A levels in PDAC correlated with a worse OS in patients. However, in contradiction, it has also been shown that elevated levels of vascular endothelial marker CD31 correlated with a higher OS in PC patients (Niedergethmann et al. 2002; Nishida et al. 2016; Katsuta et al. 2019) As cancer cells have been shown to migrate towards and damage endothelial cells, before taking over the lining of these tumour blood vessels, it could indicate that the large amount of blood vessels that causes the worse OS, are leakier and lacking in their structural components (Di Maggio et al. 2016; Nguyen, D.-H.T. et al. 2019). Tumours with higher CD31, and therefore increased numbers of endothelial cells, also had upregulated signalling pathways involved in vascular stability and immune response (Katsuta et al. 2019). This indicates that allowing the stabilisation and strengthening of the vasculature in PDAC tumours could improve therapy response, reduce the immunosuppressive environment and improve patient survival rates (Ansardamavandi et al. 2023).

In other cancers, hyper-vascularity is seen as a sign of poor prognosis, so anti-angiogenic therapies are investigated as potential treatments. However, in PDAC, preventing angiogenesis increased metastases as it upregulated the secretion of proinflammatory cytokines, leading to sustained inflammation and a more aggressive phenotype (Carbone et al. 2011; Tamburrino et al. 2013; Aguilera et al. 2014). The focus shifted to "normalising" vasculature in tumours, reducing the hypoxic environment, improving drug delivery to the tumour and enhancing immune cell infiltration (Qian, C. et al. 2023). Vascular normalisation occurs through increased pericyte recruitment and coverage, fewer sprouting endothelial cells and increased pruning, resulting in a continuous luminal diameter and blood pressure, thereby increasing oxygen levels and decreasing hypoxia (Magnussen and Mills, I.G. 2021).

Tumour angiogenesis can alter the immune cell population within tumours. Angiogenesis disrupts immune cell interaction, allowing cancer immune evasion and perpetuating immune suppression (Zhou, X. et al. 2015) An immunosuppressive environment is characteristic to PDAC and contributes to early metastasis and poor patient survival, with the dense desmoplastic stroma, hypoxic microenvironment and disrupted vasculature all contributing (Falcomatà et al. 2023; Gautam et al. 2023). Angiogenic therapies that allow vascular normalisation have been shown to affect immune cell population, by inducing dendritic cell maturation, and improving the uptake of immune cells into the tumour, allowing immune mediated control of tumour growth and improving effectiveness of immunotherapies (Shrimali et al. 2010; Fukumura et al. 2018).

Tumour vasculature normalisation allows for improved vessel structure, IFP reduction and increased levels of oxygen and immune cells. Combined, these features reduce metastasis and further stimulation of angiogenic factors, leading to easier delivery of chemotherapies to tumour tissue. This indicates that vessel normalisation could be an effective treatment in combination with standard-of-care chemotherapy to improve efficacy and patient response.

1.5 Transforming Growth Factor-β

TGF-β is an anti-inflammatory cytokine with many roles, including regulation of apoptosis, cell growth, and differentiation (Deng et al. 2024). In the initial stages of PDAC formation TGF-β acts as a tumour suppressor, triggering apoptosis of pre-malignant cells, and blocking fibroblasts and inflammatory cells from producing paracrine factors that encourage tumour formation (Seoane and Gomis 2017). In later stages of the disease, mutations in other tumour suppressors, signalling mediators, and receptors changes TGF-β into a tumour promoter, which increases fibrosis, angiogenesis, and immune cell infiltration leading to more invasive and metastatic tumours (Hao et al. 2019). TGF-β induces the expression of many pro-angiogenic factors, including VEGF-A, connective tissue growth factors, basic fibroblast growth factor (bFGF) and IL-1, emphasising its integral role in regulating angiogenesis in tumours (Fang et al. 2020; Liu, Z.-L. et al. 2023b). As a key molecule in cancer development and progression, with roles in epithelial-to-mesenchymal transition (EMT) and angiogenesis, it is a potential target to minimise metastasis and improve the effectiveness of current treatments.

TGF-β controls cellular processes through two main pathways: the canonical, and non-canonical. The canonical pathway (Figure 1.2) is controlled by SMAD proteins and is activated by TGF-β binding to serine/threonine kinase receptor, TGF-β receptor II (TGF-βRII). This binding activates the assembly of a complex of TGF-βRII and TGF-β receptor I (TGF-βRI), which phosphorylates regulator SMAD (r-SMAD) proteins SMAD2 and SMAD3. The phosphorylated SMAD2/SMAD3 complex binds to the common SMAD (co-SMAD), SMAD4, and translocates into the nucleus to control target gene expression (Hata and Chen, Y.-G. 2016; Verrecchia and Rédini 2018). There are large numbers of genes that TGF-β controls through the SMAD signalling pathway; however, this pathway predominantly regulates epithelial growth suppression and EMT through changes in the expression of genes, including: cyclin-dependent kinase inhibitors p15 and p21, and E-cadherin, a molecule heavily involved in EMT (Ten Dijke et al. 2002).

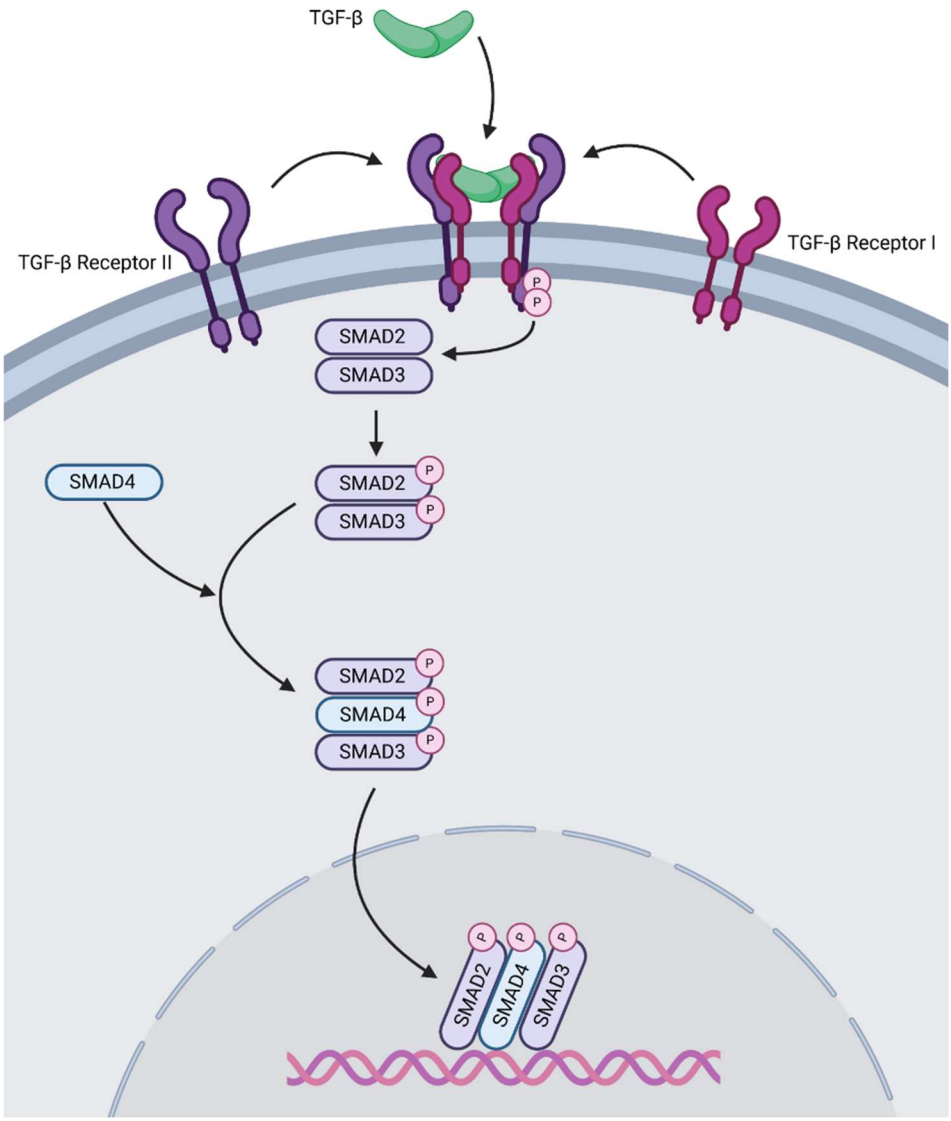


Figure 1.2 – The canonical TGF-β Pathway. This pathway is activated after the binding of TGF-β to TGF-βRII, and is mediated through r-SMADS, SMAD2 and SMAD3 and co-SMAD, SMAD4. Created in BioRender.

SMAD4 has important roles in the TGF-β signalling pathway, and it is mutated in roughly 55% of PDAC patients, altering this pathway's function (Ahmed, S. et al. 2019). *SMAD4* mutations typically occur in late stages, resulting from increased genomic instability. Patients with mutated SMAD4 had a 5-year OS of 12.3%, in comparison to 15.8% in patients with non-mutated SMAD4 (Qian, Z.R. et al. 2018). *SMAD4* mutations prevent TGF-β-induced growth suppression, leading to increased invasiveness and metastatic potential (Malkoski and Wang, X.-J. 2012; Ahmed, S. et al. 2019). Furthermore, in the absence of SMAD4, SMAD2 and SMAD3 can mediate the oncogenic effects of TGF-β through a transcriptional migration program where cells gain a collective migratory ability through Rho signalling, facilitating invasion and migration (Bertrand-Chapel et al. 2022; Murimwa et al. 2025).

In addition to the canonical signalling pathway, non-canonical signalling has many roles in tumour suppression and progression. These non-canonical pathways occur when components of the canonical pathway "crosstalk" with other signalling molecules (Moustakas and Heldin 2005). Some of these non-SMAD pathways include MAPK, Rho-like GTPase, PI3K/AKT, and JNK/p38 signalling cascades, which are all necessary for TGF-β induced EMT (Bakin et al. 2000, 2002; Bhowmick et al. 2001; Davies et al. 2005).

The TGF-β signalling pathway is regulated in many ways. The two TGF-βRs can be regulated through phosphorylation, with TGF-βRII being constitutively active and able to autophosphorylate (Chen, F. and Weinberg 1995). TGF-βRI cannot autophosphorylate but can be phosphorylated by TGF-βRII on ligand binding (Luo, K. and Lodish 1997). This phosphorylation can be reversed by the formation of the TGF-β-regulated protein phosphatase 1 (PP1) complex, which de-phosphorylates TGF-βRI when downregulation of TGF-β signalling is needed (Huang, F. and Chen, Y.-G. 2012). One of the main negative regulators of the canonical signalling pathway is SMAD7, an inhibitory SMAD (Yan, X. et al. 2009). SMAD7 mediates TGF-β signalling through many mechanisms. Firstly, it binds to DNA and interferes with the SMAD2/3/4 complex bound to target gene promoters and prevents gene transcription (Zhao, B. and Chen, Y.-G. 2014). SMAD7 can also form a complex with TGF-βRI, preventing SMAD2/3 phosphorylation and recruiting PP1 to dephosphorylate the receptor (Shi, W. et al. 2004)

Due to TGF-β signalling becoming dysregulated in cancer, attempts at inhibiting TGF-β signalling have been explored as potential treatment options (Zhang, M. et al. 2011; Melisi et al. 2021;

Xiong et al. 2025). TGF-β signalling inhibition is investigated in cancer to improve the efficacy of standard-of-care chemotherapies. Previously, TGF-βRI inhibitor LY3200882 was investigated in bladder cancer in combination with gemcitabine. Not only did LY3200882 promote apoptosis and inhibit invasion in bladder cancer cell lines, but when used with gemcitabine, it suppressed cell viability, increased apoptosis and reduced invasion, in comparison to treatment with gemcitabine alone (Xiong, Y. et al. 2025). This effect has also been investigated in metastatic PDAC, with TGF-βRI and II inhibitor LY2109671. LY2109671 inhibited cell growth in metastatic PDAC cell lines, and significantly reduced primary tumour growth, suppressed metastasis and prolonged survival in mice models when used in combination with gemcitabine (Melisi et al. 2008). Increases in treatment response with TGF-β inhibitors is linked to preventing EMT and tumour aggressiveness, allowing chemotherapy to be more effective against cancer cells, prior to metastasis formation (Melisi et al. 2008; Xiong, Y. et al. 2025).

How TGF-β inhibition affects blood vessels has been investigated to potentially improve treatment responses. In breast carcinoma, TGF-β blockade with a TGF-β neutralising antibody, reduced VEGF expression, increased recruitment of perivascular cells into tumour blood vessels, promoted vessel normalisation, and improved efficacy of the drug Doxil (Liu, J. et al. 2012). Previously, TGF-β inhibition has also been shown to prevent endothelial cell death in tumours, inhibit cell invasion, prevent lymph node metastasis, reverse the immunosuppressive environment, and enhance tumour cell susceptibility to treatment (Neuzillet et al. 2014; Nguyen, D.-H.T. et al. 2019). Previously, the angiotensin II receptor inhibitor losartan was used in PDAC, where it reduced collagen production and decreased CAF density through downstream TGF-β signalling inhibition. This change in TME composition reduced solid stress, decompressed tumour blood vessels, and enhanced 5-FU delivery and significantly decreased tumour growth and increased median survival in a mouse model (Chauhan et al. 2013).

TGF-β inhibition in cancer prevents EMT but also enhances chemotherapy response in a range of cancers and experimental models. This improvement in chemotherapy response with TGF-β inhibition is not only due to its many roles in regulating EMT, but also to its role in regulating angiogenesis. Targeting TGF-β, directly and indirectly, has improved tumour blood vessel structure and function, allowed greater intratumoral distribution of chemotherapy, and reduced stromal components of the TME (Liu, J. et al. 2012). Despite this, the direct effect of TGF-β on vascular normalisation has not been investigated in PDAC (Qiang et al. 2023).

1.6 Aims & Objectives

This project aims to investigate TGF-β inhibition with multiple components of the pancreatic cancer TME. A TGF-β inhibitor will be used in PDAC cell lines to investigate effects on cell viability and protein and mRNA expression. Fibroblastic and endothelial cell lines will be used to identify how these changes would affect the greater TME structure. Finally, TGF-β inhibition in co-culture angiogenesis assays will explore the effect on vascular formation and normalisation in PDAC. Overall, this study will expand understanding of how TGF-β influences the pancreatic cancer tumour microenvironment and blood vessel normalisation, to improve chemotherapy distribution and response.

2. Methods

2.1 Cell Culture

Human PC cell lines Panc1 (CRL-1469), MiaPaCa2 (CRM-CRL-1420) and BxPc3 (CRL-1687) were obtained from the American Tissue Culture Collection (ATCC, USA). Panc1 cells were cultured in Dulbecco's Modified Eagles Media (DMEM, Corning, 10-013-CV) and MiaPaCa2 cells and BxPc3 cells were cultured in Roswell Park Memorial Institute 1640 (RPMI 1640, Corning, 10-040-CV), both supplemented with 10% foetal bovine serum (FBS, Gibco, A5256801) and 1% penicillin/streptomycin (P/S, Gibco, 15140-122).

Primary umbilical vein endothelial cells (HUVEC, PromoCell, C-12203) were cultured in endothelial cell growth medium (ECGM, Cell Applications Inc., 211-500), supplemented with 1% P/S.

Primary human dermal fibroblasts (HDF) were provided by Dr Adam Odell and cultured in a fibroblast culture medium consisting of a 1:1 mixture of DMEM and RPMI, supplemented with 5% FBS and 1% P/S.

Patient-derived pancreatic cancer-associated fibroblasts (CAFs) were provided by Professor Thomas Hughes and cultured in a 1:1 mixture of ECGM and fibroblast culture media.

Cells were passaged every 3-4 days, when 70-80% confluent, using Trypsin-EDTA (Fisher Scientific, 10779413) for detachment, before centrifugation (300xg, 5 minutes) and subculturing in fresh media. All cell lines were cultured in humidified incubators maintained at 37^{o}C and 5% CO_2.

2.2 Test Compounds

LY2109761 (SLS, SML2051), Dexamethasone (Sigma, D1756), and SB431542 (Sigma, 61646) were prepared by resuspending the powder in sterile dimethyl sulfoxide (DMSO, Sigma D2650) to create stock concentrations of 100mM, 50mM and 100mM, respectively. Stock concentrations of LY2109761 were stored at -20^{o}C, and stock concentrations of Dexamethasone and SB431542 were stored at 4^{o}C.

2.3 MTT Viability Assays

All cell lines were seeded in 96-well plates at a density of 5000 cells/well and incubated overnight. Working drug concentrations were diluted in culture media, added to plates at the indicated final concentrations, and incubated for 72 hours.

MTT (3-(4,5-Dimethylthiazol-2-yl)-2,5-Diphenltetrazolium Bromide) (Invitrogen, M6494) prepared in PBS at a stock concentration of 5mg/ml, was added to each well at a final concentration of 0.25µg/µl and incubated for 4 hours at 37^{o}C. After incubation, the cell media was removed, and 150µl of DMSO (Fisher Scientific, D/4120/PB08) was added to each well and left until the precipitate dissolved. Absorbances were measured at 570nm using the ThermoFisher Varioskan LUX Microplate Reader.

2.4 SDS-PAGE

Cell lines were seeded in 6-well plates at a density of 2.5x10^{5} cells/well for Panc1, MiaPaCa2, BxPc3 and HUVEC cell lines, and at a density of 2x10^{5} cells/well for HDF and CAF and incubated overnight. Separate wells were treated accordingly before lysate collection. For lysate collection, well plates were placed on ice, media was removed, and wells were washed three times with 1X phosphate buffered saline (PBS) (1ml/30cm^{2}). SDS lysis buffer (2% SDS in a buffer containing 50mM Tris, 150mM NaCl, 2mM EDTA, 2mM EGTA) was added to each well, the cells were scraped off the well, and lysates were collected. Lysates were boiled (95^{o}C, 5 minutes), centrifuged (10,000xg, 30 seconds) and sonicated (20 kHz, 3-5 seconds), before further centrifugation (10,000xg, 1 min). A Pierce BCA assay kit (ThermoFisher Scientific) was used as per the manufacturer's instructions to determine protein concentration, and samples were made up to 50 µg total protein. 5X loading buffer (0.1M Tris, 4% SDS, 20% glycerol, 0.1% bromophenol blue in dH_2O) containing 10% (v/v) β-mercaptoethanol was added to the samples for a final 1X concentration, and the samples were boiled for 5 minutes at 95^{o}C before loading onto a resolving 6-15% gradient SDS-polyacrylamide gel. Samples and a PageRuler Plus pre-stained protein ladder (ThermoFisher Scientific, 26619) were separated at 200V for 60 minutes in a 1X SDS running buffer (200mM Tris, 25mM glycine, 3.5mM SDS) prior to Western blotting.

2.5 Western Blotting

SDS polyacrylamide gels were transferred onto Amersham Portran 0.45µM nitrocellulose membrane (Cytiva, 10600002) at 60mA overnight in 1X transfer buffer (25mM Tris, 200mM glycine, 4% methanol) at 4°C. Membranes were stained with Ponceau (1.3mM Ponceau S, 5% acetic acid in dH_2O) to assess consistency of protein loading, before washing 3x in TBST containing 1X TBS (1.4M NaCl, 51mM KCl, 250mM Tris in dH_2O) and 0.075% (v/v) Tween 20. Membranes were blocked in 5% non-fat dried milk in TBST for 30-60 minutes and washed with TBST. Primary antibodies were diluted in 1% bovine serum albumin (BSA) (Sigma-Aldrich, A7030) prepared in TBST containing 0.02% sodium azide and incubated with the membranes overnight at 4°C. Primary antibodies used were TGF-β (1:1000, Cell Signalling Technology, 3711S), TGF-βRII (1:20,000, Proteintech, 66636-1-Ig), α-SMA (1:1000, Cell Signalling Technology, D4K9N), COL1A1 (1:1000, Cell Signalling Technology, E8I9Z), phospho-SMAD2 (ser465/467)/SMAD3 (Ser423/425) (1:1000, Cell Signalling Technology, D27F4), SMAD2/3 (1:1000, Cell Signalling Technology, D7G7), α-tubulin (1:20,000, Abcam, ab4074) and GAPDH (1:500, Biolegend, 649202). After incubation, membranes were washed 3x for 30 minutes total in TBST. Appropriate HRP-conjugated secondary antibodies (1:3000 Anti-rabbit HRP-linked antibody, Cell Signalling Technology, 7074P2 or 1:1000 Anti-mouse IgG HRP-conjugated antibody, R&D Systems, HAF007) were diluted in TBST and added to the membranes for 1 hour, after which membranes were washed 3x in TBST prior to development using Clarity Western ECL reagent (Bio-Rad, 1705061). Membranes were imaged using the Invitrogen iBright CL1500 Imaging System (ThermoFisher Scientific). Protein expression was quantified using ImageLab software.

2.6 qPCR

RNA isolation was performed using the RNeasy Mini Kit (Qiagen) in accordance with the manufacturers protocol. cDNA synthesis was performed on 0.4 µg total RNA using the Ultrascript cDNA synthesis kit (PCR Biosystems) in accordance with the manufacturer's instructions. qPCR was performed on a QuantStudio 5 Real-time PCR System using a PowerUP SYBR Green master mix (Applied Biosystems) in accordance with the provided protocol, and the specific human primers are listed in Table 1 (Origene). Data were analysed using the $2^{-\Delta\Delta Ct}$

method to examine relative expression, presented as the fold change over control and normalised to GAPDH.

Table 1. Primer sequences used in qPCR

Gene Target	Primer Sequence
VEGF-A	F: TTGCCTTGCTGCTCTACCTCCA
	R: GATGGCAGTAGCTGCGCTGATA
TGF-β	F: TACCTGAACCCGTGTTGCTCTC
	R: TACCTGAACCCGTGTTGCTCTC
bFGF	F: AGCGGCTGTACTGCAAAAACGG
	R: CCTTTGATAGACACAACTCCTCTC
α-SMA	F: CTATGCCTCTGGACGCACAACT
	R: CAGATCCAGACGCATGATGGCA
COL1A1	F: GATTCCCTGGACCTAAAGGTGC
	R: AGCCTCTCCATCTTTGCCAGCA
COL4A1	F: TGTTGACGGCTTACCTGGAGAC
	R: GGTAGACCAACTCCAGGCTCTC
IL-6	F: AGACAGCCACTCACCTCTTCAG
	R: TTCTGCCAGTGCCTCTTTGCTG
GAPDH	F: GTCTCCTCTGACTTCAACAGCG
	R: ACCACCCTGTTGCTGTAGCCAA

2.7 Co-cpulture angiogenesis assays

Co-culture angiogenesis assays were adapted from the method described previously (Odell and Mannion 2022). Forty-eight-well plates were coated in 0.2% gelatin for 30 minutes prior to cell seeding. HDFs or CAFs were seeded at 20,000 cells/well and incubated overnight. Media was removed, and HUVECs were seeded at 5000 cells/well and incubated for 24 hours. The co-cultures were treated for 6 days, with culture media being changed every 2-3 days and

containing combinations of recombinant VEGF-A protein (Gibco, 17809912), recombinant TGF-β protein (Proteintech, HZ-1011) and LY2109761.

For the collection of conditioned media, cells were seeded at 15,000 cells/cm^2, incubated overnight, before the media was replaced with fresh growth media. When cells reached 70-80% confluency, conditioned media was removed and filter-sterilised (0.2μm). The conditioned media was diluted 50:50 with ECGM before addition to cells.

For immunofluorescence staining, media was removed, and co-cultures were fixed with ice-cold 70% ethanol for 30 minutes. Ethanol was removed, and cells were washed 2x with 1xPBS before primary antibody addition. Fixed co-cultures were incubated overnight at 4°C with primary antibody anti-CD31-APC (1:500, Biolegend, 303116) diluted in PBS with lectin-essential cations (PBLEC) solution (0.2% BSA, 1mM $MgCl_2$, 0.1mM $MnCl_2$, 1% Tween 20 and 0.05% sodium azide in 1xPBS). After incubation, co-cultures were washed 3x with PBS, and a Hoechst 33342 (1:10,000, Chemometec, 910-3015) solution diluted in PBLEC added for a further 5-10 minutes. Co-cultures were washed 1x in PBS and imaged using an EVOS FL Microscope (Thermo Fisher Scientific). Five images were taken per well at the top, bottom, left, right and middle of each well. AngioTool was used to quantify total vessel length (mm) and number of branch points. Images containing blood islands were altered to increase the brightness and contrast to limit the number of HUVEC junctions picked up as branch points (Zudaire et al. 2011).

2.8 HUVEC Immunofluorescence

Prior to seeding, 96-well plates were coated with 0.2% gelatin for 30 minutes. HUVECs were seeded at 5000 cells/well and incubated overnight. Working concentrations of LY2109761 and recombinant TGF-β protein were diluted in culture media, added to plates, and incubated for 48-72 hours as indicated.

Media was removed and HUVECs fixed with 10% neutral-buffered formalin solution (Sigma, HT501128) for 10 minutes. Formalin was removed, and cells were washed 2x with PBS. Primary antibody anti-CD31 APC (1:500, Biolegend, 303116) was diluted in PBLEC solution and incubated overnight at 4°C. Cells were washed 3x with PBS and incubated with Hoechst 33342 for a further 5-10 minutes. Cells were washed 1x with PBS and imaged using an EVOS FL Microscope.

2.9 Statistical analysis

Statistical analysis was performed in Prism version 11.0.2 (GraphPad). One-way ANOVA tests with Tukey's multiple comparison tests were used to determine statistical significance, as described in the figure legends.

3. Inhibiting TGF-β signalling in PDAC cell lines

3.1. Three TGF-β inhibitors LY2109671, Dexamethasone, and SB431542 affected cell viability and the phosphorylation of SMAD2/3 in PDAC cell lines.

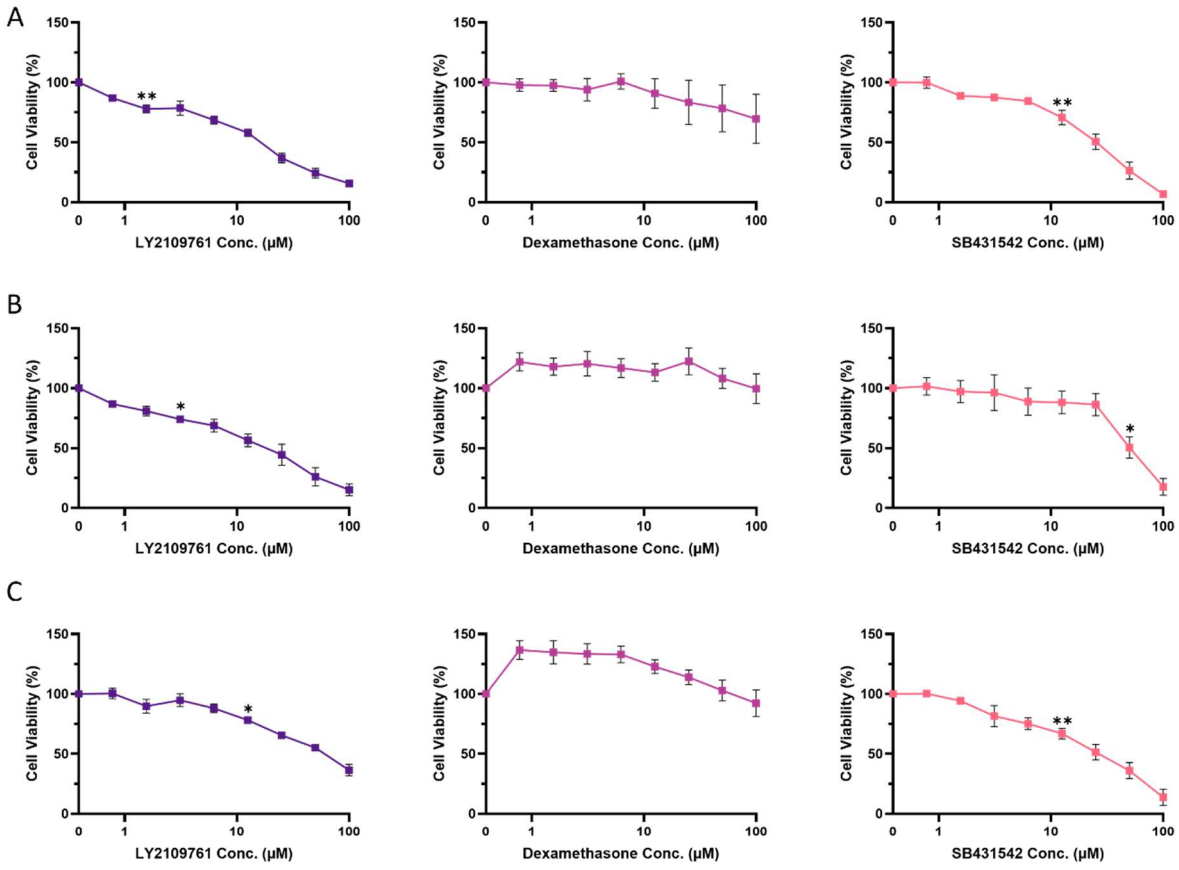
The first aim of this study was to determine the effect of TGF-β inhibition within PDAC. To investigate this, Panc1, MiaPaCa2 and BxPc3 cells were used to examine responses in PDAC with different TGF-β pathway-related genotypes and phenotypes. Panc1 cells were chosen as a cell line with no alterations affecting this pathway; MiaPaCa2 cells have a non-functional TGF-βRII, and BxPc3 cells were used as a cell line with mutated SMAD4, a key signalling molecule in the TGF-β pathway (Deer et al. 2010; Principe et al. 2022). Three TGF-β inhibitors were initially tested to assess their effects on cell viability and SMAD2/3 phosphorylation. These were LY2109671 (LY), a selective TGF-βRII and TGF-BRI inhibitor; SB431542 (SB), a TGF-βRI kinase inhibitor; and dexamethasone (DEX), a corticosteroid that inhibits TGF-β downstream signalling pathways.

MTT assays were used to assess the effect of TGF-β pathway inhibition on 72-hour cell viability at concentrations starting at 100μM, decreasing 2-fold until 0.78μM (Figure 3.1). Panc1 cells were the most sensitive to TGF-β pathway inhibition (Figure 3.1A), with viability at 100μM being 15.70% for LY, 69.58% for DEX and 6.71% for SB. LY had a dose-dependent response in Panc1 cells, significantly reducing viability at and above 1.56μM ($p = 0.005$), whereas SB did not significantly reduce viability until 12.5μM and above ($p = 0.004$), and DEX causing no significant decreases in viability.

In MiaPaCa2 cells (Figure 3.1B), LY caused a dose-dependent response, ending with a viability of 15.17%, and significantly decreased viability at and above 3.13μM ($p = 0.05$). DEX had little effect in MiaPaCa2 cells, with a viability of 99.50% at 100μM. As with Panc1 cells, SB reduced viability dramatically to 20.11% at the highest concentration of 100μM; however, it had little effect on viability until 50μM ($p = 0.03$).

In BxPc3 cells (Figure 3.1C), both LY and SB exhibited dose-dependent responses, with viability reaching 36.46% and 13.83% at 100μM, respectively. Neither inhibitor significantly decreased viability until 12.5μM and above ($p = 0.01$, $p = 0.009$). In the MiaPaCa2 cells, DEX had little effect on viability in BxPc3 cells, with the lowest viability reaching 92.32%. Finally, the IC50's for the drugs in each cell line were calculated (Figure 3.1D). There was no detectable IC50 for DEX in

any cell line. Panc1 cells exhibited the lowest IC50 for LY and SB, with an IC50 of 14.19µM, and 22.85µM, respectively. MiaPaCa2 cells had a similar IC50 to the Panc1's in LY, with 15.17µM. Despite this low IC50, MiaPaCa2 cells showed the highest IC50 in SB, with 50.52µM. BxPc3 cells had the highest IC50 in LY, with 56.47µM and the second highest IC50 in SB, with 23.61µM.



D

Cell Line	IC50 (μM)		
	LY2109671	Dexamethasone	SB431542
Panc1	14.19	N/A	22.85
MiaPaCa2	15.17	N/A	50.52
BxPc3	56.47	N/A	23.61

Figure 3.1. TGF-β inhibitors LY2109761, dexamethasone and SB431542 decrease cell viability in PDAC cell lines in dose-dependent manners. Panc1 (A), MiaPaCa2 (B) and BxPc3 (C), were treated with LY2109761 (left), dexamethasone (centre) and SB431542 (right) for 72 hours, prior to MTT assay. All data was normalised to the vehicle-treated control for each cell line. IC50's for drug in each cell line were calculated in GraphPad Prism 11.0.2 (D). Data represents means ± standard error of the mean (SEM) of 3 independent biological replicates. Statistical Analyses were performed using one-way ANOVA, with a Tukey's multiple comparison test. The asterisks indicate the first point at which significance is seen in comparison to the vehicle-treated control, * indicates $p < 0.05$ and ** indicates $p < 0.005$.

To further investigate the effect of the three TGF-β inhibitors, cell viability and protein expression analysis was performed on each PDAC cell line after exposure for 72 hours at a concentration less than the IC75 for each cell line. Based on the results from dose-response assays, 5μM was chosen as the treatment concentration in the remainder of the study (Figure 3.2).

Panc1 cells were the least sensitive to LY in comparison to the other two cell lines, with a viability of 78.94% (Figure 3.2A). BxPc3 cells had the lowest viability to LY with 66.49%, followed by MiaPaCa2 cells with 73.53%. DEX had minimal effect on the three cell lines, ending with 89.95%, 90.80% and 93.31% in Panc1, MiaPaCa2 and BxPc3 cells, respectively (Figure 3.2B). Finally, Panc1 cells were the most sensitive to SB, with a viability of 73.16%, followed by BxPc3 cells with a viability of 83.51% (Figure 3.2C). MiaPaCa2 cells were the least sensitive to SB, with a viability of 101.58%.

In addition to assessing the impact on viability, the three inhibitors were tested for efficacy at 5μM using SMAD2/3 phosphorylation as a downstream marker for TGF-β pathway activation. Panc1 cells were seeded in 6-well plates until 70% confluent, before serum-starvation for 2 hours. After 2 hours, cells were treated with 5μM of each inhibitor and 5ng/ml TGF-β for 1 hour before lysis. This allowed investigation into how effective the inhibitors were at preventing the phosphorylation of SMAD2/3. Untreated cells were shown to have very minimal expression of p-SMAD2/3, and after treatment with TGF-β, the levels of p-SMAD2/3 increased dramatically (Figure 3.2D). LY inhibited p-SMAD2/3 the most out of the three inhibitors, followed by SB. DEX did not inhibit the phosphorylation of SMAD2/3 at 5μM, with phosphorylation levels almost identical to those in the untreated, TGF-β stimulated control.

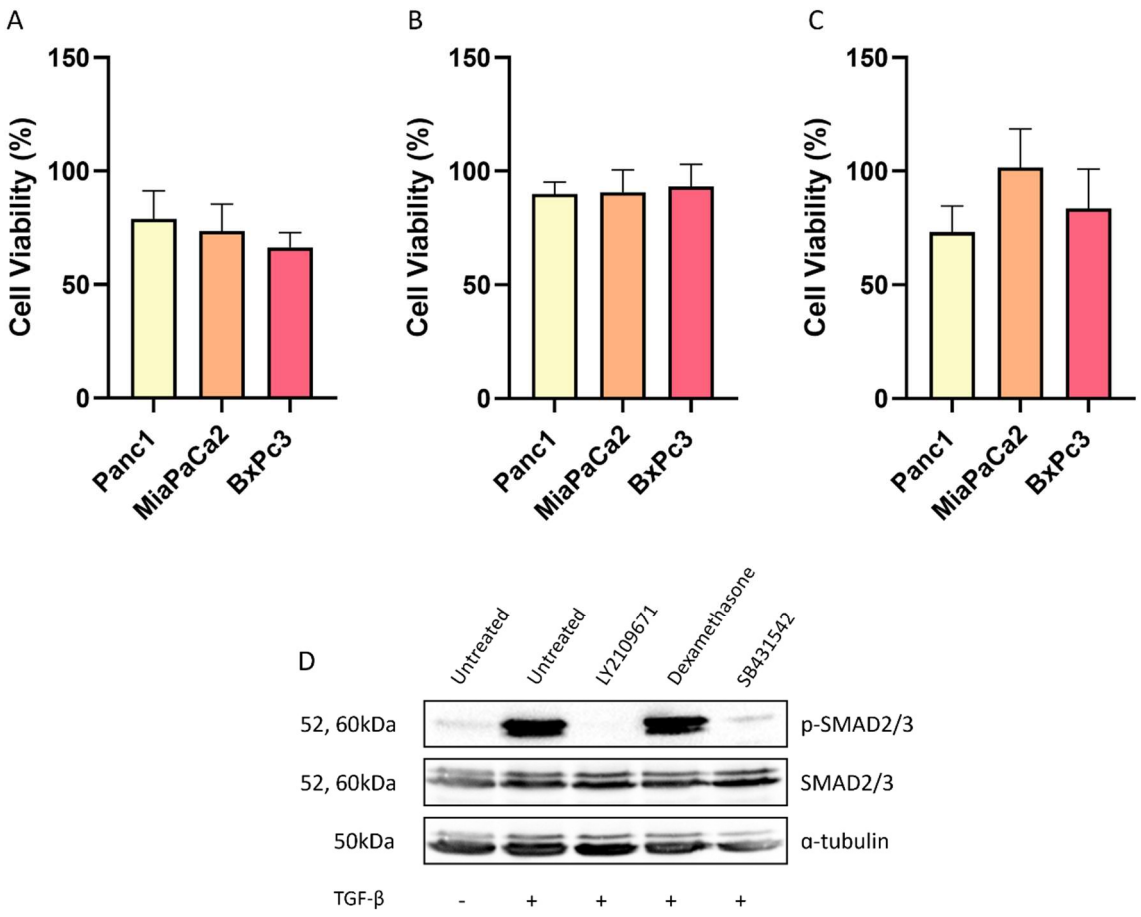


Figure 3.2. TGF-β inhibitors LY2109671 and SB431542 decrease cell viability and prevent the phosphorylation of SMAD2/3 at 5µM. Panc1, MiaPaCa2 and BxPc3, were treated with LY2109761 (A), dexamethasone (B), and SB431542 (C) for 72 hours, prior to MTT assay. Mean cell viability at 5µM was measured. Data was normalised to the vehicle-treated control for each cell line. Data represents means ± SEM of 3 independent biological replicates. Panc1 cells were serum-starved for 2 hours before treatment with 5µM of inhibitor and 5ng/ml of TGF-β for 1 hour. Protein lysates were analysed by western blot for expression of p-SMAD2/3 and SMAD2/3 (D). α-tubulin was used to determine equal protein loading between lanes. Negative (unstimulated) and untreated positive (TGF-β stimulated) controls are in the first 2 lanes.

After assessing the effect of all three inhibitors on the PDAC cell lines through cell viability and SMAD2/3 phosphorylation, LY was chosen as the inhibitor used through the remainder of the study due to its effect in all cell lines despite differences in phenotypes, without significantly decreasing viability. The effect of TGF-β induced SMAD2/3 phosphorylation at set time points, with and without LY treatment, was investigated to assess how effective LY was at 5μM in all three cell lines.

Panc1, MiaPaCa2 and BxPc3 cells were grown until 70% confluent and serum starved for 2 hours, with 5μM of LY. At this timepoint, 5ng/ml of TGF-β was added at 2-hour, 1-hour, 40-minute and 20-minute time points before lysis. Protein lysates were analysed by Western blot for the expression of p-SMAD2/3 and SMAD2/3 (Figure 3.3).

Panc1 cells showed no phosphorylation of SMAD2/3 in the untreated, unstimulated control, but showed strong levels of p-SMAD2/3 in all stimulated samples, with the 20-minute time-point showing the weakest levels. In the treated samples, LY was able to fully inhibit the phosphorylation of SMAD2/3. MiaPaCa2 cells exhibited very low levels of p-SMAD2/3 in all samples, including the untreated, TGF-β stimulated samples (Figure 3.3B). BxPc3 cells showed a similar response to that of the Panc1 cells. They had a low response of p-SMAD2/3 in the untreated, unstimulated sample, with TGF-β treatment dramatically increasing the phosphorylation of SMAD2/3 in the BxPc3 cells. This phosphorylation was inhibited by LY in the treated samples (Figure 3.3C).

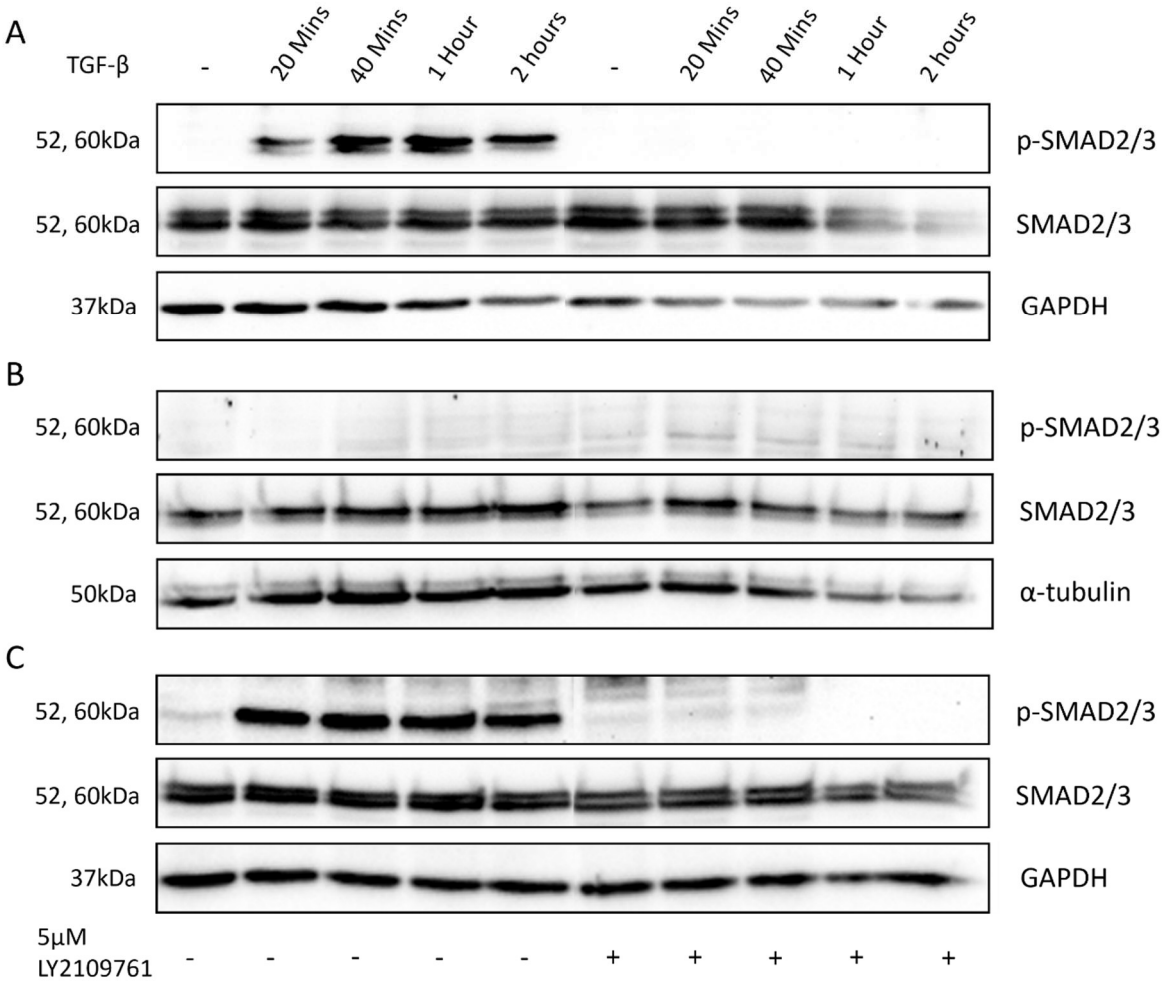


Figure 3.3. LY2109671 prevents the phosphorylation of SMAD2/3 after TGF-β stimulation in Panc1 and BxPc3 cells. Panc1 (A), MiaPaCa2 (B), and BxPc3 (C) cells were serum starved for 2 hours and treated with 5μM LY before stimulation with 5ng/ml of TGF-β for various timepoints. Protein lysates were analysed by western blot for expression of p-SMAD2/3 and SMAD2/3. α-tubulin and GAPDH were used to determine equal protein loading between lanes. Negative (unstimulated) control is in the first lane.

3.2. LY2109671 affects the protein and mRNA expression of TGF-β and VEGF-A in PDAC cell lines.

To determine the effect of LY on TGF-βRII and TGF-β protein and mRNA expression within PDAC cell lines after treatment, all three cell lines were treated with varying concentrations of LY for 72 hours, with or without 5ng/ml TGF-β, before lysis. The protein expression of TGF-βRII and TGF-β was analysed (Figure 3.4).

In Panc1 cells, LY did not alter the expression of TGF-βRII at any concentration (Figure 3.4A). Additionally, LY had limited effect in suppressing levels of TGF-β, with the protein expression levels being maintained to levels close to the untreated control. Treatment with TGF-β significantly increased the detected expression levels to 2.02 ($p = 0.02$). This increase was significantly reduced in with the addition of 5μM LY, reducing the detected protein levels to 0.35 ($p = 0.001$).

MiaPaCa2 cells showed a slight increase in detected TGF-βRII protein in cells treated with 5μM or 20μM of LY (Figure 3.4B). However, there was minimal effect on detected TGF-β protein after LY treatment. Treatment with TGF-β caused the detected protein levels to increase to 1.61, with combination treatment lowering this to 1.47.

TGF-βRII protein was slightly decreased in BxPc3 cells in the 20μM and combination-treated groups (Figure 3.4C). BxPc3 cells demonstrated a similar response to LY as in the Panc1 cells, with all treatments maintaining detected TGF-β levels at a level similar to the untreated control. Detected protein level increased to 2.52 after TGF-β treatment, and these expression levels were brought back down to 0.59 in the combination-treated cells.

An increase in detected TGF-β expression in the BxPc3 cells after TGF-β treatment, followed by a decrease back down to the levels of the untreated control, was seen as a common trend, but was deemed non-significant, likely due to a lack of statistical power, as n=2.

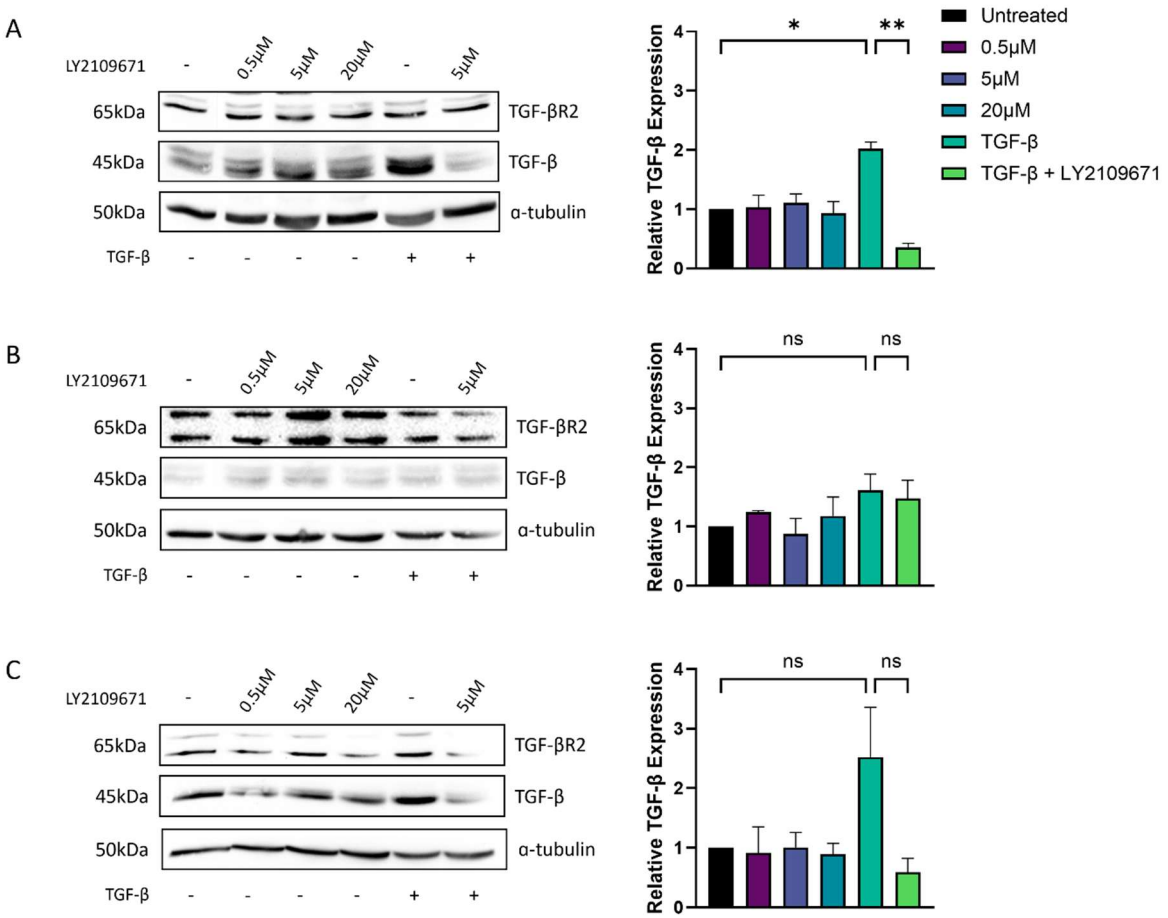


Figure 3.4. LY2109671 inhibits TGF-β protein expression in PDAC cell lines. Protein expression of TGF-βRII and TGF-β was analysed in Panc1 (A), MiaPaCa2 (B) and BxPc3 (C) after 72 hours of treatment with LY2109671 and/or 5ng/ml TGF-β. α-tubulin was used to determine equal protein loading between lanes. TGF-β expression was quantified using ImageLab (BioRad), normalised to α-tubulin expression before normalisation to the untreated control. Data represents means ± SEM of 2 independent biological replicates. Statistical analyses were performed using one-way ANOVA, with Tukey's multiple comparison test, * indicates $p < 0.05$ and ** indicates $p < 0.005$.

After analysing differences in protein expression, changes in mRNA expression were also analysed in the three PDAC cell lines. All three cell lines were treated with 5μM LY and/or 5ng/ml TGF-β for 24 hours before undergoing mRNA isolation, and qPCR to determine if this treatment altered the expression of VEGF-A and TGF-B (Figure 3.5).

In Panc1 cells, treatment with LY caused minimal change in mRNA expression of both genes (Figure 3.5A). In TGF-β treatment, a fold-increase in VEGF-A and TGF-β gene expression of 0.53 and 1.18, respectively, was observed. The combination treatment caused a fold-decrease in gene expression to 0.14 in VEGF-A and 0.04 in TGF-β.

MiaPaCa2 cells demonstrated minimal effect on TGF-β-induced mRNA expression (Figure 3.5B). VEGF-A expression was increased by 0.77-fold over the untreated control after LY treatment. This changed to a 0.46-fold increase with TGF-β treatment, which increased to a 0.53-fold increase with the combination treatment. LY and TGF-β individual treatments caused no-fold change in TGF-β mRNA expression in MiaPaCa2 cells, and the combination treatment caused a 0.63-fold decrease in comparison to the untreated control.

VEGF-A mRNA expression remained unchanged in BxPc3 cells (Figure 3.5C). Treatment with TGF-β caused a 1.08-fold increase of TGF-β mRNA expression, and although LY treatment alone did not cause a decrease in the mRNA expression of TGF-β, it did cause a 0.46-fold decrease in TGF-β mRNA expression in the combination treatment.

All data shown was deemed non-significant. An increase in TGF-β mRNA expression in the Panc1 and BxPc3 cells after TGF-β treatment, followed by a decrease back down to the levels of the untreated control, or lower, was seen as a common trend, but was deemed non-significant, likely due to a lack of statistical power, as n=2.

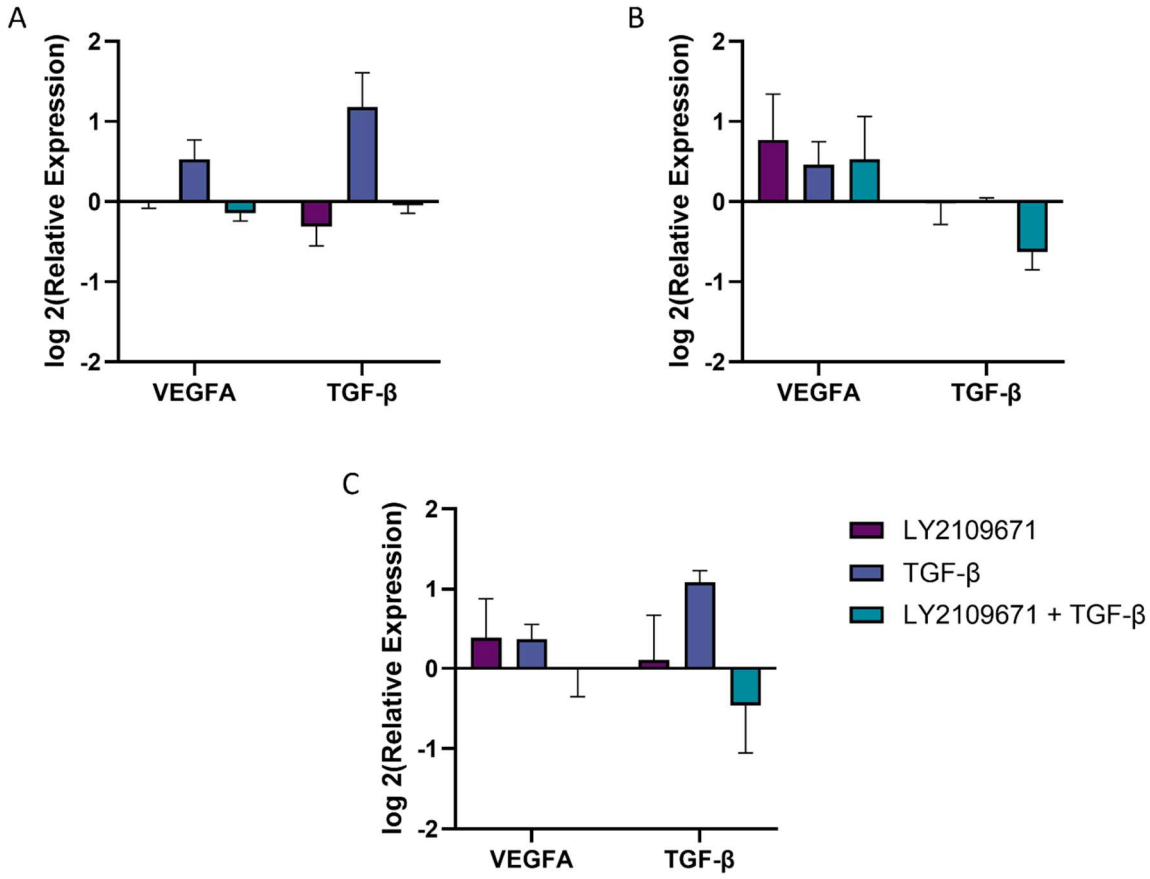


Figure 3.5. LY2109671 inhibits TGF-β induced gene expression in Panc1 and BxPc3 cells. qPCR measured mRNA expression levels of VEGFA and TGF-β in Panc1 (A), MiaPaCa2 (B), and BxPc3 (C), after 24 hours of treatments with 5μM LY2109671 and/or 5ng/ml TGF-β. Data was analysed using the $2^{-\Delta\Delta Ct}$ method, with values normalised to GAPDH and presented as the log2(fold change) over the untreated control. Data represents means ± SEM of 2 independent biological replicates. Statistical analyses were performed using one-way ANOVA, with Tukey's multiple comparison test.

4. Inhibiting TGF-β signalling in fibroblast cell lines

4.1. Human Dermal Fibroblasts

After investigating the effects of TGF-β inhibition in PDAC cell lines, the study expanded to investigate this effect on other areas of the TME. One of the other cell types investigated were fibroblasts, with HDF and CAF being the two fibroblasts used in this study. Firstly, HDFs were treated with LY and TGF-β to determine the effects on the protein expression of TGF-β as well as an ECM factor, COL1A1 (Figure 4.1).

There was no observable change in TGF-βRII protein levels in HDFs after any treatment (Figure 4.1A). Lower concentrations of LY had no effect on TGF-β expression, in comparison to the untreated control, until reaching 20μM, where detected levels decreased to 0.36. TGF-β treatment increased detected protein levels to 3.38, and combination treatment decreased these levels back down to 0.27.

The expression levels of a common protein linked to PDACs' characteristic dense desmoplastic stroma and dense ECM, COL1A1, were also analysed (Figure 4.1B). All LY treated groups caused no change in COL1A1 protein expression. TGF-β treatment caused a significant increase in detected protein to 9.51 ($p = 0.005$), which was significantly reduced to 0.43 in combination treatment ($p = 0.004$).

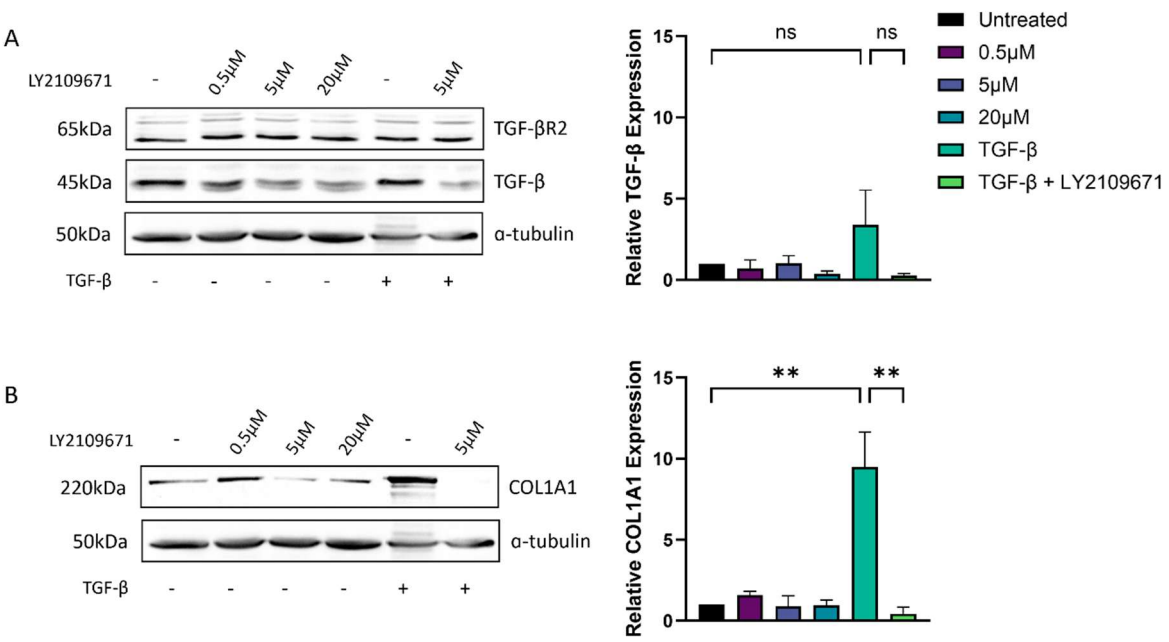


Figure 4.1. LY2109671 prevents the TGF-β induced increase in COL1A1 protein expression in HDF. Protein expression of TGF-βRII, TGF-β, and COL1A1 was analysed in HDF cells after 72 hours of treatment with LY2109671 and/or 5ng/ml TGF-β. α-tubulin was used to determine equal protein loading between lanes. Levels of TGF-β (A), and COL1A1 (B) expression was quantified using ImageLab (BioRad) and normalised to α-tubulin expression before normalisation to the untreated control. Data represents means ± SEM of 2 independent biological replicates. Statistical analyses were performed using one-way ANOVA, with Tukey's multiple comparison test, ** indicates $p < 0.005$.

Quantitative PCR was used to analyse the expression of VEGF-A, TGF-β and COL1A1, COL4A1 and bFGF in HDF cells after 24 hours of treatment with LY and/or TGF-β (Figure 4.2). For both VEGF-A and TGF-β, treatment with LY suppressed gene expression by half, whereas treatment with TGF-β stimulated a 0.84- and 0.33-fold increase in gene expression, respectively (Figure 4.2A). Combination treatment caused a 0.04-fold increase in VEGF-A expression and a 0.45-fold decrease in TGF-β expression; however, none of these changes in mRNA expression was deemed significant.

For the ECM proteins, LY treatment alone caused a decrease in mRNA expression (Figure 4.2B). TGF-β treatment caused minimal 1.10-fold and 0.19-fold increases in COL1A1 and COL4A1 mRNA expression, respectively. This was followed by 0.65-fold and 1.92-fold decreases in the respective mRNA expression levels in the combination treatment groups; however, none of these changes in mRNA expression were deemed significant. mRNA expression of bFGF was significantly increased by 1.26-fold in TGF-β-treated cells ($p = 0.0207$), and in the combination-treated group, the expression levels significantly decreased by 1.08-fold, in comparison to the TGF-β-treated group ($p = 0.0067$).

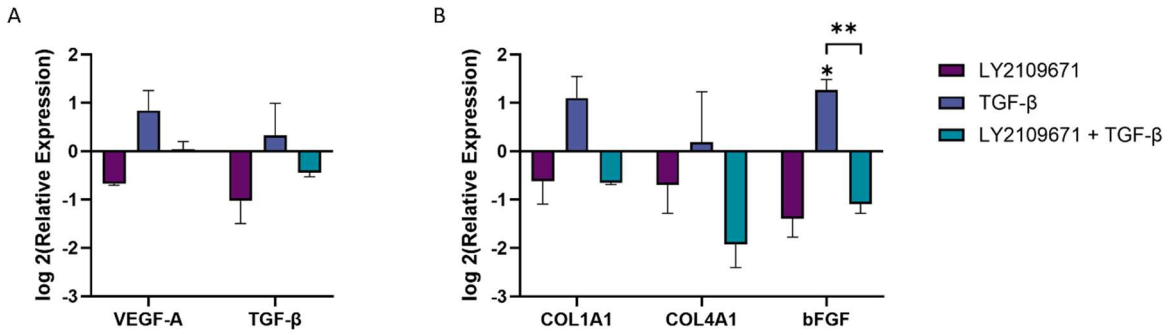


Figure 4.2. LY2109671 inhibits the TGF-β induced increase in bFGF mRNA expression. qPCR measured mRNA expression levels of VEGFA, TGF-β (A), COL1A1, COL4A1 and bFGF (B) after 24 hours of treatments with 5µM LY2109671 and/or 5ng/ml TGF-β. Data was analysed using the $2^{-\Delta\Delta Ct}$ method, with values normalised to GAPDH and presented as the log2(fold change) over the untreated control. Data represents means ± SEM of 2 independent biological replicates. Statistical analyses were performed using one-way ANOVA, with Tukey's multiple comparison test. Non-linked asterisks representing significance in comparison to the untreated control, * indicates $p < 0.05$, and ** indicates $p < 0.005$.

4.2. Pancreatic Cancer Associated Fibroblasts

In addition to HDF, patient-derived CAFs were also utilised in this study to provide a more accurate depiction of fibroblastic behaviour within a PDAC tumour. CAFs were treated for 72 hours with decreasing concentrations of LY, starting at 20μM, and/or TGF-β before being lysed. Western blotting was used to determine changes in protein expression (Figure 4.3).

TGF-βRII expression was constant throughout the treatment groups (Figure 4.3A). There were minimal changes in detected TGF-β protein expression until 5μM of LY, at which point there was a decrease of expression to 0.28. Treatment with TGF-β significantly increased detected expression to 1.61 ($p = 0.03$), before combination treatment with LY significantly decreased detected expression back down to 0.16 ($p < 0.001$).

A similar pattern was observed with COL1A1 expression. LY decreased protein expression in a dose-dependent manner, with 20μM decreasing protein expression to 0.05 (Figure 4.3B). Treatment with TGF-β significantly increased COL1A1 expression to 4.29 ($p < 0.001$), in comparison to the untreated control. This change was reversed in the combination treatment, with COL1A1 expression decreasing to 0.71, which was a significant decrease in comparison to the TGF-β alone treated ($p < 0.001$). LY and TGF-β had no effect on α-SMA protein expression in CAFs (Figure 4.3C).

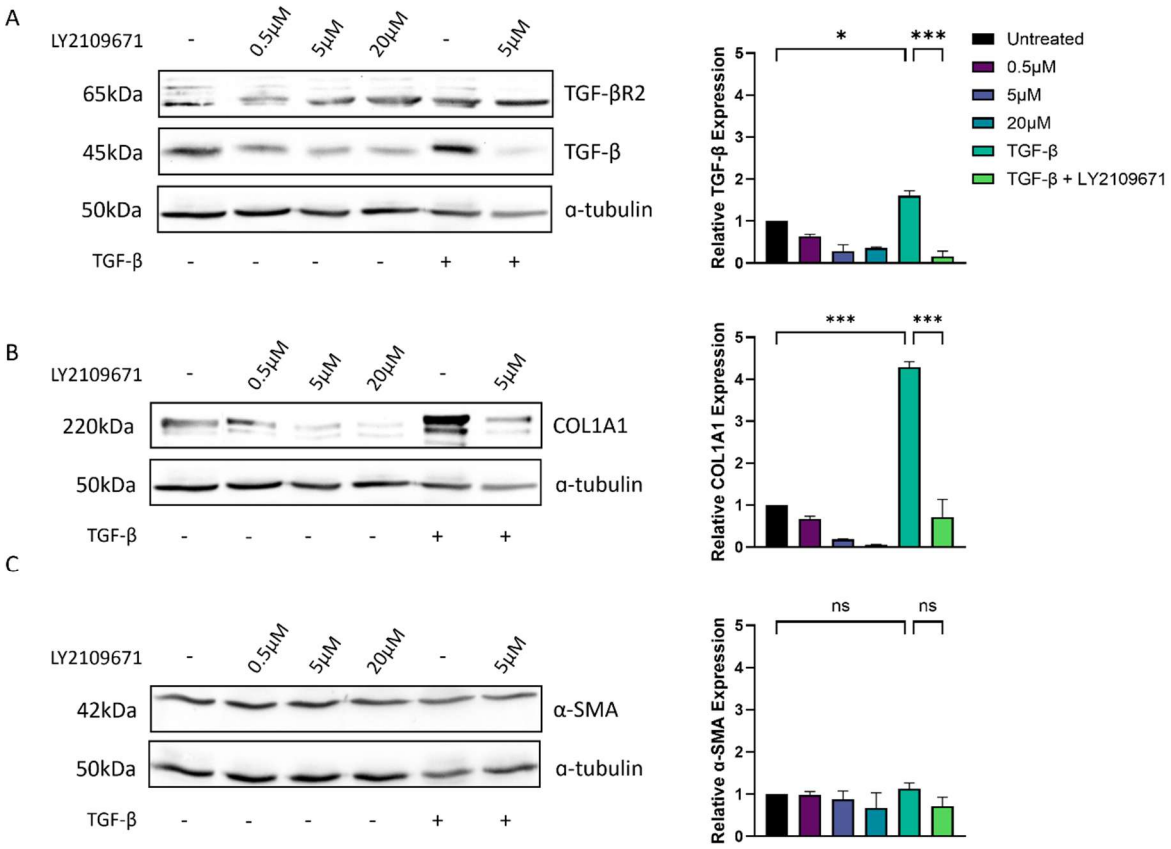


Figure 4.3. LY2109671 prevents the TGF-β induced increase of TGF-β and COL1A1 protein expression. Protein expression of TGF-βRII, TGF-β, COL1A1 and α-SMA were analysed in CAF cells after 72 hours of treatment with LY2109671 and/or 5ng/ml TGF-β. α-tubulin was used to determine equal protein loading between lanes. Levels of TGF-β (A), COL1A1 (B), and α-SMA (C) expression was quantified using ImageLab (BioRad) and normalised to α-tubulin expression before normalisation to the untreated control. Data represents means ± SEM of 2 independent biological replicates. Statistical analyses were performed using a one-way ANOVA with Tukey's multiple comparison test, * indicates $p < 0.05$, and *** indicates $p < 0.001$.

In addition to analysing protein expression, further analysis of changes in mRNA expression after TGF-β and LY treatment was performed. CAF cells were treated with 5μM LY and/or 5ng/ml TGF-β for 24 hours before their RNA was isolated and qPCR was performed, as seen in Figure 4.4.

Initially, VEGF-A and TGF-β mRNA expression levels were analysed (Figure 4.4A). TGF-β treatment had a large effect on the expression of VEGF-A in CAF cells, with the mRNA expression significantly increasing 1.38-fold in comparison to the untreated control ($p = 0.023$). Treatment with TGF-β and LY significantly decreased VEGF-A expression back to the levels in the untreated control ($p = 0.020$). This trend was seen with TGF-β expression with TGF-β treatment causing a non-significant 0.54-fold increase in TGF-β mRNA expression with the combination of LY reducing this change back down to levels seen in the untreated control.

The levels of ECM proteins and bFGF were investigated to analyse the effects of TGF-β on their mRNA expression (Figure 4.4B). Minimal change was observed in mRNA expression of COL1A1, with TGF-β treatment causing a 0.68-fold decrease in expression, which was brought back up to the levels in the untreated control in the combination treatment with LY. COL4A1 expression levels were increased 0.82-fold in TGF-β treatment, with the levels being brought back to untreated control in the combination treatment. Finally, bFGF followed this same pattern, with TGF-β treatment significantly increasing the levels of expression 1.84-fold ($p = 0.031$), in comparison to the untreated control. Once again, the population treated with TGF-β, and LY significantly reduced this increase back to levels seen in the untreated control ($p = 0.024$).

Finally, the expression levels of α-SMA and IL-6, markers of myCAF and iCAF cell populations were analysed to determine if TGF-β or LY influenced the CAF populations seen within the pancreatic TME (Figure 4.4C). α-SMA expression levels with TGF-β treatment caused a significant 1.96-fold increase in expression, in comparison to the untreated control ($p = 0.023$). This was decreased to a 0.27-fold increase combination treated population and was deemed a significant decrease in expression, in comparison to the TGF-β treated population ($p = 0.030$). TGF-β and LY treatment had no effect on IL-6 mRNA expression levels in CAFs.

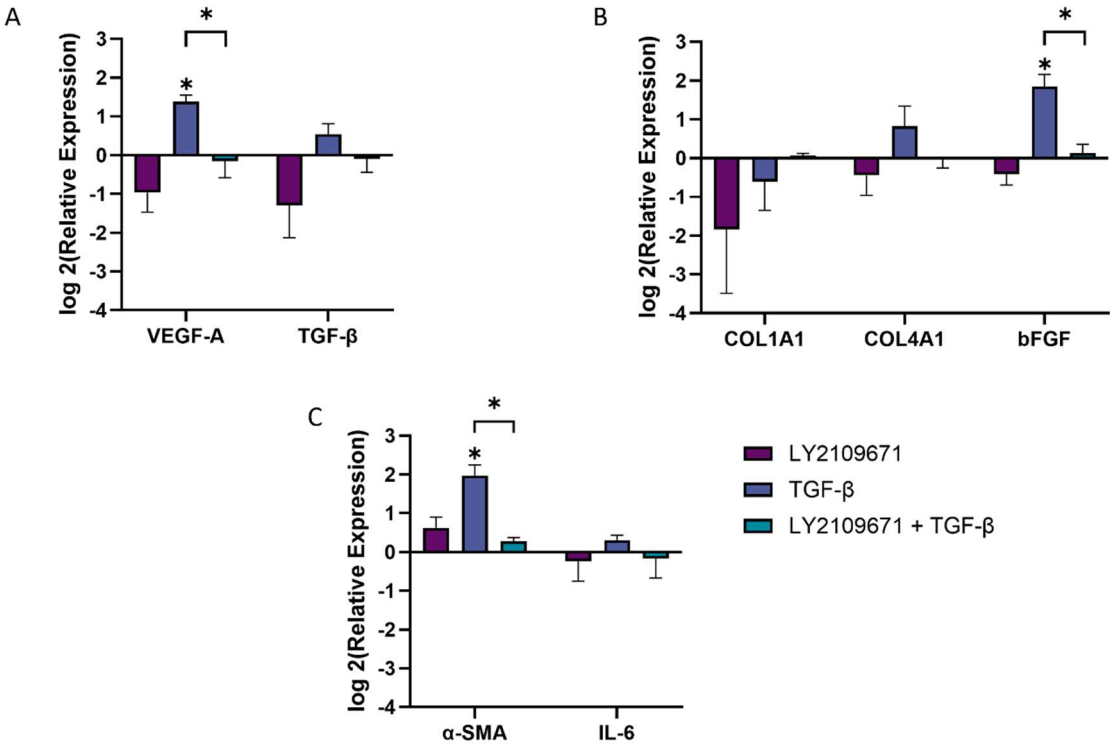


Figure 4.4. TGF-β significantly increased mRNA expression of VEGF-A, bFGF, and α-SMA in CAFs that was reversed by LY2109671. qPCR measured mRNA expression levels of VEGFA, TGF-β in CAF after 24 hours of treatment with 5μM LY2109671 and/or 5ng/ml TGF-β (A). Additional expression levels of mRNA including, COL1A1, COL1A4 and bFGF were analysed after 24 hours of the same treatment as A (B). Two markers for different CAF types, α-SMA and IL-6 were also measured (C). Data was analysed using the $2^{-\Delta\Delta Ct}$ method, with values normalised to GAPDH and presented as the log2(fold change) over the untreated control. Data represents means ± SEM of 2 independent biological replicates. Statistical analyses were performed using a one-way ANOVA with Tukey's multiple comparison test, * indicates $p < 0.05$.

5. Inhibiting TGF-β signalling affects HUVEC morphology and the formation of blood vessels in co-cultures

5.1. The effect of TGF-β signalling on HUVECs

To further expand and build upon the effect of TGF-β inhibition on other cell lines, HUVECs were used to explore this effect on endothelial cell and blood vessels in the PDAC TME. HUVECs were treated for 72 hours with varying concentrations of LY and/or 5ng/ml TGF-β before being lysed and used for western blotting, when protein levels were then quantified (Figure 5.1).

There was a decrease in TGF-βRII expression in HUVECs treated with the higher concentrations of LY (Figure 5.1A). As seen with most other cell lines in this study, LY reduced the detected TGF-β protein expression in HUVECs, with the lowest concentration of 0.5μM decreasing protein expression to 0.42. TGF-β treatment increased detected protein expression to 1.49, before combination treatment with LY significantly reduced protein expression to 0.24 ($p = 0.01$).

HUVECs were treated for 24 hours before RNA isolation. There was very minimal change seen in VEGF-A and TGF-β mRNA expression after any treatment type (Figure 5.1B). All treatments caused a 0.49- to 0.87-fold decrease in VEGF-A expression, with TGF-β expression also decreasing in all treatment groups, with LY treatment decreasing it further, causing a roughly 1.2-fold decrease in both groups with LY treatment.

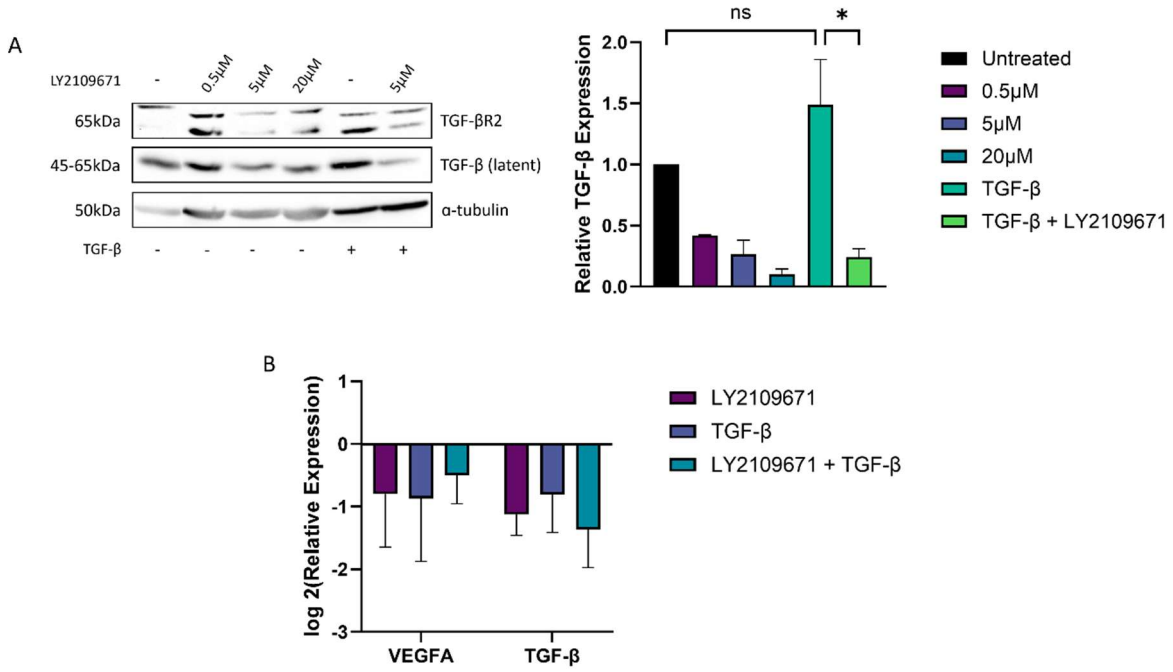


Figure 5.1. LY2109671 inhibits the TGF-β induced increase in detected protein expression in HUVECs. Protein expression of TGF-βRII and TGF-β were analysed in HUVECs after 72 hours of treatment with LY2109671 and/or 5ng/ml TGF-β. α-tubulin was used to determine equal protein loading between lanes. Levels of TGF-β (A) expression was quantified using ImageLab (BioRad) and normalised to α-tubulin expression, before normalisation to the untreated control. Data represents means ± SEM of 2 independent biological replicates. Statistical analyses were performed using one-way ANOVAs with Tukey's multiple comparison test, * indicates $p < 0.05$. qPCR measured mRNA expression levels of VEGFA, TGF-β in HUVECs after 24 hours of treatment with 5μM LY2109671 and/or 5ng/ml TGF-β (B). Data was analysed using the $2^{-\Delta\Delta Ct}$ method, with values normalised to GAPDH and presented as the log2(fold change) over the untreated control. Data represents means ± SEM of 2 independent biological replicates. Statistical analyses were performed using a one-way ANOVA with Tukey's multiple comparison test.

After assessing protein and mRNA expression changes in HUVECs, immunofluorescence was used to determine if there were any changes in morphology after TGF-β inhibition.

HUVECs were treated for 48 hours with different concentrations of LY to compare morphological differences against an untreated control (Figure 5.2). After treatment, cells were fixed and stained with CD31 and DAPI to visualise any morphological changes. In the untreated HUVEC population, HUVECs are spread widely and clump together, with cells taking on circular shapes (Figure 5.2A). In the 5µM treated population, HUVECs have spread out more, with cells starting to have a longer, less spherical shape. This pattern is seen even further in the 20µM treated group, with HUVECs exhibiting an increased length: width ratio.

The pixel intensity of each condition's images was measured with ImageJ to determine if TGF-β inhibition had any effect on CD31 expression in HUVECs (Figure 5.2B). There were no significant differences in CD31 expression in comparison to the control, with the 10µM condition reducing the expression levels the most to 0.84.

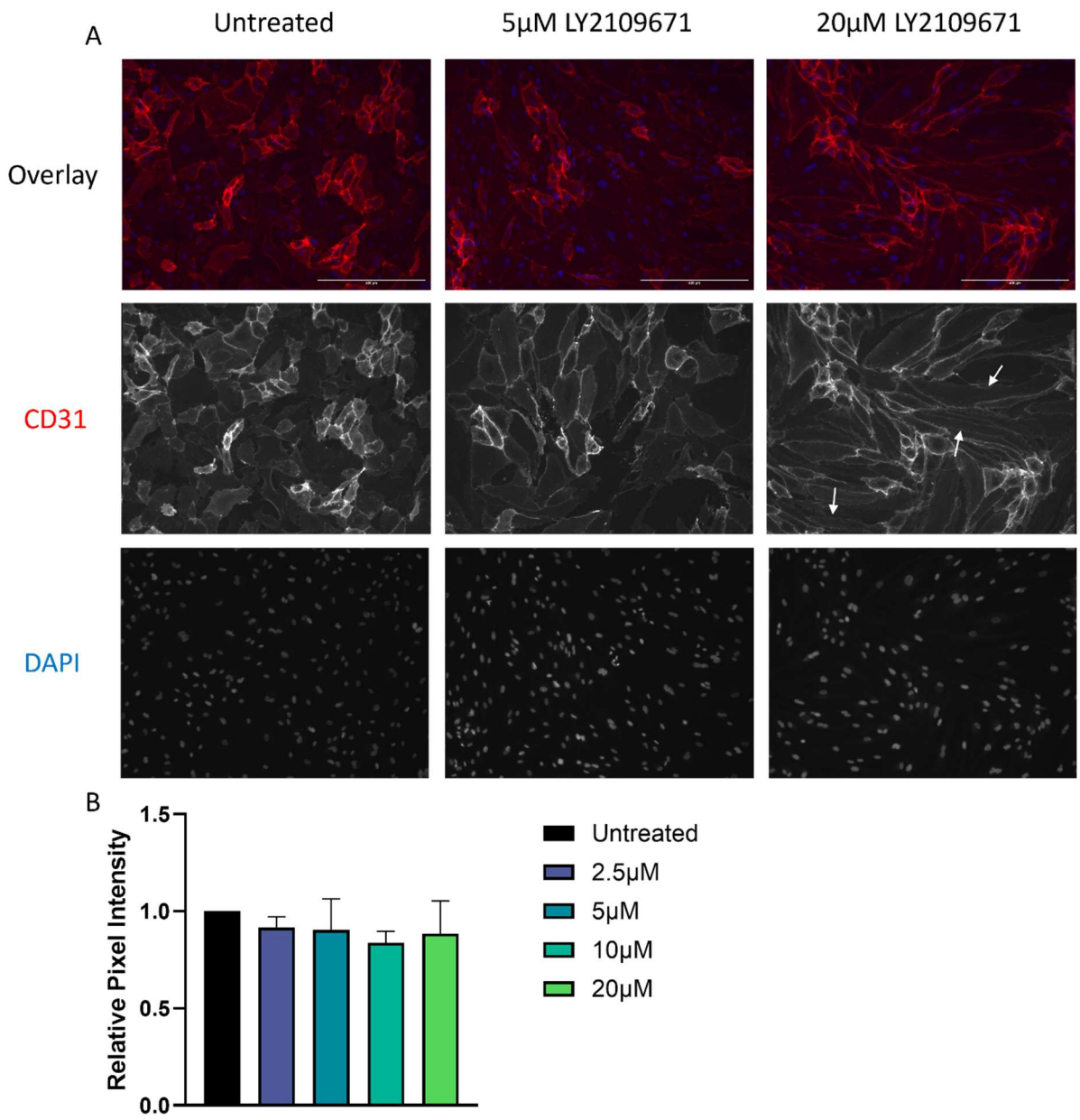


Figure 5.2. 48-hour LY2109671 treatment changes the morphology of HUVECs after treatment but has no impact on CD31 expression. HUVECs were grown in untreated media (left), or treated with 5µM (middle) and 20µM (right) of LY2109671 for 48 hours before staining for CD31 (red) and DAPI (blue) (A). Top row shows representative overlay images, middle row shows CY5 (CD31) channel alone, with elongated cells indicated with white arrows, bottom row shows DAPI nuclear stain alone. Scale bar = 400µM. Pixel intensity was measured using ImageJ and normalised to the untreated control (B). Statistcial analyases were performed with a one-way ANOVA with Tukey's multiple comparison test.

The study then extended the treatment time to 72 hours to determine if a longer treatment time had a harsher effect on the morphological effects on the HUVECs (Figure 5.3). After treatment, cells were fixed and stained with CD31 and DAPI to visualise any morphological changes. In the untreated HUVEC population, HUVECs are spread widely and clump together, with cells taking on circular shapes (Figure 5.3A). Very similar morphological differences were seen at 72 hours as well as during the 48-hour treatment period. The untreated cells exhibited the same structure, with lots of circular cells close together. In the 5µM treated population, HUVECs have spread out and taken on a more elongated shape. This pattern is seen even further in the 20µM treated group, with HUVECs exhibiting an increased length: width ratio.

Once again, the pixel intensity was measured with to determine if TGF-β inhibition had any effect on CD31 expression in HUVECs with a 72-hour treatment time (Figure 5.2B). There were no significant differences in CD31 expression in comparison to the control, with the 20µM condition reducing the expression levels the most to 0.80.

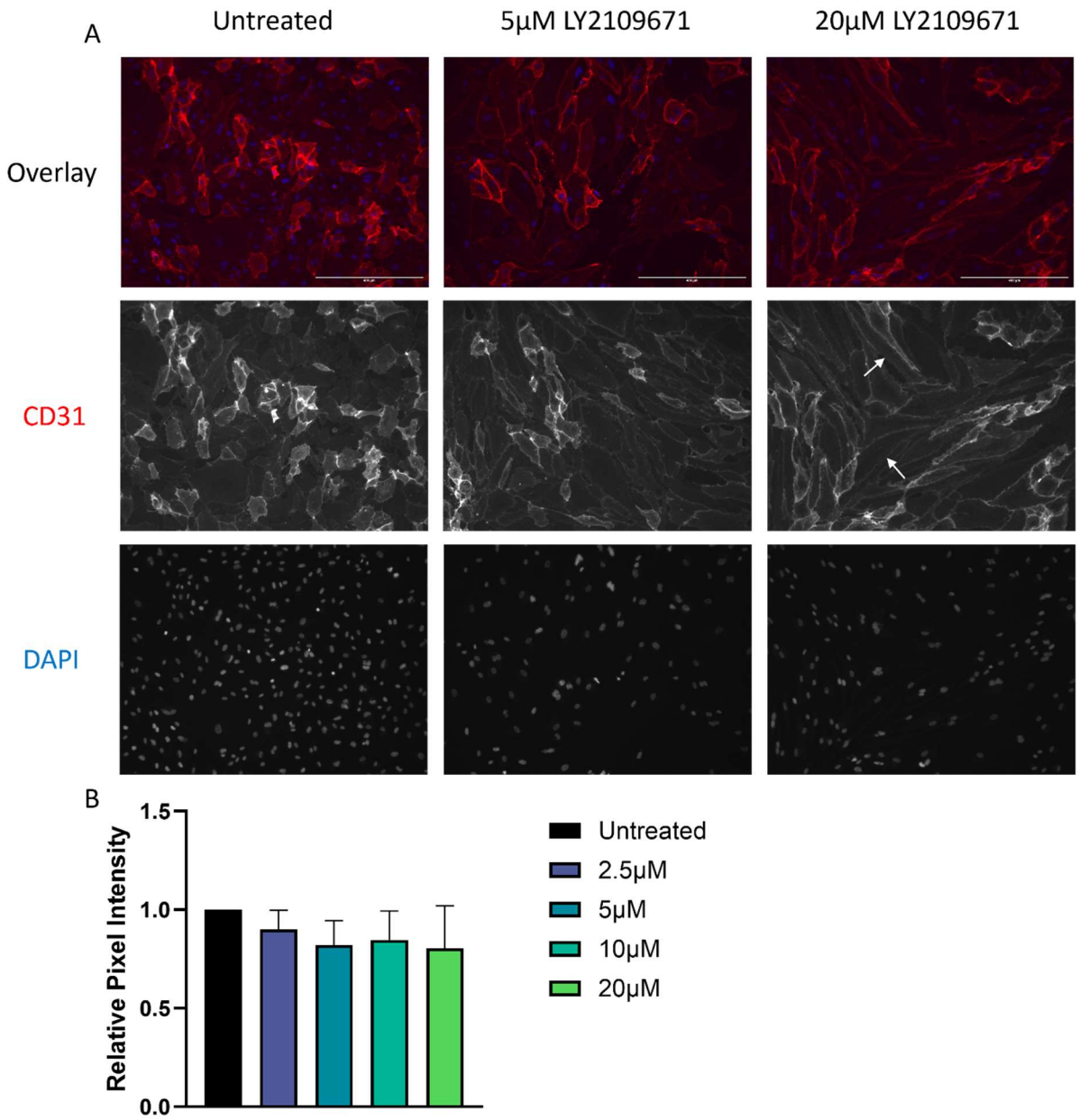


Figure 5.3. 72-hour LY2109671 treatment changes the morphology of HUVECs after treatment but has no impact on CD31 expression. HUVECs were grown in untreated media (left), or treated with 5µM (middle) and 20µM (right) of LY2109671 for 72 hours before staining for CD31 (red) and DAPI (blue) (A). Top row shows representative overlay images, middle row shows CY5 (CD31) channel alone, with elongated cells indicated with white arrows, bottom row shows DAPI nuclear stain alone. Scale bar = 400µM. Pixel intensity was measured using ImageJ and normalised to the untreated control (B). Statistcial analyases were performed with a one-way ANOVA with Tukey's multiple comparison test.

5.2 HDF Angiogenesis Assays

To finally investigate the effect of TGF-β inhibition on vessel formation within a PDAC TME environment, this study used co-cultures with the two fibroblast cell types and endothelial cells.

There are 2 main types of structures that are formed from the co-culture angiogenesis assay, which are a vessel or a blood island (Figure 5.4). These vessel structures are made up of connected HUVEC cells that have formed into a capillary-like vessel (Figure 5.4A). Blood islands are typically seen before this formation into a vessel, demonstrating the HUVECs coming together but not yet formed into a vessel (Figure 5.4B).

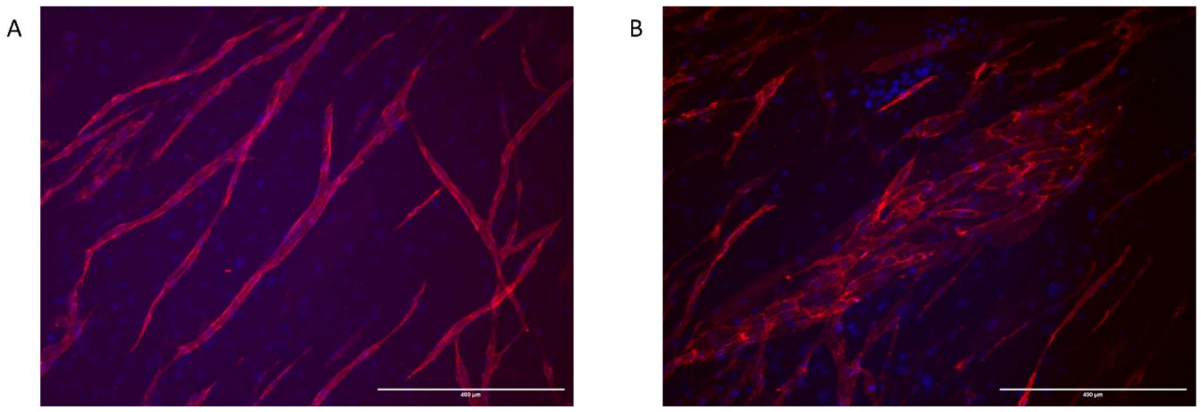


Figure 5.4. Co-cultures of fibroblasts and HUVECs can produce vessels or blood islands. CAFs and HUVECs were cultured together for 10 days before being stained with CD31 (red) and DAPI (blue). Co-culture media was changed every 2-3 days with untreated media to produce an example of vessels (A), and co-cultures with media containing 5µM LY210671 produced an example of a blood island (B). Scale bar = 400µM.

HDFs were used initially to demonstrate the general effect of the angiogenesis assays with and without VEGF-A, TGF-β, and LY treatment, in a way that was non-specific to the PDAC TME. HUVECs were cultured with the HDF cells for 10 days, and the co-cultures were treated with combinations of VEGF-A, TGF-β, and LY for 6 days before staining with CD31 and imaging (Figure 5.5). Co-cultures with HDF and HUVECs were shown to have lots of shorter vessels, with less branching seen, as well as blood islands. Co-cultures were treated individually or in combination with VEGF-A and TGF-β (Figure 5.5A) and with or without LY (Figure 5.5B) to analyse the differences in vessel formation. The immunofluorescent images showed an increase in the number of vessels in VEGF-A treated co-cultures, with very small blood islands being predominantly produced in the TGF-β-treated co-cultures.

The images were analysed through AngioTool to measure the total vessel length (Figure 5.5C), and the number of branch points (Figure 5.5D) within each condition, with the final values being normalised to the untreated control. The VEGF-A treated population increased the total vessel length and number of branch points to 1.38 and 2.03, respectively. Treatment with TGF-β decreased the total vessel length to 0.90 and the number of branch points to 0.75. The combination of VEGF-A and TGF-β, as well as the individual treatment with LY, had similar effects on both factors. The addition of LY to the TGF-β-treated co-cultures increased the number of branch points to 2.17 and the total vessel length to 1.21, however, there were no significant differences in total vessel length or the number of branch points detected in any condition.

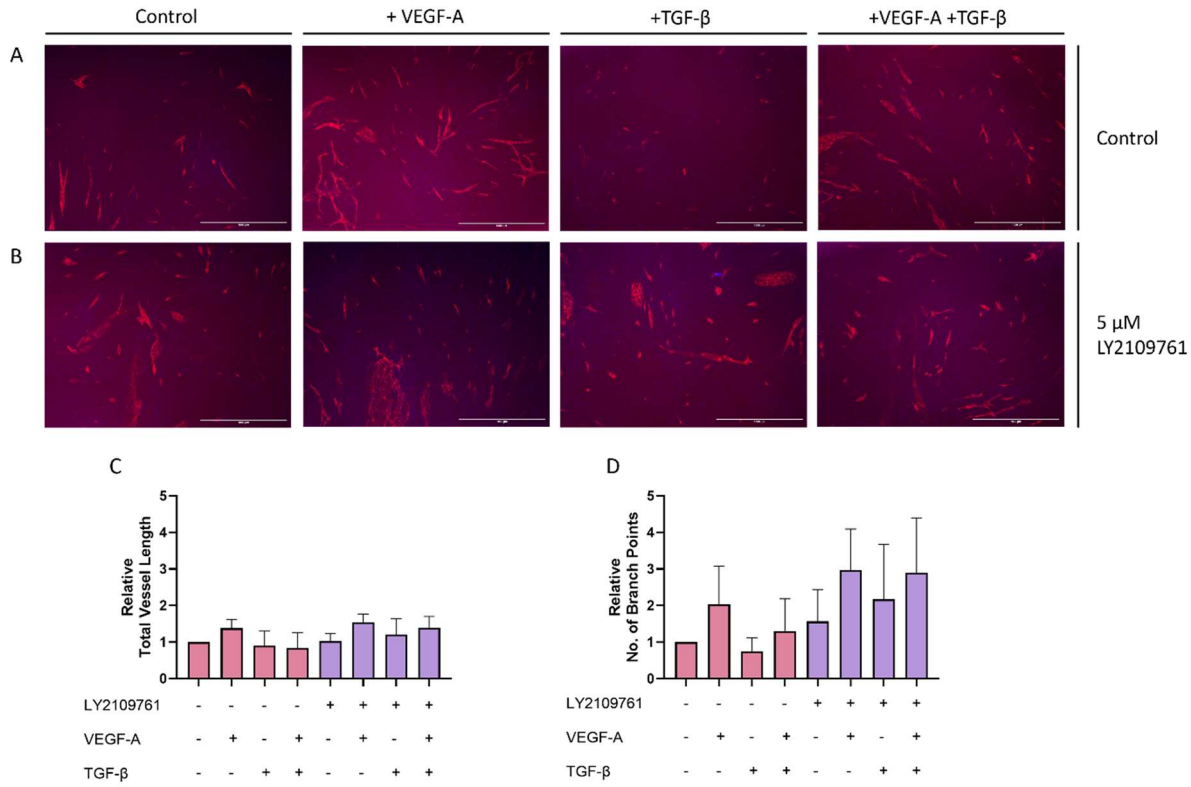


Figure 5.5. LY2109671 prevents the effect of TGF-β on total vessel length and the number of branch points in HDF and HUVEC co-cultures. Co-cultures of HDF and HUVEC were stained for CD31 (red) after 10 days of growth. Co-cultures were treated with 5ng/ml VEGF-A or TGF-β (A) and 5µM LY2109671 (B) for 6 days before staining. Scale bar = 1000µM. Total vessel length (C) and number of branch points (D) were analysed using AngioTool and normalised to the untreated control. Data represents means ± SEM of 4 technical replicates within 3 biological replicates. Statistical analyses were performed using one-way ANOVAs with Tukey's multiple comparison test.

To create a more accurate depiction of the PDAC TME, PDAC cell media was collected and used in the co-culture experiments. This allowed investigation into whether the growth factors produced by PC cells influence the formation of vessels in HDF and HUVEC co-cultures.

HUVECs were cultured with the HDF cells for 10 days, and the co-cultures were treated with combinations of VEGF-A, TGF-β, and LY in non-conditioned media or conditioned media, containing media from 70-80% confluent Panc1 cells. Panc1 cells were chosen due to their lack of mutations within the TGF-β signalling pathway and being the most susceptible to TGF-β stimulation and inhibition. Co-cultures were treated for 6 days before staining with CD31, imaging and measuring total vessel length and number of branch points in AngioTool. All values were then normalised to the non-conditioned media untreated control (Figure 5.6).

Conditioned media had no significant effect on total vessel length in these co-cultures (Figure 5.6A). A minimal increase in total vessel length was seen with TGF-β treatment in both groups, with relative total vessel length increasing to 1.46 in non-conditioned media and 1.11 in conditioned media. In all groups containing LY, total vessel length increased to over 2.00, but no increase was deemed significant.

The number of branch points was also analysed in these co-cultures (Figure 5.7B). There was a non-significant decrease in the number of branch points to 0.55 in conditioned untreated media. This pattern was also seen in the TGF-β treated group, with the conditioned media group having a smaller number of branch points in comparison to the non-conditioned media group. All groups treated with LY increased the number of branch points to 1.50, with no difference between media types.

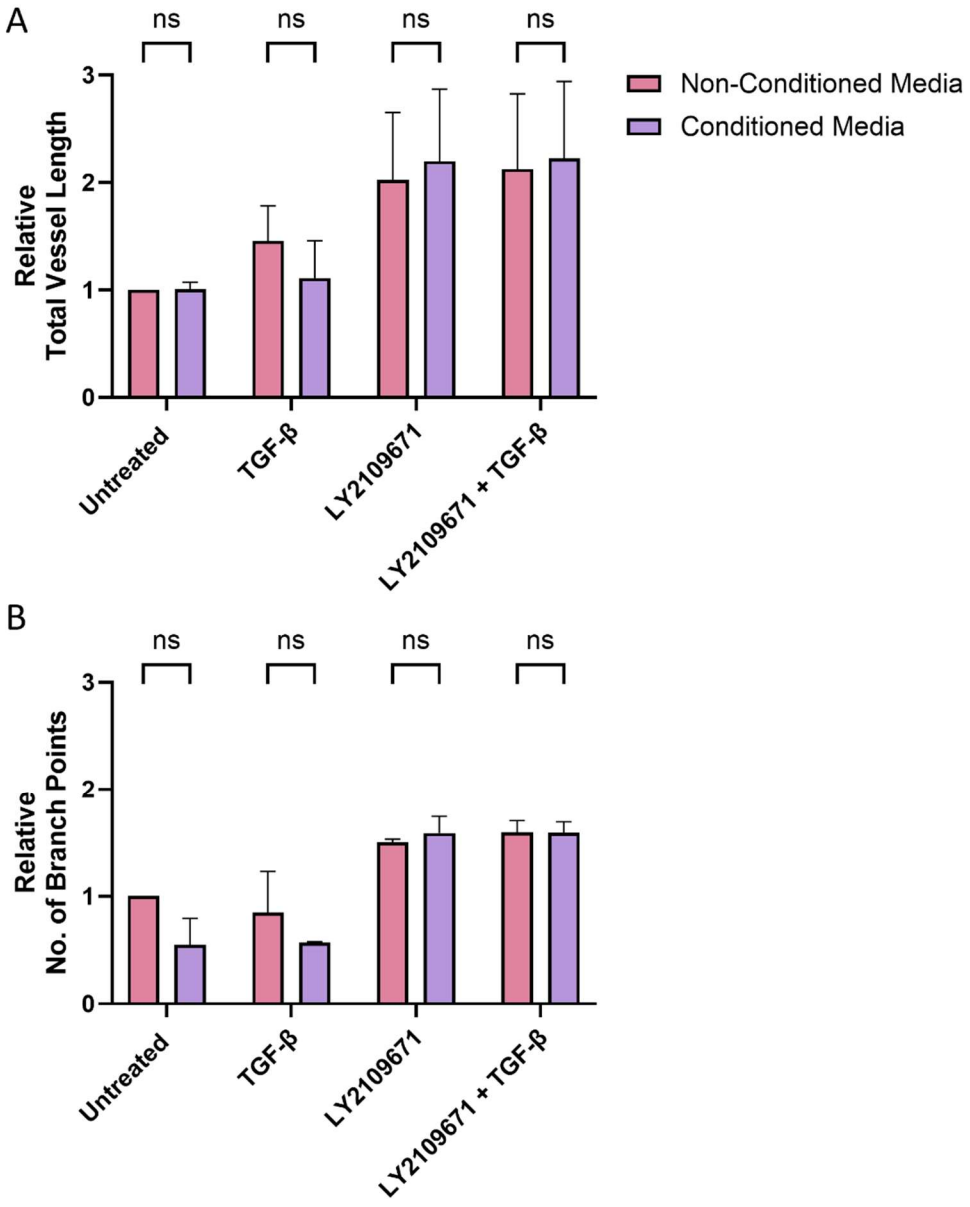


Figure 5.6. PDAC cell conditioned media had no effect on vessel formation in HDF and HUVEC co-cultures. HDF and HUVEC co-cultures were grown together for 10 days. Culture media from Panc1 cells was used for conditioned media condition 1:1 with ECGM. Non-conditioned media consisted of a 1:1 mix of DMEM and ECGM. Co-cultures were treated with TGF-β and/or LY for 6 days before fixation, staining with CD31 and imaging. Images were analysed with AngioTool to measure total vessel length (A), and number of branch points (B). Values normalised to non-conditioned media untreated control. Data represents means ± SEM of 3 technical replicates within 2 biological replicates. Statistical analyses were performed using one-way ANOVAs with Tukey's multiple comparison test.

5.3 CAF Angiogenesis Assays

After observing the effect of TGF-β in co-cultures with HDF cells, further investigation was performed to determine if this effect would be seen in co-cultures containing CAFs that had been isolated from PDAC patient tumours. HUVECs were cultured with the CAF cells for 10 days, and the co-cultures were treated with combinations of VEGF-A, TGF-β, and LY for 6 days before staining with CD31 and imaging (Figure 5.7).

Within the CAF co-cultures, there were larger networks of tubules formed in the untreated controls, with VEGF-A having little effect on vessel formation in these co-cultures (Figure 5.7A). Treatment with TGF-β largely inhibited the formation of tubules, and this effect was also seen in the VEGF-A and TGF-β treated population. LY treatment alone increased vessel formation in these co-cultures and was able to reverse the effects to TGF-β treatment when used in combination (Figure 5.7B).

These patterns were further seen once quantified; CAF co-cultures showed similar levels of total vessel length in comparison to the VEGF-A treated group (Figure 5.7C). CAF co-cultures exhibited a larger number of branch points in the untreated co-cultures, in comparison to the VEGF-A-treated, with the number of branch points in the VEGF-A-treated being 0.73 (Figure 5.7D). The addition of TGF-β to the co-cultures reduced the number of branch points to 0.53 and the total vessel length to 0.77. Treatment with LY increased the total vessel length and number of branch points in all populations used. Particularly in combination treatment with TGF-β and LY significantly increased the total vessel length to 1.43 ($p = 0.01$), and the number of branch points to 1.54 ($p = 0.01$), in comparison to the only-TGF-β-treated co-cultures.

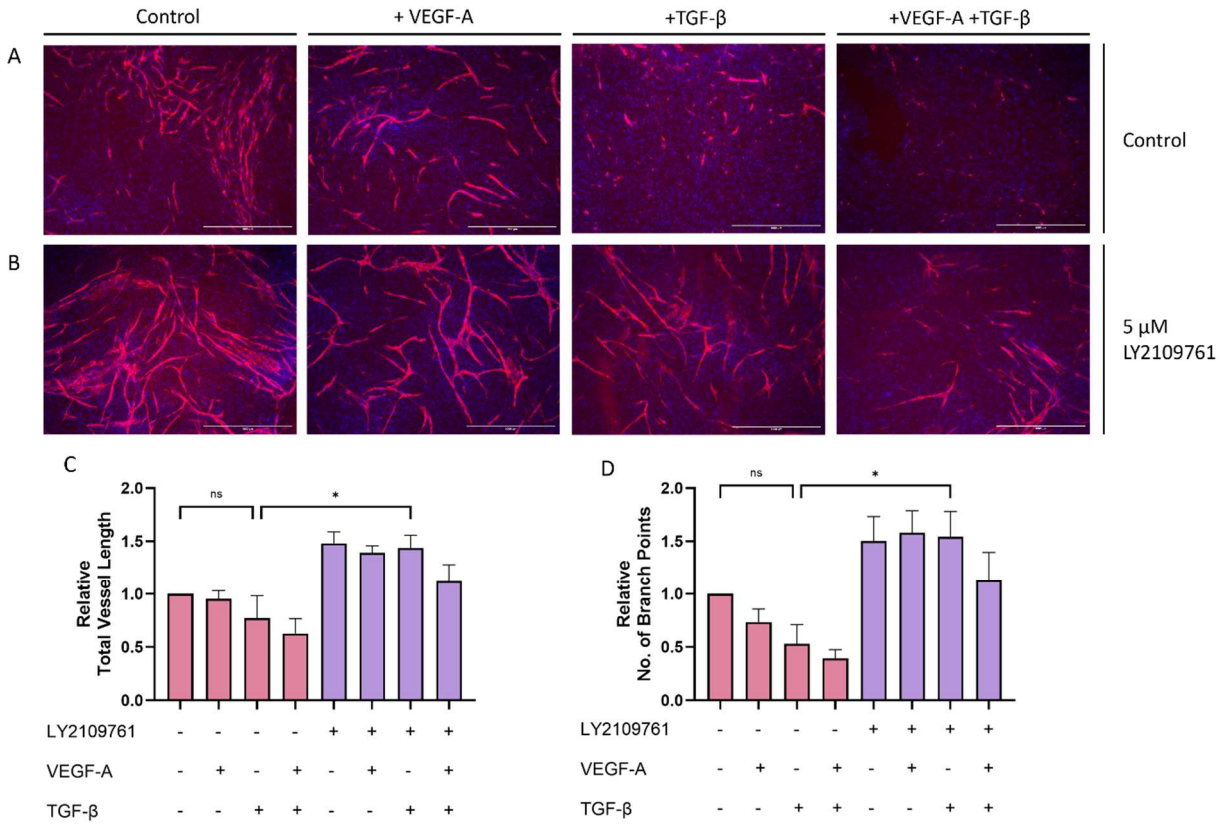


Figure 5.7. LY2109671 reverses the effect of TGF-β on total vessel length and the number of branch points in CAF and HUVEC co-cultures. Co-cultures of CAF and HUVEC were stained for CD31 after 10 days of growth. Co-cultures were treated with 5ng/ml VEGF-A or TGF-β (A) and 5μM LY2109671 (B) for 6 days before staining. Scale bar = 1000μM. Total vessel length (C) and number of branch points (D) were analysed using AngioTool and normalised to the untreated control. Data represents means ± SEM of 4 technical replicates within 5 biological replicates. Statistical analyses were performed using one-way ANOVA with Tukey's multiple comparison test, * indicates $p < 0.05$.

6. Discussion

In this study, TGF-β signalling was investigated as a potential inhibitory target in PDAC to normalise vasculature and improve the effect of chemotherapy in patients. The main objectives of this study were to show the effect of TGF-β inhibition in PDAC cell lines, before expanding this investigation into additional cell types enriched within the TME, including fibroblasts and endothelial cells. Finally, co-cultures with two types of fibroblasts used together with HUVECs to analyse the effect of TGF-β and its inhibition on the formation of vasculature.

6.1 TGF-βR inhibitors LY2109671 and SB431542 reduce PDAC cell line viability and reduce the phosphorylation of SMAD2/3

The three PDAC cell lines were chosen due to their mutational and structural differences. Panc1 cells have no identified alterations in the TGF-β signalling pathway, the MiaPaCa2 cell line responds poorly to TGF-β, due to low expression of TGF-βRII, and BxPc3 cells have a homologous deleted *SMAD4* gene, a key signalling molecule in the TGF-β pathway (Principe et al. 2022). Three TGF-β inhibitors were initially used on these cell lines and included LY2109671 (LY), a selective dual TGF-βRI and II inhibitor, SB431542 (SB), a TGF-βRI kinase inhibitor and dexamethasone (DEX), a corticosteroid that inhibits TGF-β downstream signalling pathways.

MTT assays were performed with the three inhibitors, on the three PDAC cell lines to test the inhibitors initial toxicity (Figure 3.1). After inhibition treatment, Panc1 cells were the most sensitive to the three inhibitors, exhibiting the lowest IC50's and all inhibitors displaying a dose-dependent decrease in viability. LY demonstrated this same decrease in the other two cell lines, and SB has a similar effect in BxPc3 cells. In MiaPaCa2 cells, SB had minimal effect on viability until higher concentrations of 50μM were reached, and DEX had no effect on viability at any concentration examined. DEX had a similar effect on BxPc3 cells, with viability decreasing to 92% at its highest concentration.

TGF-β signalling is linked to cell proliferation and growth, and targeting this signalling pathway can affect the growth of PDAC cell lines. Previously, blocking TGF-β signalling in human derived PDAC cell lines with a neutralising anti-human TGF-β antibody, significantly decreased cell viability, suggesting that TGF-β signalling is linked to cell growth and survival in PDAC (Ligorio et al. 2019). One of the signalling pathways that TGF-β contributes to, canonically and non-canonically, is the extracellular signal regulated kinase (ERK) signalling pathway which in

oncogenic cells, accelerates tumour formation through enhancing cell proliferation (Neuzillet et al. 2013; Principe et al. 2021). Previously, removing TGF-β receptor signalling in mice has been shown to lower ERK activation, indicating TGF-β signalling is required for this process and has an integral role in cell proliferation and growth (Principe et al. 2017). Additionally, SB has been used in Panc1 cells previously and was shown to inhibit the TGF-β-induced increase in cell viability (Ye et al. 2025). Through blocking TGF-βRI and II, this study demonstrated that inhibiting TGF-β signalling decreased pancreatic cancer cell viability, with Panc1 cells being the most sensitive to LY and SB treatment of the three cell lines tested.

The deletion of SMAD4 in PDAC cells can dramatically change the role and function of TGF-β in tumour growth and development, as this signalling protein has a key role in the TGF-β canonical signalling pathway. SMAD4 deficient cell lines have previously been shown to have hyperactivated ERK and AKT signalling pathways (Chen, Y.-W. et al. 2014). The less sensitive response to LY in BxPc3 cells, could be explained by their homologous deletion of SMAD4 and hyperactive ERK pathway. This requires more TGF-β signalling suppression before the prevention of cell proliferation and growth. In SB treatment, BxPc3 cells exhibit a similar response to Panc1 cells. The response of SB for 24-hour treatments has been compared between SMAD4-deficient and wild-type cell lines previously, showing a non-significant decrease in cell viability in SMAD4 wild-type cell lines in comparison to the SMAD4-deficient cell lines, which is similarly seen in this study (Chen, Y.-W. et al. 2014).

With LY treatment, MiaPaCa2 cells exhibited a similar effect to Panc1 cells, demonstrating a similar IC50 and dose-dependent response to cell viability. Despite this, MiaPaCa2 cells were the least sensitive of the three cell lines to SB treatment, with significant differences in viability only occurring at concentrations of 50μM and above. Previously, MiaPaCa2 cells have been shown to lack or exhibit faulty TGF-βRII (Freeman et al. 1995; Ungefroren et al. 2024). As MiaPaCa2 cells demonstrated a less sensitive response to SB in comparison to LY, it would suggest that the MiaPaCa2 cells used in this study have a more functional TGF-βRII than previously described. Despite this argument TGF-β was unable to cause the phosphorylation of SMAD2/3 in MiaPaCa2 cells in this study (Figure 3.3), meaning further investigation into the TGF-βRII status in the used MiaPaCa2 cells would need to be investigated.

Treatment with DEX exhibited minimal effect on the three PDAC cell lines, with no IC50s able to be calculated. DEX is a corticosteroid used in the treatment of many inflammatory conditions. It has been investigated for its effect in many cancers as its anti-inflammatory properties can decrease inflammatory responses and reduce cancer treatment side effects (Madamsetty et al. 2022). It targets TGF-β signalling through suppression of SMAD3 transcriptional activity but does not inhibit the phosphorylation of SMAD2/3 (Song et al. 1999; Iu et al. 2005). Previously, DEX has been used to treat PDAC patients who underwent a pancreaticoduodenectomy and was found to significantly improve OS and prevent tumour growth with Panc1 cells (Sandini et al. 2018; Yao, Y. et al. 2020). Despite this, DEX has also been shown to enhance tumour proliferation, which was seen in this study at lower concentrations with slightly increased BxPc3 and MiaPaCa2 viability (Liu, L. et al. 2017).

After initial viability testing, the three inhibitors were tested for exposure at a concentration less than the IC75 for each cell line, which was chosen to be 5µM. In addition to assessing viability at 5µM, the inhibitors were assessed for the effectiveness of inhibiting the phosphorylation of SMAD2/3 in Panc1 cells, the most sensitive cell line and the cell lines with no alterations to the TGF-β pathway (Figure 3.2). LY had the greatest effect on cell viability, in comparison to the other two inhibitors, without dramatically reducing cell viability. LY also had the greatest effect on the phosphorylation of SMAD2/3, supporting its use throughout the remainder of the study.

Finally, LY was used to assess the effect of TGF-β and its inhibition of SMAD2/3 phosphorylation in the three PDAC cell lines (Figure 3.3). TGF-β successfully induced the phosphorylation of SMAD2/3 in Panc1 and BxPc3 cells at 5µM, with LY successfully inhibiting this effect. In MiaPaCa2 cells, TGF-β stimulation did not induce SMAD2/3 phosphorylation, with no p-SMAD2/3 protein being seen in any condition. This observation indicates not only that MiaPaCa2 cells have a potential non-functional TGF-βRII but there are additional faults within the cell line that prevents TGF-β signalling and phosphorylation of SMAD2/3, an effect that has been reported previously (Simeone et al. 2000).

6.2 TGF-β suppression reduces TGF-β protein and mRNA expression in PDAC cell lines

To determine the effect of TGF-β signalling on PDAC cells and its effect on TME structure and blood vessels, TGF-β protein and mRNA expression were evaluated in the three cell lines.

TGF-β treatment significantly increased the detected protein levels of TGF-β in Panc1 cells, with a similar, increase seen in the BxPc3 cells. The increase in detected protein expression seen with TGF-β treatment, was reversed when cells were additionally treated with LY (Figure 3.4). This pattern in Panc1 and BxPc3 cells was also supported through analysis of changes in mRNA expression, with TGF-β stimulation increasing the mRNA expression of TGF-β, before combination treatment with LY, which reversed this increase (Figure 3.5).

Within cells, the release of TGF-β requires production of the latent version of TGF-β, where the active growth factor is bound to a latency-associated protein. This complex is further bound to latent TGF-β binding proteins (LTBP) in the endoplasmic reticulum prior to release into the ECM (Robertson, I.B. and Rifkin 2016). These binding proteins influence the receptor binding activity of TGF-β and must be removed to release the active TGF-β molecule necessary for its receptor activation (Robertson, I.B. et al. 2015). It has previously been shown that TGF-β increased the expression and production of LTBPs in lung fibroblasts (Ahmed, W. et al. 1998). As TGF-β has been shown to contribute to transcriptional regulation of its binding proteins, it could also be a controller of its own expression.

There have been many reports of TGF-β being able to induce its own mRNA expression in cartilage, renal glomerular cells, and osteoblast-like cells (Dallas et al. 1994; Kato, M. et al. 2011; Wang, T. et al. 2024). Many studies stimulated cells with TGF-β and observed both increased mRNA levels and increased levels of latent TGF-β (~45kDa) indicating this detected TGF-β was newly synthesised, similarly to the TGF-β detected in this study (Kelley et al. 1993; Dallas et al. 1994; Wang, T. et al. 2024). It has been reported previously that this autoinduction of TGF-β is mediated by the AP-1 complex, a group of transcription factors that control cell cycle, proliferation, apoptosis and autophagy and are implicated in cancer and its development (Kim, S.-J. et al. 1990; Wu, Z. et al. 2021).

In addition to autoinduction of TGF-β in many non-cancerous cell types, this process is also observed in various cancers including, gastric and breast cancer, and has been inhibited through blocking SMAD3-mediated autoinduction (Li, N.S. et al. 2016; Zou, J. et al. 2021). In cancer, the positive feedback loop created by TGF-β autoinduction leads to the accumulation of TGF-β within the TME, promoting further angiogenesis, EMT, migration and invasion (Zhang et al.

2014; Witte et al. 2016). This positive feedback loop could be a good target for PDAC treatment, to alter the TME and reduce metastasis.

Panc1 and BxPc3 cells did exhibit similar effects in response to TGF-β, despite BxPc3 cells lacking SMAD4, a key signalling molecule within the TGF-β canonical signalling pathway. It is unclear as to whether the TGF-β autoinduction seen is caused by the canonical or non-canonical signalling pathway. As BxPc3 cells lack this key canonical signalling molecule but still demonstrate TGF-β autoinduction, it would imply the production of latent TGF-β is stimulated from the non-canonical signalling pathway (Hariyanto et al. 2021). In contrast, it has been previously shown that in the absence of SMAD4, SMAD2 and SMAD3 are able to mediate the oncogenic effects of TGF-β, which could be how BxPc3 cells show the capability for autoinduction (Bertrand-Chapel et al. 2022).

There was no effect of TGF-β stimulation seen in MiaPaCa2 cells with regards to detected TGF-β protein and mRNA expression. Once again this could be caused by the reported faulty TGF-βRII seen within this cell line. It has previously been reported that mutations within TGF-βRII, cause a loss of sensitivity to TGF-β (Sun, L. et al. 1994; Luo, K. and Lodish 1997). This may provide an explanation for the observations seen within this current study, where MiaPaCa2 cells failed to demonstrate TGF-β autoinduction.

In addition to evaluation of TGF-β-induced TGF-β mRNA and protein expression, the effect of TGF-β stimulation on the production of VEGF-A in PDAC cell lines was also explored. This was to determine if PDAC cells could further influence angiogenesis and blood vessel formation within a pancreatic tumour through TGF-β signalling. There were no significant changes in VGEF-A mRNA expression observed in any cell lines examined, with Panc1 cells showing a minimal increase in expression following TGF-β stimulation, MiaPaCa2s showing an increase in expression in all three conditions, and LY and TGF-β treatments inducing VEGF-A increase in BxPc3 cells.

TGF-β has prominent roles in regulating the expression of angiogenic factors, such as VEGF-A, and has previously been shown to increase the release of VEGF-A without substantial upregulation of VEFG-A mRNA expression (Sánchez-Elsner et al. 2001; Zhou, Q. et al. 2019). This lack of substantial effect on mRNA expression is similar to what was observed here. As such, further investigations into whether TGF-β influences the release of VEGF-A from PDAC cell lines

would need to be performed to gain a wider understanding of the consequences of TGF-β stimulation and inhibition on the release of growth factors from PDAC cells.

6.3 TGF-β suppression prevents expression of ECM proteins and TGF-β in fibroblastic cell lines

In addition to investigating the effect of TGF-β inhibition on PDAC cell lines, observing the effects of this inhibition on other cell types seen within a PDAC tumour was also investigated. The main other cell types used in this study to reflect common TME components were endothelial cells (HUVECs) and fibroblasts. Two different types of fibroblasts were used, human dermal fibroblasts (HDF) and patient-derived cancer-associated fibroblasts (CAF), that were isolated from a primary pancreatic cancer tumour. Fibroblasts were chosen for study due to their key roles in the production of the ECM, collagen, and their contributions to PDACs dense desmoplastic stroma. The two different primary fibroblast cells were chosen to investigate differences between non-cancerous and cancerous versions of fibroblasts, in particular their ability to support tumour angiogenesis. CAFs can be derived from local fibroblast populations, they can have origins in other cell types that have differentiated into CAFs, or they can have migrated from different tissue locations (Pape et al. 2020). In particular, when differentiated from fibroblasts, they become myofibroblasts, which are characterised by the expression of α-SMA. Within tumours they typically excrete large amounts of growth factors including TGF-β, VEGF-A and IL-6 which modify the tumour microenvironment, cancer development, and treatment response (Melegová et al. 2022).

As with the PDAC cell lines, TGF-β treatment induced increased TGF-β protein expression, significantly in the CAFs and non-significantly in the HDFs (Figure 4.1 and 4.3). LY treatment decreased these levels back to baseline control levels, reaching significance in the CAFs only. This trend was further seen, though less dramatically, in both cell lines for mRNA expression, with TGF-β increasing its own expression, and LY reducing the effect back to untreated control levels or lower (Figure 4.2 and 4.4). TGF-β has been shown previously to increase protein and mRNA expression of its latent form in HDF and other fibroblast types, however it is unclear if this effect has been seen in pancreatic CAFs before (Kelley et al. 1993; Dallas et al. 1994). The

autocrine activation of TGF-β expression by fibroblast populations may further contribute to the immunosuppressive environment observed in pancreatic tumours.

In addition to TGF-β, changes in the expression of VEGF-A were investigated in fibroblasts. The mRNA expression of VEGF-A was significantly increased in CAFs after treatment with TGF-β, with combination treatment significantly decreasing this expression. CAFs have been shown to directly affect angiogenesis and the production of VEGF-A in a number of cancer types, including colorectal, breast and gastric cancer, with CAFs typically acting as a secondary source of VEGF in addition to tumour cells (Guo, X. et al. 2008; Vong and Kalluri 2011; De Francesco et al. 2013; Pape et al. 2020). In particular, the control of VEGF expression within gastric CAFs has been shown to be controlled by galectin-1, a member of the β-galactoside-binding soluble lectin family that has many roles in inflammatory conditions and the promotion of cancer growth (Novák et al. 2025). Galectin-1 was found to be highly expressed in gastric CAFs and was correlated with higher VEGF levels (Tang, D. et al. 2016). Similarly, galectin-1 was reportedly increased in pancreatic CAFs and is associated with reduced survival and increased tumour progression (Tang, D. et al. 2014). It was also observed that TGF-β causes a dose-dependent increase in galectin-1 expression in CAFs, which could explain the TGF-β induced increase in VEGF-A mRNA expression in CAFs, and the subsequent decrease with LY treatment (Tang, D. et al. 2014).

The change in CAF VEGF-A mRNA expression was also evident in HDFs; however, this did not reach significance. Within a non-cancerous environment, TGF-β functions as a growth factor with roles in wound healing and stimulates fibroblast collagen deposition and normal angiogenesis. This suggests that TGF-β could stimulate the release of VEGF-A in non-cancerous fibroblasts to mediate faster wound healing, as seen in this study (Taherpour et al. 2025).

In addition to VEGF-A and TGF-β, bFGF is another growth factor implicated in cell proliferation, differentiation, survival and motility. It is commonly overexpressed in PDAC, and its crosstalk with TGF-β promotes EMT and cancer cell invasion (Basilico and Moscatelli 1992; Xelwa et al. 2021). Independent of TGF-β, bFGF is a prominent angiogenic factor that regulates the migration of endothelial cells to form new blood vessels (Dow and deVere White 2000). Within cancer, bFGF maintains its role as an angiogenic factor and is produced by CAFs (Parma et al. 2020). In this study, both HDFs and CAFs demonstrated a significant increase in bFGF expression after

TGF-β stimulation. This increase was significantly decreased in the groups treated with LY, showing TGF-β also regulates the expression of bFGF in fibroblasts.

As mentioned, TGF-β and bFGF signalling pathways are often interlinked and the two growth factors can influence the expression of each other (Boes et al. 1991). Previously, TGF-β was reported to induce the expression of bFGF in fibroblast cell lines through the phosphorylation of SMAD3 and activation of p38 and ERK signalling pathways. Elevated bFGF levels induced angiogenesis in the TME and increased the rate of tumour growth (Strand et al. 2014). Additionally, the enhanced release of bFGF from CAFs has been shown to increase the survival of pancreatic cancer cells and correlated with a shorter post-operative survival in patients (Awaji et al. 2019). Another role of bFGF is in inhibiting TGF-β signalling in CAFs, where bFGF prevented TGF-β-induced differentiation of CAFs through ERK pathway activation and, downregulation of collagen and α-SMA in fibroblasts (Mardhian et al. 2020; Tian, X. et al. 2023). This behaviour has also been seen in non-cancerous environments related to wound-healing (Song, Q.H. et al. 2002). As bFGF has roles in inhibiting TGF-β, this molecule could be used to regulate TGF-β signalling, however further investigation would be needed to confirm this effect.

After investigating the effects of TGF-β inhibition on fibroblast expression of TGF-β, VEGF-A, and bFGF, further exploration into how this growth factor affects ECM molecules was performed. Both fibroblast lines experienced significant increases in COL1A1 protein expression after TGF-β stimulation, followed by significant decreases in expression after combination treatment with LY. Despite the dramatic changes in COL1A1 protein expression, there were minimal differences observed in mRNA expression. However, there was a non-significant increase in COL1A1 after TGF-β stimulation in HDFs, and this increase was reversed following combination treatment with LY. On the other hand, CAFs exhibited minimal changes in COL1A1 mRNA expression. The mRNA expression of the basement membrane protein COL4A1 was also analysed. In CAFs, there was minimal increase in COL4A1 mRNA expression after TGF-β treatment, which was lowered to baseline levels after inhibition with LY. Similarly, in HDFs, TGF-β treatment increased COL4A1, and combination treatment with LY decreased mRNA expression.

Collagen is the predominant protein found within the PDAC ECM, with COL1A1 being the main type found in this environment. COL1A1 is produced by CAFs, and its production is typically stimulated by TGF-β (Shin et al. 2022; Li, Q. et al. 2025). TGF-β inhibitors have been used

previously in PDAC and demonstrated a reduction of stromal content, through decreased collagen deposition, which increased the effect of drug delivery (Biffi et al. 2019). COL1A1 is heavily involved in promoting a fibrotic stroma, with large amounts of collagen deposition causing the dense physical barrier seen in PDAC and preventing the formation of functioning blood vessels, as well as preventing immune cells and treatment from entering the tumour (Song, X. et al. 2023). Suppressing TGF-β signalling in PDAC may reduce the level of COL1A1 deposition from CAFs into the ECM. This would create a less dense environment, allowing for better blood vessel formation and structure, and improving intratumoral drug penetration.

COL4A1 is another prominent collagen found in PDAC. It is predominantly expressed in CAFs and is a key component of basement membranes, providing a barrier to tumour invasion (Khoshnoodi et al. 2008). Despite this suppressive role, COL4A1 is also associated with EMT and, inflammation, with high expression levels linked to increased metastasis risk and decreased survival rates in PDAC (Shin et al. 2022; Li, Q. et al. 2025). Despite TGF-β inducing the expression of many proteins in CAFs, it has minimal effects on COL4A1, as reported in this study. In addition, COL4A1 is implicated as an oncogene in PDAC and other cancers such as glioma, skin melanoma, and stomach adenocarcinoma, with high expression correlating with poor patient prognosis (Wang, H. et al. 2021; Shin et al. 2022). *COL4A1* mutations were shown to dysregulate the TGF-β signalling pathway, alter CAF behaviour to promote an immunosuppressive environment (Shin et al. 2022).

Finally, the effect of TGF-β on the differentiation of CAFs was explored. The protein and mRNA expression of the myCAFs and iCAFs markers, α-SMA and IL-6 respectively, were investigated. There were no changes seen in α-SMA protein expression in CAFs after 72 hours of TGF-β treatment or inhibition. However, there were significant increases in α-SMA mRNA expression after TGF-β treatment, with LY treatment suppressing the response.

There are several growth factors, including TGF-β that can shift fibroblasts to the myCAF subtype, which express α-SMA and are predominantly responsible for the production of the dense desmoplastic stroma (Kim, D.K. et al. 2022). In PDAC, the change to this phenotype is reportedly mediated by the release of TGF-β from cancer cells (Roger et al. 2026). TGF-β inhibition has been used previously in CAFs to prevent differentiation into a myCAF phenotype, with inhibition also reducing collagen production and the dense stroma (Biffi et al. 2019; Liu, X.

et al. 2021). Furthermore, bFGF treatment decreased α-SMA synthesis and reduced collagen production in CAFs, directly counteracting the effects of TGF-β on the TME (Mardhian et al. 2020; Tian, X. et al. 2023).

IL-6 is one of the main markers for the iCAF subtype of CAFs found in the PDAC tumours and no change in IL-6 mRNA expression was observed in the pancreatic CAFs (Figure 4.4). The main roles of TGF-β include inducing myCAF phenotypes in fibroblast cells, and this typically correlated with low levels of iCAF markers, due to TGF-β induced inhibition (di Miceli et al. 2024). In this study, even in groups containing LY, there was no increase in the iCAF marker IL-6, despite TGF-β inhibition. This correlated with other studies, showing that while TGF-β inhibition does reduce the expression of α-SMA and the production of collagen, it does not significantly increase iCAF content (Biffi et al. 2019).

This analysis was not performed in the HDF, but investigation into this cell line and a pancreatic CAF precursor cell line, would be interesting to determine how TGF-β influences fibroblastic differentiation in non-cancerous cells, in comparison to the CAFs. Furthermore, investigating the interconnected relationship between PDAC cell lines and CAFs to show how this relationship is affected by TGF-β inhibition would allow a more well-rounded representation of the PDAC TME.

6.4 TGF-β suppression effect on endothelial cells

The final cell type used to investigate the effect of TGF-β within the PDAC TME were endothelial cells, represented by HUVECs in this study. The protein and mRNA expression of TGF-β was analysed in HUVECs after TGF-β stimulation and inhibition (Figure 5.1). TGF-β stimulation caused a non-significant increase in TGF-β protein expression, with LY combination treatment causing a significant decrease in TGF-β expression. This pattern was not seen in mRNA expression analysis, with all treatment groups decreasing levels of TGF-β expression. Additionally, TGF-β treatment and inhibition with LY also decreased VEGF-A mRNA expression in all treatment groups.

The autoregulation of detected TGF-β protein expression observed in HUVECs aligns with earlier findings in PDAC and fibroblasts (see Figure 3.4, 4.1 and 4.3) and autoregulation of this protein reported previously (Kelley et al. 1993; Dallas et al. 1994). Within endothelial cells, TGF-β can

act as an angiogenesis inhibitor or stimulator though different signalling pathways and has previously been shown to increase VGEF-A expression, although this was not replicated in this study (Ferrari et al. 2012).

Additionally, HUVECs were analysed by immunofluorescence microscopy to determine if TGF-β inhibition induced phenotypic changes (Figure 5.2 and 5.3). HUVECs treated for 48 or 72 hours with LY compound, demonstrated concentration-dependent changes in HUVEC morphology. HUVECs became more elongated and spindle shaped when treated with LY at higher concentrations, although total CD31 expression was not influenced by LY addition. Despite TGF-β having major roles in the stimulation and inhibition of angiogenesis, TGF-β has predominantly been shown to prevent endothelial cell proliferation and tube formation, with inhibition of TGF-β signalling increasing proliferation and promoting angiogenic vessel formation (Watabe et al. 2003; Goumans et al. 2009). As longer treatment times and higher LY concentrations increasingly altered HUVEC shape, the response may reflect the morphological changes which would occur in endothelial cells during their differentiation into new blood vessels.

In addition to its many roles supporting angiogenesis, TGF-β is also involved in endothelial-to-mesenchymal transition. This process occurs in cancer, whereby endothelial cells differentiate into a CAF sub-type, subsequently expressing more α-SMA and less CD31 (Zeisberg, E.M. et al. 2007; van Meeteren and ten Dijke 2012). As LY did not change CD31 expression in this study, as determines by microscopy analysis, it is not clear if it would influence this process if HUVECs were used in a co-culture with PDAC cells to model a more accurate depiction of the PDAC TME.

6.5 LY2109671 supported the formation of vessels in HDF and CAF co-cultures

To apply the previous findings and to investigate how TGF-β signalling affects the formation of blood vessels within a PDAC tumour, HUVECs were cultured with both fibroblast types. The co-cultures grown together for 10 days, with the latter 6 days involving treatment with VEGF-A, TGF-β and LY combinations, before fixation and staining with anti-CD31 to visualise vessel formation. This study focused on two main structures found in these co-cultures, vessels and blood islands (Figure 5.4). Blood islands are typically found as a precursor to the formation of blood vessels and are shown by the grouping of HUVECs before they become more connected and elongated to form the capillary-like vessel structures (Risau et al. 1988).

HDFs were used first to analyse how TGF-β and inhibition of its receptors would affect blood vessel formation in a non-cancerous environment (Figure 5.5). HDFs were unable to facilitate substantive vessel formation under control conditions, however there was an increase in vessel length and branch points numbers following VEGF-A treatment. In contrast, TGF-β treatment reduced overall vessel length and number of branch points. Conversely, treatment with LY increased the total vessel length and number of branch points, although the change did not reach significance. Blocking TGF-β signalling has been shown to stimulate vessel formation, through reversing the anti-angiogenic effect of TGF-β on endothelial cells (Watabe et al. 2003). HDFs have been shown to facilitate vessel formation within co-cultures previously, but in comparison to the CAF co-cultures, HDFs exhibited minimal vessel formation (Costa-Almeida et al. 2015; Pape et al. 2020).

HDF co-cultures were used further to investigate the effects of cultured media on vessel formation (Figure 5.6). Co-cultures were grown with either non-conditioned control media or conditioned media, from Panc1 cells. In these co-cultures, there were minimal differences in total vessel length and number of branch points between treatments with the two media types. There was a general increase in vessel length and branch point number following LY treatment, similar to the increases noted in the standard co-culture assays reported above. However, there were no significant changes observed between co-culture growth in the two media types. As the cultured media used was derived from standard untreated PDAC cells, this research area could be expanded to investigate how conditioned media from TGF-β or LY treated PDAC cultures may affect vessel formation. Within a pancreatic tumour, PDAC cells heavily influence the fibroblast populations through release of signalling molecules such as TGF-β. Previously, 3D cultures containing PDAC cancer cells, CAFs and HUVECs have been used to determine the effect of cancer cells on HUVECs. These cultures showed inhibition of vessel formation in co-cultures containing cancer cells, in comparison to CAF-HUVEC only co-cultures (Di Maggio et al. 2016). As such, PDAC cells could be grown in similar conditions more reflective of the complex TME of a PDAC tumour, to provide a more accurate representation of blood vessel formation in a tumour (Bailey, J.M. et al. 2008; Yauch et al. 2008).

The final co-cultures investigated were with performed with patient-derived CAFs (Figure 5.7). CAFs were able to support vessel formation more efficiently than the HDFs, with the addition of VEGF-A to the co-cultures having minimal effect on vessel length. This could be due to CAFs

secreting high concentrations of endogenous VEGF-A, reducing the influence of additional VEGF-A (Vong and Kalluri 2011). TGF-β decreased total vessel length and number of branch points in CAF-HUVEC co-cultures, although this did not reach significance. This suppression could be due to TGF-β-mediated production and release of COL1A1 from CAFs. As increased collagen levels in the ECM prevents the formation of blood vessels, inhibiting this pathway conceivably reduces the physical barrier created by high collagen levels, and allows for more efficient vessel formation (Li, Q. et al. 2025). The addition of LY increased the total vessel length and branch points, regardless of any other treatments used, with the effect reaching significance in the LY and TGF-β-treated group. This suggests not only is the anti-angiogenic effect of TGF-β inhibited by LY addition, but TGF-β receptor inhibition prevents further COL1A1 formation and deposition by CAFs, alongside altering CAF differentiation into myCAFs. As myCAFs are the predominant producers of collagen, the decrease in myCAF levels would contribute to an environment that allows for the better formation of blood vessels (Biffi et al. 2019).

To expand on this, repeating the CAF co-cultures together with conditioned media from PDACs or addition of PDAC cells themselves into the co-culture system, would provide an alternative environment to more accurately depict the PDAC TME. The PDAC cells would potentially alter how the CAFs support angiogenesis, possibly due to their increased expression of VEGF-A and other stromal components (Pape et al. 2020). Experiments using PDAC cells would allow further investigation into the long-term effects of LY on these cells, as they were only treated with the inhibitor for a maximum of 72 hours. PDAC cell lines have been shown previously to migrate towards and cluster around endothelial cells. This causes endothelial cell damage and the re-lining of tumour blood vessels with cancer cells, in process heavily involving TGF-β signalling (Di Maggio et al. 2016; Nguyen, D.-H.T. et al. 2019). Investigating the effect of this inhibitor in, a co-culture model with CAFs, HUVECs, and PDAC cell lines would further inform how cancer cells migrate and interact with blood vessels to regulate tumour angiogenesis and cancer growth within pancreatic tumours.

In this study, vascular density in fibroblast-endothelial cell co-cultures was the primary quality of vascular normalisation assessed. To expand, investigation into vascular structure and leakiness could be performed through Transwell permeability assays to assess the effect of TGF-β receptor inhibition. Finally, microfluidic systems could further assess vascular stability, with

additional investigation into how TGF-β receptor inhibition affects the immune population across different co-cultures.

7. General Conclusion

In PDAC, poor patient outcomes and treatment response can be correlated with the characteristic dense desmoplastic stroma and the poorly formed blood vessels found within the TME. These leaky, functionally impaired blood vessels struggle to form due to the presence of CAFs which secrete excessive collagen and contribute to the dense tumour stroma. These factors contribute to a hypoxic environment that prevents effective drug delivery to cancer cells. A critical mediator of the suppressive and fibrotic TME is TGF-β, a key signalling molecule in cancer which also contributes to EMT and angiogenesis responses. This study targeted TGF-β signalling through receptor inhibition with small molecule drugs, to determine the effect on TME components, including new blood vessel formation. TGF-β receptor inhibition in PDAC cell lines led to decreased cell viability. It also prevented TGF-β autoinduction and the release of VEGF-A from PDAC cells.

The effect of receptor inhibition on down-regulation of TGF-β and VEGF-A levels was seen in fibroblasts. Additionally, TGF-β receptor inhibition reduced the production of COL1A1 and bFGF in CAFs and HDFs, potentially altering the structure of the dense desmoplastic stroma. Co-culture models analysing differences in vessel formation between HDFs and CAFs, found that CAFs supported vessel formation more effectively than HDFs. Both fibroblast co-cultures responded to TGF-β stimulation with reduced vessel formation, an effect that was reversed with TGF-β receptor inhibition.

Overall, this study demonstrated TGF-β receptor inhibition reduced collagen production by fibroblasts and increased the formation of blood vessels in co-culture models. Inhibition of TGF-β signalling also directly reduced the viability and growth of PDAC cells. Consequently, this approach could be utilised clinically to reduce the characteristic stiff extracellular matrix present in PDAC tumours and allow the formation of more patent and structured blood vessels. This would lead to improved intratumoral penetration of treatments, improving the effectiveness of chemotherapy, and leading to better clinical outcomes following treatment.

8. Bibliography

Addadi, Y., Moskovits, N., Granot, D., Lozano, G., Carmi, Y., Apte, R.N., Neeman, M. and Oren, M. (2010) p53 Status in Stromal Fibroblasts Modulates Tumor Growth in an SDF1-Dependent Manner. *Cancer Research*, 70 (23), pp. 9650–9658.

Aguilera, K.Y., Rivera, L.B., Hur, H., Carbon, J.G., Toombs, J.E., Goldstein, C.D., Dellinger, M.T., Castrillon, D.H. and Brekken, R.A. (2014) Collagen Signaling Enhances Tumor Progression after Anti-VEGF Therapy in a Murine Model of Pancreatic Ductal Adenocarcinoma. *Cancer Research*, 74 (4), pp. 1032–1044.

Aguirre, A.J., Nowak, J.A., Camarda, N.D., Moffitt, R.A., Ghazani, A.A., Hazar-Rethinam, M., Raghavan, S., Kim, J., Brais, L.K., Ragon, D., Welch, M.W., Reilly, E., McCabe, D., Marini, L., Anderka, K., Helvie, K., Oliver, N., Babic, A., Da Silva, A., Nadres, B., Van Seventer, E.E., Shahzade, H.A., St Pierre, J.P., Burke, K.P., Clancy, T., Cleary, J.M., Doyle, L.A., Jajoo, K., McCleary, N.J., Meyerhardt, J.A., Murphy, J.E., Ng, K., Patel, A.K., Perez, K., Rosenthal, M.H., Rubinson, D.A., Ryou, M., Shapiro, G.I., Sicinska, E., Silverman, S.G., Nagy, R.J., Lanman, R.B., Knoerzer, D., Welsch, D.J., Yurgelun, M.B., Fuchs, C.S., Garraway, L.A., Getz, G., Hornick, J.L., Johnson, B.E., Kulke, M.H., Mayer, R.J., Miller, J.W., Shyn, P.B., Tuveson, D.A., Wagle, N., Yeh, J.J., Hahn, W.C., Corcoran, R.B., Carter, S.L. and Wolpin, B.M. (2018) Real-time Genomic Characterization of Advanced Pancreatic Cancer to Enable Precision Medicine. *Cancer discovery*, 8 (9), pp. 1096–1111.

Ahmed, S., Schwartz, C., Dewan, M. and Xu, R. (2019) The Promising Role of TGF- β/SMAD4 in Pancreatic Cancer: The future targeted therapy. *Journal of Cancer Treatment and Diagnosis*, 3 (2), pp. 1–7.

Ahmed, W., Kucich, U., Abrams, W., Bashir, M., Rosenbloom, J., Segade, F., Mecham, R. and Rosenbloom, J. (1998) Signaling Pathway by which TGF-β1 Increases Expression of Latent TGF-β Binding Protein-2 at the Transcriptional Level. *Connective Tissue Research* [Post-print], 37 (3–4), pp. 263–276.

An, Y.-F., Pu, N., Jia, J.-B., Wang, W.-Q. and Liu, L. (2023) Therapeutic advances targeting tumor angiogenesis in pancreatic cancer: Current dilemmas and future directions. *Biochimica et Biophysica Acta (BBA) - Reviews on Cancer* [Post-print], 1878 (5), p. 188958.

Ansardamavandi, A., Nikfarjam, M. and He, H. (2023) PAK in Pancreatic Cancer-Associated Vasculature: Implications for Therapeutic Response. *Cells* [Post-print], 12 (23), p. 2692.

Awaji, M., Futakuchi, M., Heavican, T., Iqbal, J. and Singh, R.K. (2019) Cancer-Associated Fibroblasts Enhance Survival and Progression of the Aggressive Pancreatic Tumor Via FGF-2 and CXCL8. *Cancer Microenvironment*, 12 (1), pp. 37–46.

Baeriswyl, V. and Christofori, G. (2009) The angiogenic switch in carcinogenesis. *Seminars in Cancer Biology*, 19 (5), pp. 329–337.

Bailey, J.M., Swanson, B.J., Hamada, T., Eggers, J.P., Singh, P.K., Caffery, T., Ouellette, M.M. and Hollingsworth, M.A. (2008) Sonic Hedgehog Promotes Desmoplasia in Pancreatic Cancer. *Clinical Cancer Research*, 14 (19), pp. 5995–6004.

Bailey, P., Chang, D.K., Nones, K., Johns, A.L., Patch, A.-M., Gingras, M.-C., Miller, D.K., Christ, A.N., Bruxner, T.J.C., Quinn, M.C., Nourse, C., Murtaugh, L.C., Harliwong, I., Idrisoglu, S., Manning, S.,

Nourbakhsh, E., Wani, S., Fink, L., Holmes, O., Chin, V., Anderson, M.J., Kazakoff, S., Leonard, C., Newell, F., Waddell, N., Wood, S., Xu, Q., Wilson, P.J., Cloonan, N., Kassahn, K.S., Taylor, D., Quek, K., Robertson, A., Pantano, L., Mincarelli, L., Sanchez, L.N., Evers, L., Wu, J., Pinese, M., Cowley, M.J., Jones, M.D., Colvin, E.K., Nagrial, A.M., Humphrey, E.S., Chantrill, L.A., Mawson, A., Humphris, J., Chou, A., Pajic, M., Scarlett, C.J., Pinho, A. V., Giry-Laterriere, M., Rooman, I., Samra, J.S., Kench, J.G., Lovell, J.A., Merrett, N.D., Toon, C.W., Epari, K., Nguyen, N.Q., Barbour, A., Zeps, N., Moran-Jones, K., Jamieson, N.B., Graham, J.S., Duthie, F., Oien, K., Hair, J., Grützmann, R., Maitra, A., Iacobuzio-Donahue, C.A., Wolfgang, C.L., Morgan, R.A., Lawlor, R.T., Corbo, V., Bassi, C., Rusev, B., Capelli, P., Salvia, R., Tortora, G., Mukhopadhyay, D., Petersen, G.M., Munzy, D.M., Fisher, W.E., Karim, S.A., Eshleman, J.R., Hruban, R.H., Pilarsky, C., Morton, J.P., Sansom, O.J., Scarpa, A., Musgrove, E.A., Bailey, U.-M.H., Hofmann, O., Sutherland, R.L., Wheeler, D.A., Gill, A.J., Gibbs, R.A., Pearson, J. V., Waddell, N., Biankin, A. V. and Grimmond, S.M. (2016) Genomic analyses identify molecular subtypes of pancreatic cancer. *Nature* [Post-print], 531 (7592), pp. 47–52.

Bakin, A. V., Rinehart, C., Tomlinson, A.K. and Arteaga, C.L. (2002) p38 mitogen-activated protein kinase is required for TGFβ-mediated fibroblastic transdifferentiation and cell migration. *Journal of Cell Science*, 115 (15), pp. 3193–3206.

Bakin, A. V., Tomlinson, A.K., Bhowmick, N.A., Moses, H.L. and Arteaga, C.L. (2000) Phosphatidylinositol 3-Kinase Function Is Required for Transforming Growth Factor β-mediated Epithelial to Mesenchymal Transition and Cell Migration. *Journal of Biological Chemistry*, 275 (47), pp. 36803–36810.

Basilico, C. and Moscatelli, D. (1992) The Fgf Family of Growth Factors and Oncogenes. In: *Advances in Cancer Research*. Elsevier , pp. 115–165.

Basturk, O., Hong, S.-M., Wood, L.D., Adsay, N.V., Albores-Saavedra, J., Biankin, A. V., Brosens, L.A.A., Fukushima, N., Goggins, M., Hruban, R.H., Kato, Y., Klimstra, D.S., Klöppel, G., Krasinskas, A., Longnecker, D.S., Matthaei, H., Offerhaus, G.J.A., Shimizu, M., Takaori, K., Terris, B., Yachida, S., Esposito, I. and Furukawa, T. (2015) A Revised Classification System and Recommendations From the Baltimore Consensus Meeting for Neoplastic Precursor Lesions in the Pancreas. *American Journal of Surgical Pathology*, 39 (12), pp. 1730–1741.

Bertrand-Chapel, A., Caligaris, C., Fenouil, T., Savary, C., Aires, S., Martel, S., Huchedé, P., Chassot, C., Chauvet, V., Cardot-Ruffino, V., Morel, A.-P., Subtil, F., Mohkam, K., Mabrut, J.-Y., Tonon, L., Viari, A., Cassier, P., Hervieu, V., Castets, M., Mauviel, A., Sentis, S. and Bartholin, L. (2022) SMAD2/3 mediate oncogenic effects of TGF-β in the absence of SMAD4. *Communications Biology* [Post-print], 5 (1), p. 1068.

Bhowmick, N.A., Ghiassi, M., Bakin, A., Aakre, M., Lundquist, C.A., Engel, M.E., Arteaga, C.L. and Moses, H.L. (2001) Transforming Growth Factor-β1 Mediates Epithelial to Mesenchymal Transdifferentiation through a RhoA-dependent Mechanism. *Molecular Biology of the Cell*, 12 (1), pp. 27–36.

Biffi, G., Oni, T.E., Spielman, B., Hao, Y., Elyada, E., Park, Y., Preall, J. and Tuveson, D.A. (2019) IL1-Induced JAK/STAT Signaling Is Antagonized by TGFβ to Shape CAF Heterogeneity in Pancreatic Ductal Adenocarcinoma. *Cancer Discovery* [Post-print], 9 (2), pp. 282–301.

Boes, M., Dake, B.L. and Bar, R.S. (1991) Interactions of cultured endothelial cells with TGF-β, bFGF, PDGF and IGF-I. *Life Sciences*, 48 (8), pp. 811–821.

Brichkina, A., Polo, P., Sharma, S.D., Visestamkul, N. and Lauth, M. (2023) A Quick Guide to CAF Subtypes in Pancreatic Cancer. *Cancers*, 15 (9), p. 2614.

Cancer Research UK (2024) *Pancreatic Cancer Statistics* [Internet]. Available from https://www.cancerresearchuk.org/health-professional/cancer-statistics/statistics-by-cancer-type/pancreatic-cancer. [Accessed 28th April 2026].

Carbone, C., Moccia, T., Zhu, C., Paradiso, G., Budillon, A., Chiao, P.J., Abbruzzese, J.L. and Melisi, D. (2011) Anti-VEGF Treatment–Resistant Pancreatic Cancers Secrete Proinflammatory Factors That Contribute to Malignant Progression by Inducing an EMT Cell Phenotype. *Clinical Cancer Research*, 17 (17), pp. 5822–5832.

Chakkera, M., Foote, J.B., Farran, B. and Nagaraju, G.P. (2024) Breaking the stromal barrier in pancreatic cancer: Advances and challenges. *Biochimica et Biophysica Acta (BBA) - Reviews on Cancer*, 1879 (1), p. 189065.

Chauhan, V.P., Boucher, Y., Ferrone, C.R., Roberge, S., Martin, J.D., Stylianopoulos, T., Bardeesy, N., DePinho, R.A., Padera, T.P., Munn, L.L. and Jain, R.K. (2014) Compression of Pancreatic Tumor Blood Vessels by Hyaluronan Is Caused by Solid Stress and Not Interstitial Fluid Pressure. *Cancer Cell*, 26 (1), pp. 14–15.

Chauhan, V.P., Martin, J.D., Liu, H., Lacorre, D.A., Jain, S.R., Kozin, S. V., Stylianopoulos, T., Mousa, A.S., Han, X., Adstamongkonkul, P., Popović, Z., Huang, P., Bawendi, M.G., Boucher, Y. and Jain, R.K. (2013) Angiotensin inhibition enhances drug delivery and potentiates chemotherapy by decompressing tumour blood vessels. *Nature Communications*, 4 (1), p. 2516.

Chen, F. and Weinberg, R.A. (1995) Biochemical evidence for the autophosphorylation and transphosphorylation of transforming growth factor beta receptor kinases. *Proceedings of the National Academy of Sciences*, 92 (5), pp. 1565–1569.

Chen, Y.-W., Hsiao, P.-J., Weng, C.-C., Kuo, K.-K., Kuo, T.-L., Wu, D.-C., Hung, W.-C. and Cheng, K.-H. (2014) SMAD4 Loss triggers the phenotypic changes of pancreatic ductal adenocarcinoma cells. *BMC Cancer*, 14 (1), p. 181.

Collisson, E.A., Bailey, P., Chang, D.K. and Biankin, A. V. (2019) Molecular subtypes of pancreatic cancer. *Nature Reviews Gastroenterology & Hepatology*, 16 (4), pp. 207–220.

Collisson, E.A., Sadanandam, A., Olson, P., Gibb, W.J., Truitt, M., Gu, S., Cooc, J., Weinkle, J., Kim, G.E., Jakkula, L., Feiler, H.S., Ko, A.H., Olshen, A.B., Danenberg, K.L., Tempero, M.A., Spellman, P.T., Hanahan, D. and Gray, J.W. (2011) Subtypes of pancreatic ductal adenocarcinoma and their differing responses to therapy. *Nature Medicine*, 17 (4), pp. 500–503.

Connor, A.A. and Gallinger, S. (2022) Pancreatic cancer evolution and heterogeneity: integrating omics and clinical data. *Nature Reviews Cancer* [Post-print], 22 (3), pp. 131–142.

Conroy, T., Castan, F., Lopez, A., Turpin, A., Ben Abdelghani, M., Wei, A.C., Mitry, E., Biagi, J.J., Evesque, L., Artru, P., Lecomte, T., Assenat, E., Bauguion, L., Ychou, M., Bouché, O., Monard, L., Lambert, A., Hammel, P., Francois, E., Ramee, J.-F., Castanie, H., Pracht, M., Ghiringhelli, F., Maillard, E., Couffon, C., Volet, J., Bourgeois, V., Chauvenet, M., Blanc, J.-F., Péré-Vergé, D., De La Fouchardiere, C., Adenis, A., El

Hajbi, F., Bennouna, J., Texereau, P., Faroux, R., Miglianico, L., Platini, C., Legoux, J.-L., Caroli-Bosc, F.-X., Bouhier-Leporrier, K., Gagnaire, A., Granger, V., Lebrun-Ly, V., Guimbaud, R., Touchefeu, Y., Gasmi, M., Di Fiore, F., Seitz, J.F., Etienne, P.-L., Ligeza Poisson, C., Rinaldi, Y., Baba-Hamed, N., Bachet, J.B., Aparicio, T., Chone, L., Guillet, M., Forestier, J., Terrebonne, E., Hebbar, M., Breysacher, G., Andre, T., Khemissa-Akouz, F., Hautefeuille, V., Guerin-Meyer, V., Hartwig, J., Becouarn, Y., Malka, D., Louvet, C., Raoul, J.-L., Cany, L., Juzina, B., Jouffroy, C., Gourgou, S., Rassouli, M., Chalchal, H., Renouf, D., Wong, R., Lemay, F., Aubin, F., Couture, F., Mc Whirter, E., Welch, S., Kavan, P., Findlay, B., Cripps, C., Cano, P., Ahmed, S., Harb, M., Pressnail, B., Dowden, S. and O'Callaghan, C. (2022) Five-Year Outcomes of FOLFIRINOX vs Gemcitabine as Adjuvant Therapy for Pancreatic Cancer. *JAMA Oncology* [Post-print], 8 (11), p. 1571.

Costa-Almeida, R., Gomez-Lazaro, M., Ramalho, C., Granja, P.L., Soares, R. and Guerreiro, S.G. (2015) Fibroblast-Endothelial Partners for Vascularization Strategies in Tissue Engineering. *Tissue Engineering Part A*, 21 (5–6), pp. 1055–1065.

Dallas, S.L., Park-Snyder, S., Miyazono, K., Twardzik, D., Mundy, G.R. and Bonewald, L.F. (1994) Characterization and autoregulation of latent transforming growth factor beta (TGF beta) complexes in osteoblast-like cell lines. Production of a latent complex lacking the latent TGF beta-binding protein. *Journal of Biological Chemistry*, 269 (9), pp. 6815–6821.

Davies, M., Robinson, M., Smith, E., Huntley, S., Prime, S. and Paterson, I. (2005) Induction of an epithelial to mesenchymal transition in human immortal and malignant keratinocytes by TGF-β1 involves MAPK, Smad and AP-1 signalling pathways. *Journal of Cellular Biochemistry*, 95 (5), pp. 918–931.

Deer, E.L., González-Hernández, J., Coursen, J.D., Shea, J.E., Ngatia, J., Scaife, C.L., Firpo, M.A. and Mulvihill, S.J. (2010) Phenotype and Genotype of Pancreatic Cancer Cell Lines. *Pancreas*, 39 (4), pp. 425–435.

Deng, Z., Fan, T., Xiao, C., Tian, H., Zheng, Y., Li, C. and He, J. (2024) TGF-β signaling in health, disease and therapeutics. *Signal Transduction and Targeted Therapy*, 9 (1), p. 61.

Ten Dijke, P., Goumans, M., Itoh, F. and Itoh, S. (2002) Regulation of cell proliferation by Smad proteins. *Journal of Cellular Physiology*, 191 (1), pp. 1–16.

Dow, J.K. and deVere White, R.W. (2000) Fibroblast growth factor 2: its structure and property, paracrine function, tumor angiogenesis, and prostate-related mitogenic and oncogenic functions. *Urology*, 55 (6), pp. 800–806.

Drizyte-Miller, K., Talabi, T., Somasundaram, A., Cox, A.D. and Der, C.J. (2025) KRAS: the Achilles' heel of pancreas cancer biology. *Journal of Clinical Investigation*, 135 (16).

DuFort, C.C., DelGiorno, K.E., Carlson, M.A., Osgood, R.J., Zhao, C., Huang, Z., Thompson, C.B., Connor, R.J., Thanos, C.D., Scott Brockenbrough, J., Provenzano, P.P., Frost, G.I., Michael Shepard, H. and Hingorani, S.R. (2016) Interstitial Pressure in Pancreatic Ductal Adenocarcinoma Is Dominated by a Gel-Fluid Phase. *Biophysical Journal*, 110 (9), pp. 2106–2119.

Fadhal, E. (2023) A Comprehensive Analysis of the PI3K/AKT Pathway: Unveiling Key Proteins and Therapeutic Targets for Cancer Treatment. *Cancer Informatics*, 22.

Falcomatà, C., Bärthel, S., Schneider, G., Rad, R., Schmidt-Supprian, M. and Saur, D. (2023) Context-Specific Determinants of the Immunosuppressive Tumor Microenvironment in Pancreatic Cancer. *Cancer Discovery*, 13 (2), pp. 278–297.

Fang, L., Li, Y., Wang, S., Li, Y., Chang, H.-M., Yi, Y., Yan, Y., Thakur, A., Leung, P.C.K., Cheng, J.-C. and Sun, Y.-P. (2020) TGF-β1 induces VEGF expression in human granulosa-lutein cells: a potential mechanism for the pathogenesis of ovarian hyperstimulation syndrome. *Experimental & Molecular Medicine*, 52 (3), pp. 450–460.

Ferrara, B., Pignatelli, C., Cossutta, M., Citro, A., Courty, J. and Piemonti, L. (2021) The Extracellular Matrix in Pancreatic Cancer: Description of a Complex Network and Promising Therapeutic Options. *Cancers*, 13 (17), p. 4442.

Ferrari, G., Terushkin, V., Wolff, M.J., Zhang, X., Valacca, C., Poggio, P., Pintucci, G. and Mignatti, P. (2012) TGF-β1 Induces Endothelial Cell Apoptosis by Shifting VEGF Activation of p38MAPK from the Prosurvival p38β to Proapoptotic p38α. *Molecular Cancer Research*, 10 (5), pp. 605–614.

Fink, D.M., Steele, M.M. and Hollingsworth, M.A. (2016) *The lymphatic system and pancreatic cancer*. Elsevier Ireland Ltd, pp. 217–236.

De Francesco, E.M., Lappano, R., Santolla, M.F., Marsico, S., Caruso, A. and Maggiolini, M. (2013) HIF-1α/GPER signaling mediates the expression of VEGF induced by hypoxia in breast cancer associated fibroblasts (CAFs). *Breast Cancer Research*, 15 (4), p. R64.

Freeman, J.W., Mattingly, C.A. and Strodel, W.E. (1995) Increased tumorigenicity in the human pancreatic cell line MIA PaCa-2 Is associated with an aberrant regulation of an IGF-1 autocrine loop and lack of expression of the TGF-β type RII receptor. *Journal of Cellular Physiology*, 165 (1), pp. 155–163.

Fukumura, D., Kloepper, J., Amoozgar, Z., Duda, D.G. and Jain, R.K. (2018) Enhancing cancer immunotherapy using antiangiogenics: opportunities and challenges. *Nature Reviews Clinical Oncology*, 15 (5), pp. 325–340.

Gautam, S.K., Batra, S.K. and Jain, M. (2023) Molecular and metabolic regulation of immunosuppression in metastatic pancreatic ductal adenocarcinoma. *Molecular Cancer*, 22 (1), p. 118.

Goumans, M.-J., Liu, Z. and ten Dijke, P. (2009) TGF-β signaling in vascular biology and dysfunction. *Cell Research*, 19 (1), pp. 116–127.

Guenther, M., Surendran, S.A., Steinke, L.M., Liou, I., Palm, M.A., Heinemann, V., Haas, M., Boeck, S. and Ormanns, S. (2025) The Prognostic, Predictive and Clinicopathological Implications of KRT81/HNF1A- and GATA6-Based Transcriptional Subtyping in Pancreatic Cancer. *Biomolecules*, 15 (3), p. 426.

Guo, X., Oshima, H., Kitmura, T., Taketo, M.M. and Oshima, M. (2008) Stromal Fibroblasts Activated by Tumor Cells Promote Angiogenesis in Mouse Gastric Cancer. *Journal of Biological Chemistry*, 283 (28), pp. 19864–19871.

Guo, Y., Pan, W., Liu, S., Shen, Z., Xu, Y. and Hu, L. (2020) ERK/MAPK signalling pathway and tumorigenesis (Review). *Experimental and Therapeutic Medicine*,.

Hamed, S.S., Straubinger, R.M. and Jusko, W.J. (2013) Pharmacodynamic modeling of cell cycle and apoptotic effects of gemcitabine on pancreatic adenocarcinoma cells. *Cancer Chemotherapy and Pharmacology*, 72 (3), pp. 553–563.

Hanahan, D. and Weinberg, R.A. (2000) The Hallmarks of Cancer. *Cell* [Post-print], 100 (1), pp. 57–70.

Hao, Y., Baker, D. and ten Dijke, P. (2019) TGF-β-Mediated Epithelial-Mesenchymal Transition and Cancer Metastasis. *International Journal of Molecular Sciences* [Post-print], 20 (11), p. 2767.

Hariyanto, N.I., Yo, E.C. and Wanandi, S.I. (2021) Regulation and Signaling of TGF-β Autoinduction. *International journal of molecular and cellular medicine*, 10 (4), pp. 234–247.

Hashizume, H., Baluk, P., Morikawa, S., McLean, J.W., Thurston, G., Roberge, S., Jain, R.K. and McDonald, D.M. (2000) Openings between Defective Endothelial Cells Explain Tumor Vessel Leakiness. *The American Journal of Pathology* [Post-print], 156 (4), pp. 1363–1380.

Hata, A. and Chen, Y.-G. (2016) TGF-β Signaling from Receptors to Smads. *Cold Spring Harbor Perspectives in Biology*, 8 (9), p. a022061.

Hernández Borrero, L.J. and El-Deiry, W.S. (2021) Tumor suppressor p53: Biology, signaling pathways, and therapeutic targeting. *Biochimica et Biophysica Acta (BBA) - Reviews on Cancer*, 1876 (1), p. 188556.

Von Hoff, D.D., Ervin, T., Arena, F.P., Chiorean, E.G., Infante, J., Moore, M., Seay, T., Tjulandin, S.A., Ma, W.W., Saleh, M.N., Harris, M., Reni, M., Dowden, S., Laheru, D., Bahary, N., Ramanathan, R.K., Tabernero, J., Hidalgo, M., Goldstein, D., Van Cutsem, E., Wei, X., Iglesias, J. and Renschler, M.F. (2013) Increased Survival in Pancreatic Cancer with nab-Paclitaxel plus Gemcitabine. *New England Journal of Medicine*, 369 (18), pp. 1691–1703.

Huang, F. and Chen, Y.-G. (2012) Regulation of TGF-β receptor activity. *Cell & Bioscience*, 2 (1), p. 9.

Iu, M.-F., Kaji, H., Sowa, H., Naito, J., Sugimoto, T. and Chihara, K. (2005) Dexamethasone suppresses Smad3 pathway in osteoblastic cells. *Journal of Endocrinology*, 185 (1), pp. 131–138.

Iwamoto, C., Ohuchida, K., Shinkawa, T., Okuda, S., Otsubo, Y., Okumura, T., Sagara, A., Koikawa, K., Ando, Y., Shindo, K., Ikenaga, N., Nakata, K., Moriyama, T., Miyasaka, Y., Ohtsuka, T., Eto, M., Akashi, K. and Nakamura, M. (2021) Bone marrow-derived macrophages converted into cancer-associated fibroblast-like cells promote pancreatic cancer progression. *Cancer Letters*, 512, pp. 15–27.

Jain, R.K., Martin, J.D. and Stylianopoulos, T. (2014) The Role of Mechanical Forces in Tumor Growth and Therapy. *Annual Review of Biomedical Engineering*, 16 (1), pp. 321–346.

Jang, C.-W., Chen, C.-H., Chen, C.-C., Chen, J., Su, Y.-H. and Chen, R.-H. (2002) TGF-β induces apoptosis through Smad-mediated expression of DAP-kinase. *Nature Cell Biology*, 4 (1), pp. 51–58.

Janssen, Q.P., van Dam, J.L., van Bekkum, M.L., Bonsing, B.A., Bos, H., Bosscha, K.P., Bouwense, S.A.W., Brouwer-Hol, L., Bruynzeel, A.M.E., Busch, O.R., Coene, P.-P.L.O., van Eijck, C.H.J., de Groot, J.W.B.,

Haberkorn, B.C.M., de Hingh, I.H.J.T., Karsten, T.M., Kazemier, G., van der Kolk, M.B., Liem, M.S.L., Loosveld, O.J.L., Luelmo, S.A.C., Luyer, M.D.P., Mekenkamp, L.J.M., Mieog, J.S.D., Nieuwenhuijs, V.B., Nuyttens, J.J.M.E., Patijn, G.A., van Santvoort, H.C., Stommel, M.W.J., Versteijne, E., de Vos-Geelen, J., de Wilde, R.F., Zonderhuis, B.M., van der Holt, B., Homs, M.Y. V, van Tienhoven, G., Besselink, M.G., Wilmink, J.W., Groot Koerkamp, B., Verkolf, E.M.M., Dekker, E.N., Beerepoot, L. V., Cirkel, G.A., ten Oever, D., Streppel, M.M. and Vrijaldenhoven, S. (2025) Neoadjuvant FOLFIRINOX versus neoadjuvant gemcitabine-based chemoradiotherapy in resectable and borderline resectable pancreatic cancer (PREOPANC-2): a multicentre, open-label, phase 3 randomised trial. *The Lancet Oncology*, 26 (10), pp. 1346–1356.

Jia, Y. and Xie, J. (2015) Promising molecular mechanisms responsible for gemcitabine resistance in cancer. *Genes & Diseases*, 2 (4), pp. 299–306.

Kato, M., Arce, L., Wang, M., Putta, S., Lanting, L. and Natarajan, R. (2011) A microRNA circuit mediates transforming growth factor-B1 autoregulation in renal glomerular mesangial cells. *Kidney International*, 80 (4), pp. 358–368.

Katsuta, E., Qi, Q., Peng, X., Hochwald, S.N., Yan, L. and Takabe, K. (2019) Pancreatic adenocarcinomas with mature blood vessels have better overall survival. *Scientific Reports*, 9 (1), p. 1310.

Kelley, J., Shull, S., Walsh, J.J., Cutroneo, K.R. and Absher, M. (1993) Auto-induction of Transforming Growth Factor- *β* in Human Lung Fibroblasts. *American Journal of Respiratory Cell and Molecular Biology*, 8 (4), pp. 417–424.

Khoshnoodi, J., Pedchenko, V. and Hudson, B.G. (2008) Mammalian collagen IV. *Microscopy Research and Technique*, 71 (5), pp. 357–370.

Kim, D.K., Jeong, J., Lee, D.S., Hyeon, D.Y., Park, G.W., Jeon, S., Lee, K.B., Jang, J.-Y., Hwang, D., Kim, H.M. and Jung, K. (2022) PD-L1-directed PlGF/VEGF blockade synergizes with chemotherapy by targeting CD141+ cancer-associated fibroblasts in pancreatic cancer. *Nature Communications*, 13 (1), p. 6292.

Kim, S.-J., Angel, P., Lafyatis, R., Hattori, K., Kim, K.Y., Sporn, M.B., Karin, M. and Roberts, A.B. (1990) Autoinduction of Transforming Growth Factor β1 Is Mediated by the AP-1 Complex. *Molecular and Cellular Biology* [Post-print], 10 (4), pp. 1492–1497.

Kleeff, J., Korc, M., Apte, M., La Vecchia, C., Johnson, C.D., Biankin, A. V., Neale, R.E., Tempero, M., Tuveson, D.A., Hruban, R.H. and Neoptolemos, J.P. (2016) Pancreatic cancer. *Nature Reviews Disease Primers*, 2 (1), p. 16022.

Larionova, I., Kazakova, E., Gerashchenko, T. and Kzhyshkowska, J. (2021) New Angiogenic Regulators Produced by TAMs: Perspective for Targeting Tumor Angiogenesis. *Cancers*, 13 (13), p. 3253.

Levi, A., Blais, E., Davelaar, J., Ebia, M.I., Minasyan, A., Nikravesh, N., Gresham, G., Zheng, L., Chuy, J.W., Shroff, R.T., Wadlow, R.C., DeArbeloa, P., Matrisian, L.M., Petricoin, E., Pishvaian, M.J., Gong, J., Hendifar, A.E. and Osipov, A. (2025) Clinical outcomes and molecular characteristics of lung-only and liver-only metastatic pancreatic cancer: results from a real-world evidence database. *The Oncologist*, 30 (3).

Li, N.S., Zou, J.R., Lin, H., Ke, R., He, X.L., Xiao, L., Huang, D., Luo, L., Lv, N. and Luo, Z. (2016) LKB1/AMPK inhibits TGF-β1 production and the TGF-β signaling pathway in breast cancer cells. *Tumor Biology*, 37 (6), pp. 8249–8258.

Li, Q., Wang, C. and Wang, G. (2025) COL4A1 as a potential prognostic biomarker with functional roles in colon cancer progression. *Scientific Reports*, 15 (1), p. 31382.

Li, Q., Yang, C., Li, J., Wang, R., Min, J., Song, Y. and Su, H. (2025) The type I collagen paradox in PDAC progression: microenvironmental protector turned tumor accomplice. *Journal of Translational Medicine*, 23 (1), p. 744.

Liao, W.-C., Chien, K.-L., Lin, Y.-L., Wu, M.-S., Lin, J.-T., Wang, H.-P. and Tu, Y.-K. (2013) Adjuvant treatments for resected pancreatic adenocarcinoma: a systematic review and network meta-analysis. *The Lancet Oncology*, 14 (11), pp. 1095–1103.

Libutti, S.K., Tamarkin, L. and Nilubol, N. (2018) Targeting the invincible barrier for drug delivery in solid cancers: interstitial fluid pressure. *Oncotarget*, 9 (87), pp. 35723–35725.

Ligorio, M., Sil, S., Malagon-Lopez, J., Nieman, L.T., Misale, S., Di Pilato, M., Ebright, R.Y., Karabacak, M.N., Kulkarni, A.S., Liu, A., Vincent Jordan, N., Franses, J.W., Philipp, J., Kreuzer, J., Desai, N., Arora, K.S., Rajurkar, M., Horwitz, E., Neyaz, A., Tai, E., Magnus, N.K.C., Vo, K.D., Yashaswini, C.N., Marangoni, F., Boukhali, M., Fatherree, J.P., Damon, L.J., Xega, K., Desai, R., Choz, M., Bersani, F., Langenbucher, A., Thapar, V., Morris, R., Wellner, U.F., Schilling, O., Lawrence, M.S., Liss, A.S., Rivera, M.N., Deshpande, V., Benes, C.H., Maheswaran, S., Haber, D.A., Fernandez-Del-Castillo, C., Ferrone, C.R., Haas, W., Aryee, M.J. and Ting, D.T. (2019) Stromal Microenvironment Shapes the Intratumoral Architecture of Pancreatic Cancer. *Cell*, 178 (1), pp. 160-175.e27.

Liu, J., Liao, S., Diop-Frimpong, B., Chen, W., Goel, S., Naxerova, K., Ancukiewicz, M., Boucher, Y., Jain, R.K. and Xu, L. (2012) TGF-β blockade improves the distribution and efficacy of therapeutics in breast carcinoma by normalizing the tumor stroma. *Proceedings of the National Academy of Sciences*, 109 (41), pp. 16618–16623.

Liu, L., Aleksandrowicz, E., Schönsiegel, F., Gröner, D., Bauer, N., Nwaeburu, C.C., Zhao, Z., Gladkich, J., Hoppe-Tichy, T., Yefenof, E., Hackert, T., Strobel, O. and Herr, I. (2017) Dexamethasone mediates pancreatic cancer progression by glucocorticoid receptor, TGFβ and JNK/AP-1. *Cell Death & Disease*, 8 (10), pp. e3064–e3064.

Liu, X., Gündel, B., Li, X., Liu, J., Wright, A., Löhr, M., Arvidsson, G. and Heuchel, R. (2021) 3D heterospecies spheroids of pancreatic stroma and cancer cells demonstrate key phenotypes of pancreatic ductal adenocarcinoma. *Translational Oncology* [Post-print], 14 (7), p. 101107.

Liu, X., Zhang, J., Yi, T., Li, H., Tang, X., Liu, D., Wu, D. and Li, Y. (2025) Decoding tumor angiogenesis: pathways, mechanisms, and future directions in anti-cancer strategies. *Biomarker Research*, 13 (1), p. 62.

Liu, Z.-L., Chen, H.-H., Zheng, L.-L., Sun, L.-P. and Shi, L. (2023a) Angiogenic signaling pathways and anti-angiogenic therapy for cancer. *Signal Transduction and Targeted Therapy*, 8 (1), p. 198.

Liu, Z.-L., Chen, H.-H., Zheng, L.-L., Sun, L.-P. and Shi, L. (2023b) Angiogenic signaling pathways and anti-angiogenic therapy for cancer. *Signal Transduction and Targeted Therapy*, 8 (1), p. 198.

Longley, D.B., Harkin, D.P. and Johnston, P.G. (2003) 5-Fluorouracil: mechanisms of action and clinical strategies. *Nature Reviews Cancer*, 3 (5), pp. 330–338.

Luo, K. and Lodish, H.F. (1997) Positive and negative regulation of type II TGF-β receptor signal transduction by autophosphorylation on multiple serine residues. *The EMBO Journal* [Post-print], 16 (8), pp. 1970–1981.

Ma, W.W. and Hidalgo, M. (2013) The Winning Formulation: The Development of Paclitaxel in Pancreatic Cancer. *Clinical Cancer Research*, 19 (20), pp. 5572–5579.

Madamsetty, V.S., Mohammadinejad, R., Uzieliene, I., Nabavi, N., Dehshahri, A., García-Couce, J., Tavakol, S., Moghassemi, S., Dadashzadeh, A., Makvandi, P., Pardakhty, A., Afshar, A.A. and Seyfoddin, A. (2022) *Dexamethasone: Insights into Pharmacological Aspects, Therapeutic Mechanisms, and Delivery Systems*. American Chemical Society, pp. 1763–1790.

Maddalena, M., Mallel, G., Belugali Nataraj, N., Shreberk-Shaked, M., Hassin, O., Mukherjee, S., Arandkar, S., Rotkopf, R., Kapsack, A., Lambiase, G., Pellegrino, B., Ben-Isaac, E., Golani D , O., Addadi, Y., Hajaj, E., Eilam, R., Straussman, R., Yarden, Y., Lotem, M. and Oren, M. (2021) TP53 missense mutations in PDAC are associated with enhanced fibrosis and an immunosuppressive microenvironment. *Proceedings of the National Academy of Sciences of the United States of America* [Internet]

Di Maggio, F., Arumugam, P., Delvecchio, F.R., Batista, S., Lechertier, T., Hodivala-Dilke, K. and Kocher, H.M. (2016) Pancreatic stellate cells regulate blood vessel density in the stroma of pancreatic ductal adenocarcinoma. *Pancreatology* [Post-print], 16 (6), pp. 995–1004.

Magnussen, A.L. and Mills, I.G. (2021) Vascular normalisation as the stepping stone into tumour microenvironment transformation. *British Journal of Cancer*, 125 (3), pp. 324–336.

Makohon-Moore, A.P., Matsukuma, K., Zhang, M., Reiter, J.G., Gerold, J.M., Jiao, Y., Sikkema, L., Attiyeh, M.A., Yachida, S., Sandone, C., Hruban, R.H., Klimstra, D.S., Papadopoulos, N., Nowak, M.A., Kinzler, K.W., Vogelstein, B. and Iacobuzio-Donahue, C.A. (2018) Precancerous neoplastic cells can move through the pancreatic ductal system. *Nature*, 561 (7722), pp. 201–205.

Malkoski, S.P. and Wang, X.-J. (2012) Two sides of the story? Smad4 loss in pancreatic cancer versus head-and-neck cancer. *FEBS Letters*, 586 (14), pp. 1984–1992.

Mardhian, D.F., Vrynas, A., Storm, G., Bansal, R. and Prakash, J. (2020) FGF2 engineered SPIONs attenuate tumor stroma and potentiate the effect of chemotherapy in 3D heterospheroidal model of pancreatic tumor. *Nanotheranostics*, 4 (1), pp. 26–39.

Masugi, Y. (2022) The Desmoplastic Stroma of Pancreatic Cancer: Multilayered Levels of Heterogeneity, Clinical Significance, and Therapeutic Opportunities. *Cancers*, 14 (13).

McCarthy, J.B., El-Ashry, D. and Turley, E.A. (2018) Hyaluronan, Cancer-Associated Fibroblasts and the Tumor Microenvironment in Malignant Progression. *Frontiers in Cell and Developmental Biology*, 6.

van Meeteren, L.A. and ten Dijke, P. (2012) Regulation of endothelial cell plasticity by TGF-β. *Cell and Tissue Research*, 347 (1), pp. 177–186.

Melegová, N., Čoma, M., Urban, L., Kaňuchová, M., Szabo, P., Jr., K.S., Mučaji, P. and Gál, P. (2022) Aesculus hippocastanum L. extract differently modulates normal human dermal fibroblasts and cancer-associated fibroblasts from basal/squamous cell carcinoma. *Neoplasma* [Post-print], 69 (01), pp. 224–232.

Melisi, D., Ishiyama, S., Sclabas, G.M., Fleming, J.B., Xia, Q., Tortora, G., Abbruzzese, J.L. and Chiao, P.J. (2008) LY2109761, a novel transforming growth factor β receptor type I and type II dual inhibitor, as a therapeutic approach to suppressing pancreatic cancer metastasis. *Molecular Cancer Therapeutics* [Post-print], 7 (4), pp. 829–840.

Melisi, D., Oh, D.-Y., Hollebecque, A., Calvo, E., Varghese, A., Borazanci, E., Macarulla, T., Merz, V., Zecchetto, C., Zhao, Y., Gueorguieva, I., Man, M., Gandhi, L., Estrem, S.T., Benhadji, K.A., Lanasa, M.C., Avsar, E., Guba, S.C. and Garcia-Carbonero, R. (2021) Safety and activity of the TGFβ receptor I kinase inhibitor galunisertib plus the anti-PD-L1 antibody durvalumab in metastatic pancreatic cancer. *Journal for ImmunoTherapy of Cancer* [Post-print], 9 (3), p. e002068.

di Miceli, N., Baioni, C., Barbieri, L., Danielli, D., Sala, E., Salvioni, L., Garbujo, S., Colombo, M., Prosperi, D., Innocenti, M. and Fiandra, L. (2024) TGF-β Signaling Loop in Pancreatic Ductal Adenocarcinoma Activates Fibroblasts and Increases Tumor Cell Aggressiveness. *Cancers*, 16 (21), p. 3705.

Miyazaki, Y., Oda, T., Mori, N. and Kida, Y.S. (2020) Adipose-derived mesenchymal stem cells differentiate into pancreatic cancer-associated fibroblasts *in vitro*. *FEBS Open Bio*, 10 (11), pp. 2268–2281.

Mizrahi, J.D., Surana, R., Valle, J.W. and Shroff, R.T. (2020) Pancreatic cancer. *The Lancet* [Post-print], 395 (10242), pp. 2008–2020.

Moustakas, A. and Heldin, C.-H. (2005) Non-Smad TGF-β signals. *Journal of Cell Science*, 118 (16), pp. 3573–3584.

Mullen, K.M., Hong, J., Attiyeh, M.A., Hayashi, A., Sakamoto, H., Kohutek, Z.A., McIntyre, C.A., Zhang, H., Makohon-Moore, A.P., Zucker, A., Wood, L.D., Myers, M.A., Arnold, B.J., Zaccaria, S., Chou, J.F., Capanu, M., Socci, N.D., Raphael, B.J. and Iacobuzio-Donahue, C.A. (2025) The Evolutionary Forest of Pancreatic Cancer. *Cancer Discovery*, 15 (2), pp. 329–345.

Murimwa, G.Z., Williams, N.E., Alzhanova, D., Mohammadi, A., Westcott, J.M., Beato, F., Dai, R., Nivelo, L., Rossi, F., Fleming, H.K., Tassielli, A.F., Yazgan, Z., Toombs, J.E., Fleming, J.B., Singhi, A.D., Ethun, C.G., Huang, H. and Brekken, R.A. (2025) SMAD4 Deficiency Promotes Pancreatic Cancer Progression and Confers Susceptibility to TGFβ Inhibition. *Cancer Research* [Post-print], 85 (16), pp. 2987–2996.

Natarajan, V., Ha, S., Delgado, A., Jacobson, R., Alhalhooly, L., Choi, Y. and Kim, J. (2022) Acquired αSMA Expression in Pericytes Coincides with Aberrant Vascular Structure and Function in Pancreatic Ductal Adenocarcinoma. *Cancers* [Post-print], 14 (10), p. 2448.

Neuzillet, C., de Gramont, A., Tijeras-Raballand, A., de Mestier, L., Cros, J., Faivre, S. and Raymond, E. (2014) Perspectives of TGF-β inhibition in pancreatic and hepatocellular carcinomas. *Oncotarget*, 5 (1), pp. 78–94.

Neuzillet, C., Hammel, P., Tijeras-Raballand, A., Couvelard, A. and Raymond, E. (2013) Targeting the Ras–ERK pathway in pancreatic adenocarcinoma. *Cancer and Metastasis Reviews*, 32 (1–2), pp. 147–162.

Nguyen, D.-H.T., Lee, E., Alimperti, S., Norgard, R.J., Wong, A., Lee, J.J.-K., Eyckmans, J., Stanger, B.Z. and Chen, C.S. (2019) A biomimetic pancreatic cancer on-chip reveals endothelial ablation via ALK7 signaling. *Science Advances* [Post-print], 5 (8).

Niedergethmann, M., Hildenbrand, R., Wostbrock, B., Hartel, M., Sturm, J.W., Richter, A. and Post, S. (2002) High expression of vascular endothelial growth factor predicts early recurrence and poor prognosis after curative resection for ductal adenocarcinoma of the pancreas. *Pancreas*, 25 (2), pp. 122–9.

Nishida, T., Yoshitomi, H., Takano, S., Kagawa, S., Shimizu, H., Ohtsuka, M., Kato, A., Furukawa, K. and Miyazaki, M. (2016) Low Stromal Area and High Stromal Microvessel Density Predict Poor Prognosis in Pancreatic Cancer. *Pancreas*, 45 (4), pp. 593–600.

Novák, J., Takács, T., Tilajka, Á., László, L., Oravecz, O., Farkas, E., Than, N.G., Buday, L., Balogh, A. and Vas, V. (2025) The sweet and the bitter sides of galectin-1 in immunity: its role in immune cell functions, apoptosis, and immunotherapies for cancer with a focus on T cells. *Seminars in immunopathology*, 47 (1), p. 24.

Odell, A.F. and Mannion, A.J. (2022) In Vitro Co-culture of Fibroblast and Endothelial Cells to Assess Angiogenesis. pp. 277–286.

Ohba, A., Ozaka, M., Mizusawa, J., Okusaka, T., Kobayashi, S., Yamashita, T., Ikeda, M., Yasuda, I., Sugimori, K., Sasahira, N., Ikezawa, K., Miki, I., Okano, N., Mizuno, N., Furukawa, M., Shirakawa, H., Sano, Y., Katayama, H., Furuse, J., Ueno, M., Okamura, K., Komatsu, Y., Katanuma, A., Unno, M., Shirakawa, H., Yamaguchi, H., Shimizu, S., Ikeda, M., Ishii, H., Kato, N., Okusaka, T., Nagashima, F., Itoi, T., Kojima, Y., Kuramochi, H., Sasahira, N., Sano, K., Takahashi, S., Sunakawa, Y., Ueno, M., Kumamoto, Y., Sugimori, K., Shioji, K., Yasuda, I., Yamashita, T., Tsuji, K., Yamazaki, K., Hara, K., Hatano, E., Eguchi, H., Kudo, M., Ohkawa, K., Gotoh, K., Satoi, S., Tobimatsu, K., Hirono, S., Miki, I., Kitano, M., Nagano, H., Asagi, A., Okabayashi, T., Furukawa, M., Fujimori, N., Nakao, K. and Ido, A. (2025) Modified Fluorouracil, Leucovorin, Irinotecan, and Oxaliplatin or S-1, Irinotecan, and Oxaliplatin Versus Nab-Paclitaxel + Gemcitabine in Metastatic or Recurrent Pancreatic Cancer (GENERATE, JCOG1611): A Randomized, Open-Label, Phase II/III Trial. *Journal of Clinical Oncology* [Post-print], 43 (31), pp. 3345–3354.

Öhlund, D., Handly-Santana, A., Biffi, G., Elyada, E., Almeida, A.S., Ponz-Sarvise, M., Corbo, V., Oni, T.E., Hearn, S.A., Lee, E.J., Chio, I.I.C., Hwang, C.-I., Tiriac, H., Baker, L.A., Engle, D.D., Feig, C., Kultti, A., Egeblad, M., Fearon, D.T., Crawford, J.M., Clevers, H., Park, Y. and Tuveson, D.A. (2017) Distinct populations of inflammatory fibroblasts and myofibroblasts in pancreatic cancer. *Journal of Experimental Medicine*, 214 (3), pp. 579–596.

Olaoba, O.T., Yang, M., Adelusi, T.I., Maidens, T., Kimchi, E.T., Staveley-O'Carroll, K.F. and Li, G. (2024) Targeted Therapy for Highly Desmoplastic and Immunosuppressive Tumor Microenvironment of Pancreatic Ductal Adenocarcinoma. *Cancers* [Post-print], 16 (8), p. 1470.

Palmer, D.H., Jackson, R., Springfeld, C., Ghaneh, P., Rawcliffe, C., Halloran, C.M., Faluyi, O., Cunningham, D., Wadsley, J., Darby, S., Meyer, T., Gillmore, R., Lind, P., Glimelius, B., Falk, S., Ma, Y.T., Middleton, G.W., Cummins, S., Ross, P.J., Wasan, H., McDonald, A., Crosby, T., Hammel, P., Borg, D., Sothi, S., Valle, J.W., Mehrabi, A., Bailey, P., Tjaden, C., Michalski, C., Hackert, T., Büchler, M.W. and Neoptolemos, J.P. (2024) Pancreatic Adenocarcinoma: Long-Term Outcomes of Adjuvant Therapy in the ESPAC4 Phase III Trial. *Journal of Clinical Oncology*,.

Pape, J., Magdeldin, T., Stamati, K., Nyga, A., Loizidou, M., Emberton, M. and Cheema, U. (2020) Cancer-associated fibroblasts mediate cancer progression and remodel the tumouroid stroma. *British Journal of Cancer*, 123 (7), pp. 1178–1190.

Parma, L., Peters, H.A.B., Sluiter, T.J., Simons, K.H., Lazzari, P., de Vries, M.R. and Quax, P.H.A. (2020) bFGF blockade reduces intraplaque angiogenesis and macrophage infiltration in atherosclerotic vein graft lesions in ApoE3*Leiden mice. *Scientific Reports*, 10 (1), p. 15968.

Pihlak, R., Weaver, J., Valle, J. and McNamara, M. (2018) Advances in Molecular Profiling and Categorisation of Pancreatic Adenocarcinoma and the Implications for Therapy. *Cancers*, 10 (1), p. 17.

Prejac, J., Tomek Hamzić, D., Librenjak, N., Goršić, I., Kekez, D. and Pleština, S. (2022) The effectiveness of nab-paclitaxel plus gemcitabine and gemcitabine monotherapy in first-line metastatic pancreatic cancer treatment: A real-world evidence. *Medicine*, 101 (39), p. e30566.

Principe, D.R., Diaz, A.M., Torres, C., Mangan, R.J., DeCant, B., McKinney, R., Tsao, M.-S., Lowy, A., Munshi, H.G., Jung, B. and Grippo, P.J. (2017) TGFβ engages MEK/ERK to differentially regulate benign and malignant pancreas cell function. *Oncogene*, 36 (30), pp. 4336–4348.

Principe, D.R., Timbers, K.E., Atia, L.G., Koch, R.M. and Rana, A. (2021) TGFβ Signaling in the Pancreatic Tumor Microenvironment. *Cancers*, 13 (20), p. 5086.

Principe, D.R., Underwood, P.W., Kumar, S., Timbers, K.E., Koch, R.M., Trevino, J.G., Munshi, H.G. and Rana, A. (2022) Loss of SMAD4 Is Associated With Poor Tumor Immunogenicity and Reduced PD-L1 Expression in Pancreatic Cancer. *Frontiers in Oncology*, 12.

Provenzano, P.P., Cuevas, C., Chang, A.E., Goel, V.K., Von Hoff, D.D. and Hingorani, S.R. (2012) Enzymatic Targeting of the Stroma Ablates Physical Barriers to Treatment of Pancreatic Ductal Adenocarcinoma. *Cancer Cell* [Post-print], 21 (3), pp. 418–429.

Pugsley, M.K. and Tabrizchi, R. (2000) The vascular system. *Journal of Pharmacological and Toxicological Methods*, 44 (2), pp. 333–340.

Puleo, F., Nicolle, R., Blum, Y., Cros, J., Marisa, L., Demetter, P., Quertinmont, E., Svrcek, M., Elarouci, N., Iovanna, J., Franchimont, D., Verset, L., Galdon, M.G., Devière, J., de Reyniès, A., Laurent-Puig, P., Van Laethem, J.-L., Bachet, J.-B. and Maréchal, R. (2018) Stratification of Pancreatic Ductal Adenocarcinomas Based on Tumor and Microenvironment Features. *Gastroenterology*, 155 (6), pp. 1999-2013.e3.

Qian, C., Liu, C., Liu, W., Zhou, R. and Zhao, L. (2023) Targeting vascular normalization: a promising strategy to improve immune–vascular crosstalk in cancer immunotherapy. *Frontiers in Immunology* [Post-print], 14.

Qian, Z.R., Rubinson, D.A., Nowak, J.A., Morales-Oyarvide, V., Dunne, R.F., Kozak, M.M., Welch, M.W., Brais, L.K., Da Silva, A., Li, T., Li, W., Masuda, A., Yang, J., Shi, Y., Gu, M., Masugi, Y., Bui, J., Zellers, C.L., Yuan, C., Babic, A., Khalaf, N., Aguirre, A., Ng, K., Miksad, R.A., Bullock, A.J., Chang, D.T., Tseng, J.F., Clancy, T.E., Linehan, D.C., Findeis-Hosey, J.J., Doyle, L.A., Thorner, A.R., Ducar, M., Wollison, B., Laing, A., Hahn, W.C., Meyerson, M., Fuchs, C.S., Ogino, S., Hornick, J.L., Hezel, A.F., Koong, A.C. and Wolpin, B.M. (2018) Association of Alterations in Main Driver Genes With Outcomes of Patients With Resected Pancreatic Ductal Adenocarcinoma. *JAMA Oncology* [Post-print], 4 (3), p. e173420.

Qiang, L., Hoffman, M.T., Ali, L.R., Castillo, J.I., Kageler, L., Temesgen, A., Lenehan, P., Wang, S.J., Bello, E., Cardot-Ruffino, V., Uribe, G.A., Yang, A., Dougan, M., Aguirre, A.J., Raghavan, S., Pelletier, M., Cremasco, V. and Dougan, S.K. (2023) Transforming Growth Factor-β Blockade in Pancreatic Cancer Enhances Sensitivity to Combination Chemotherapy. *Gastroenterology* [Post-print], 165 (4), pp. 874-890.e10.

Quinn, B.A., Lee, N.A., Kegelman, T.P., Bhoopathi, P., Emdad, L., Das, S.K., Pellecchia, M., Sarkar, D. and Fisher, P.B. (2015) The Quest for an Effective Treatment for an Intractable Cancer. In: Fisher, P.B. and Tew, K.D. eds. *Advances in Cancer Research*. pp. 283–306.

Racu, M.-L., Lebrun, L., Schiavo, A.A., Van Campenhout, C., De Clercq, S., Absil, L., Minguijon Perez, E., Maris, C., Decaestecker, C., Salmon, I. and D'Haene, N. (2022) The Role of SMAD4 Inactivation in Epithelial–Mesenchymal Plasticity of Pancreatic Ductal Adenocarcinoma: The Missing Link? *Cancers*, 14 (4), p. 973.

Raphael, B.J., Hruban, R.H., Aguirre, A.J., Moffitt, R.A., Yeh, J.J., Stewart, C., Robertson, A.G., Cherniack, A.D., Gupta, M., Getz, G., Gabriel, S.B., Meyerson, M., Cibulskis, C., Fei, S.S., Hinoue, T., Shen, H., Laird, P.W., Ling, S., Lu, Y., Mills, G.B., Akbani, R., Loher, P., Londin, E.R., Rigoutsos, I., Telonis, A.G., Gibb, E.A., Goldenberg, A., Mezlini, A.M., Hoadley, K.A., Collisson, E., Lander, E., Murray, B.A., Hess, J., Rosenberg, M., Bergelson, L., Zhang, H., Cho, J., Tiao, G., Kim, J., Livitz, D., Leshchiner, I., Reardon, B., Van Allen, E., Kamburov, A., Beroukhim, R., Saksena, G., Schumacher, S.E., Noble, M.S., Heiman, D.I., Gehlenborg, N., Kim, J., Lawrence, M.S., Adsay, V., Petersen, G., Klimstra, D., Bardeesy, N., Leiserson, M.D.M., Bowlby, R., Kasaian, K., Birol, I., Mungall, K.L., Sadeghi, S., Weinstein, J.N., Spellman, P.T., Liu, Y., Amundadottir, L.T., Tepper, J., Singhi, A.D., Dhir, R., Paul, D., Smyrk, T., Zhang, L., Kim, P., Bowen, J., Frick, J., Gastier-Foster, J.M., Gerken, M., Lau, K., Leraas, K.M., Lichtenberg, T.M., Ramirez, N.C., Renkel, J., Sherman, M., Wise, L., Yena, P., Zmuda, E., Shih, J., Ally, A., Balasundaram, M., Carlsen, R., Chu, A., Chuah, E., Clarke, A., Dhalla, N., Holt, R.A., Jones, S.J.M., Lee, D., Ma, Y., Marra, M.A., Mayo, M., Moore, R.A., Mungall, A.J., Schein, J.E., Sipahimalani, P., Tam, A., Thiessen, N., Tse, K., Wong, T., Brooks, D., Auman, J.T., Balu, S., Bodenheimer, T., Hayes, D.N., Hoyle, A.P., Jefferys, S.R., Jones, C.D., Meng, S., Mieczkowski, P.A., Mose, L.E., Perou, C.M., Perou, A.H., Roach, J., Shi, Y., Simons, J. V., Skelly, T., Soloway, M.G., Tan, D., Veluvolu, U., Parker, J.S., Wilkerson, M.D., Korkut, A., Senbabaoglu, Y., Burch, P., McWilliams, R., Chaffee, K., Oberg, A., Zhang, W., Gingras, M.-C., Wheeler, D.A., Xi, L., Albert, M., Bartlett, J., Sekhon, H., Stephen, Y., Howard, Z., Judy, M., Breggia, A., Shroff, R.T., Chudamani, S., Liu, J., Lolla, L., Naresh, R., Pihl, T., Sun, Q., Wan, Y., Wu, Y., Jennifer, S., Roggin, K., Becker, K.-F., Behera, M., Bennett, J., Boice, L., Burks, E., Carlotti Junior, C.G., Chabot, J., Pretti da Cunha Tirapelli, D., Sebastião dos Santos, J., Dubina,

M., Eschbacher, J., Huang, M., Huelsenbeck-Dill, L., Jenkins, R., Karpov, A., Kemp, R., Lyadov, V., Maithel, S., Manikhas, G., Montgomery, E., Noushmehr, H., Osunkoya, A., Owonikoko, T., Paklina, O., Potapova, O., Ramalingam, S., Rathmell, W.K., Rieger-Christ, K., Saller, C., Setdikova, G., Shabunin, A., Sica, G., Su, T., Sullivan, T., Swanson, P., Tarvin, K., Tavobilov, M., Thorne, L.B., Urbanski, S., Voronina, O., Wang, T., Crain, D., Curley, E., Gardner, J., Mallery, D., Morris, S., Paulauskis, J., Penny, R., Shelton, C., Shelton, T., Janssen, K.-P., Bathe, O., Bahary, N., Slotta-Huspenina, J., Johns, A., Hibshoosh, H., Hwang, R.F., Sepulveda, A., Radenbaugh, A., Baylin, S.B., Berrios, M., Bootwalla, M.S., Holbrook, A., Lai, P.H., Maglinte, D.T., Mahurkar, S., Triche, T.J., Van Den Berg, D.J., Weisenberger, D.J., Chin, L., Kucherlapati, R., Kucherlapati, M., Pantazi, A., Park, P., Saksena, G., Voet, D., Lin, P., Frazer, S., Defreitas, T., Meier, S., Chin, L., Kwon, S.Y., Kim, Y.H., Park, S.-J., Han, S.-S., Kim, S.H., Kim, H., Furth, E., Tempero, M., Sander, C., Biankin, A., Chang, D., Bailey, P., Gill, A., Kench, J., Grimmond, S., Johns, A., Cancer Genome Initiative (APGI, A.P., Postier, R., Zuna, R., Sicotte, H., Demchok, J.A., Ferguson, M.L., Hutter, C.M., Mills Shaw, K.R., Sheth, M., Sofia, H.J., Tarnuzzer, R., Wang, Z., Yang, L., Zhang, J. (Julia), Felau, I. and Zenklusen, J.C. (2017) Integrated Genomic Characterization of Pancreatic Ductal Adenocarcinoma. *Cancer Cell* [Post-print], 32 (2), pp. 185-203.e13.

Risau, W., Sariola, H., Zerwes, H.-G., Sasse, J., Ekblom, P., Kemler, R. and Doetschman, T. (1988) Vasculogenesis and angiogenesis in embryonic-stem-cell-derived embryoid bodies. *Development*, 102 (3), pp. 471–478.

Robertson, I.B., Horiguchi, M., Zilberberg, L., Dabovic, B., Hadjiolova, K. and Rifkin, D.B. (2015) Latent TGF-β-binding proteins. *Matrix Biology*, 47, pp. 44–53.

Robertson, I.B. and Rifkin, D.B. (2016) Regulation of the Bioavailability of TGF-β and TGF-β-Related Proteins. *Cold Spring Harbor Perspectives in Biology*, 8 (6), p. a021907.

Roger, E., Mummey, H.M., Zimmer, E., Srinivasan, D., Härle, A., Moubri, L., Michels, A.K., Singh, R., Ekizce, M., Melzer, M.K., Lee, Y., Silva, A., Härle, L., Engleitner, T., Arnold, F., Morawe, M., Naggay, B.K., Schneider, J., Gilberg, L., Mosler, J.P., Ludwig, C., Meng, C., Hirschenberger, M., Hunszinger, V., Kluck, K., Kirchner, M., Volckmar, A.-L., Wirth, M., Alhamdani, M.S.S., Hoheisel, J.D., Löhr, J.-M., Seufferlein, T., Abaei, A., Kemkemer, R., Rad, R., Budczies, J., Mulaw, M.A., Hermann, P.C., Haenle, M.M., Sparrer, K.M.J., Halbrook, C.J., Gaulton, K.J., Steinestel, K., Stenzinger, A., Dusetti, N., Perkhofer, L., Gout, J. and Kleger, A. (2026) ATM Deficiency Induces TGFβ-Mediated Stromal Programming in Pancreatic Cancer. *Cancer Research*, 86 (14), pp. 3412–3435.

Sánchez-Elsner, T., Botella, L.M., Velasco, B., Corbí, A., Attisano, L. and Bernabéu, C. (2001) Synergistic Cooperation between Hypoxia and Transforming Growth Factor-β Pathways on Human Vascular Endothelial Growth Factor Gene Expression. *Journal of Biological Chemistry*, 276 (42), pp. 38527–38535.

Sandini, M., Ruscic, K.J., Ferrone, C.R., Warshaw, A.L., Qadan, M., Eikermann, M., Lillemoe, K.D. and Fernández-del Castillo, C. (2018) Intraoperative Dexamethasone Decreases Infectious Complications After Pancreaticoduodenectomy and is Associated with Long-Term Survival in Pancreatic Cancer. *Annals of Surgical Oncology*, 25 (13), pp. 4020–4026.

Sarfaty, E., Khajoueinejad, N., Zewde, M.G., Yu, A.T. and Cohen, N.A. (2023) Surgical management of pancreatic ductal adenocarcinoma: a narrative review. *Translational Gastroenterology and Hepatology*, 8, pp. 39–39.

Seoane, J. and Gomis, R.R. (2017) TGF-β Family Signaling in Tumor Suppression and Cancer Progression. *Cold Spring Harbor Perspectives in Biology*, 9 (12), p. a022277.

Shi, W., Sun, C., He, B., Xiong, W., Shi, X., Yao, D. and Cao, X. (2004) GADD34–PP1c recruited by Smad7 dephosphorylates TGFβ type I receptor. *The Journal of Cell Biology*, 164 (2), pp. 291–300.

Shin, H.-J., Gil, M. and Lee, I.-S. (2022) Association of Elevated Expression Levels of COL4A1 in Stromal Cells with an Immunosuppressive Tumor Microenvironment in Low-Grade Glioma, Pancreatic Adenocarcinoma, Skin Cutaneous Melanoma, and Stomach Adenocarcinoma. *Journal of Personalized Medicine* [Post-print], 12 (4), p. 534.

Shrimali, R.K., Yu, Z., Theoret, M.R., Chinnasamy, D., Restifo, N.P. and Rosenberg, S.A. (2010) Antiangiogenic Agents Can Increase Lymphocyte Infiltration into Tumor and Enhance the Effectiveness of Adoptive Immunotherapy of Cancer. *Cancer Research*, 70 (15), pp. 6171–6180.

Simeone, D.M., Pham, T. and Logsdon, C.D. (2000) Disruption of TGFbeta signaling pathways in human pancreatic cancer cells. *Annals of surgery*, 232 (1), pp. 73–80.

Song, C.-Z., Tian, X. and Gelehrter, T.D. (1999) Glucocorticoid receptor inhibits transforming growth factor-β signaling by directly targeting the transcriptional activation function of Smad3. *Proceedings of the National Academy of Sciences*, 96 (21), pp. 11776–11781.

Song, Q.H., Klepeis, V.E., Nugent, M.A. and Trinkaus-Randall, V. (2002) TGF-β1 regulates TGF-β1 and FGF-2 mRNA expression during fibroblast wound healing. *Molecular Pathology*, 55 (3), pp. 164–176.

Song, X., Nihashi, Y., Yamamoto, M., Setoyama, D., Kunisaki, Y. and Kida, Y.S. (2023) Exploring the Role of Desmoplastic Physical Stroma in Pancreatic Cancer Progression Using a Three-Dimensional Collagen Matrix Model. *Bioengineering*, 10 (12), p. 1437.

Spender, L.C., O'Brien, D.I., Simpson, D., Dutt, D., Gregory, C.D., Allday, M.J., Clark, L.J. and Inman, G.J. (2009) TGF-β induces apoptosis in human B cells by transcriptional regulation of BIK and BCL-XL. *Cell Death & Differentiation*, 16 (4), pp. 593–602.

Strand, D.W., Liang, Y.-Y., Yang, F., Barron, D.A., Ressler, S.J., Schauer, I.G., Feng, X.-H. and Rowley, D.R. (2014) TGF-β induction of FGF-2 expression in stromal cells requires integrated smad3 and MAPK pathways. *American journal of clinical and experimental urology*, 2 (3), pp. 239–48.

Strobel, O., Neoptolemos, J., Jäger, D. and Büchler, M.W. (2019) Optimizing the outcomes of pancreatic cancer surgery. *Nature Reviews Clinical Oncology*, 16 (1), pp. 11–26.

Sun, L., Wu, G., Willson, J.K., Zborowska, E., Yang, J., Rajkarunanayake, I., Wang, J., Gentry, L.E., Wang, X.F. and Brattain, M.G. (1994) Expression of transforming growth factor beta type II receptor leads to reduced malignancy in human breast cancer MCF-7 cells. *Journal of Biological Chemistry*, 269 (42), pp. 26449–26455.

Taherpour, A., Mirzavi, F., Shafaei, E., Zarban, A. and Shakibaie, M. (2025) Combined effects of honey and silver nanoparticles on wound healing in human dermal fibroblast cells. *BMC Complementary Medicine and Therapies*, 25 (1), p. 446.

Tamburrino, A., Piro, G., Carbone, C., Tortora, G. and Melisi, D. (2013) Mechanisms of resistance to chemotherapeutic and anti-angiogenic drugs as novel targets for pancreatic cancer therapy. *Frontiers in Pharmacology*, 4.

Tang, D., Gao, J., Wang, S., Ye, N., Chong, Y., Huang, Y., Wang, J., Li, B., Yin, W. and Wang, D. (2016) Cancer-associated fibroblasts promote angiogenesis in gastric cancer through galectin-1 expression. *Tumor Biology* [Post-print], 37 (2), pp. 1889–1899.

Tang, D., Zhang, J., Yuan, Z., Gao, J., Wang, S., Ye, N., Li, P., Gao, S., Miao, Y., Wang, D. and Jiang, K. (2014) Pancreatic Satellite Cells Derived Galectin-1 Increase the Progression and Less Survival of Pancreatic Ductal Adenocarcinoma. *PLoS ONE*, 9 (3), p. e90476.

Tian, X., Jia, Y., Guo, Y., Liu, H., Cai, X., Li, Y., Tian, Z. and Sun, C. (2023) Fibroblast growth factor 2 acts as an upstream regulator of inhibition of pulmonary fibroblast activation. *FEBS Open Bio*, 13 (10), pp. 1895–1909.

Ungefroren, H., von der Ohe, J., Braun, R., Gätje, Y., Lapshyna, O., Schrader, J., Lehnert, H., Marquardt, J.-U., Konukiewitz, B. and Hass, R. (2024) Characterization of Epithelial–Mesenchymal and Neuroendocrine Differentiation States in Pancreatic and Small Cell Ovarian Tumor Cells and Their Modulation by TGF-β1 and BMP-7. *Cells*, 13 (23), p. 2010.

Verrecchia, F. and Rédini, F. (2018) Transforming Growth Factor-β Signaling Plays a Pivotal Role in the Interplay Between Osteosarcoma Cells and Their Microenvironment. *Frontiers in Oncology* [Post-print], 8.

Verweij, J., Clavel, M. and Chevalier, B. (1994) Paclitaxel (Taxol) and docetaxel (Taxotere): not simply two of a kind. *Annals of oncology : official journal of the European Society for Medical Oncology*, 5 (6), pp. 495–505.

Vong, S. and Kalluri, R. (2011) The Role of Stromal Myofibroblast and Extracellular Matrix in Tumor Angiogenesis. *Genes & Cancer*, 2 (12), pp. 1139–1145.

Wang, H., Liu, Z., Li, A., Wang, J., Liu, J., Liu, B., Lian, X., Zhang, B., Pang, B., Liu, L. and Gao, Y. (2021) COL4A1 as a novel oncogene associated with the clinical characteristics of malignancy predicts poor prognosis in glioma. *Experimental and Therapeutic Medicine* [Post-print], 22 (5), p. 1224.

Wang, T., Kim, S.Y., Peng, Y., Zheng, J., Layne, M.D., Murphy-Ullrich, J.E. and Albro, M.B. (2024) Autoinduction-Based Quantification of *In Situ* TGF-β Activity in Native and Engineered Cartilage. *Tissue Engineering Part C: Methods*, 30 (11), pp. 522–532.

Watabe, T., Nishihara, A., Mishima, K., Yamashita, J., Shimizu, K., Miyazawa, K., Nishikawa, S.-I. and Miyazono, K. (2003) TGF-β receptor kinase inhibitor enhances growth and integrity of embryonic stem cell–derived endothelial cells. *The Journal of Cell Biology*, 163 (6), pp. 1303–1311.

Witte, D., Zeeh, F., Gädeken, T., Gieseler, F., Rauch, B., Settmacher, U., Kaufmann, R., Lehnert, H. and Ungefroren, H. (2016) Proteinase-Activated Receptor 2 Is a Novel Regulator of TGF-β Signaling in Pancreatic Cancer. *Journal of Clinical Medicine*, 5 (12), p. 111.

Wood, L.D., Canto, M.I., Jaffee, E.M. and Simeone, D.M. (2022) Pancreatic Cancer: Pathogenesis, Screening, Diagnosis, and Treatment. *Gastroenterology*, 163 (2), pp. 386-402.e1.

Wu, Z., Nicoll, M. and Ingham, R.J. (2021) AP-1 family transcription factors: a diverse family of proteins that regulate varied cellular activities in classical hodgkin lymphoma and ALK+ ALCL. *Experimental Hematology & Oncology*, 10 (1), p. 4.

Xelwa, N., Candy, G.P., Devar, J., Omoshoro-Jones, J., Smith, M. and Nweke, E.E. (2021) Targeting Growth Factor Signaling Pathways in Pancreatic Cancer: Towards Inhibiting Chemoresistance. *Frontiers in Oncology*, 11.

Xiong, Y., Li, Y., Chen, L., Chen, M., He, W. and Qi, L. (2025) Enhancing the therapeutic efficacy of gemcitabine in bladder cancer through TGF-β1 inhibition and pluronic F-127-based microsphere delivery. *Journal of Biological Engineering* [Post-print], 19 (1), p. 62.

Xu, R., Shao, J., Liu, J., Qu, B. and Liu, J. (2024) Single-cell analysis of chemotherapy-resistant microenvironment identifies a chemo-response biomarker for pancreatic cancer. *Journal of Gastrointestinal Oncology*, 15 (4), pp. 1836–1846.

Yan, X., Liu, Z. and Chen, Y. (2009) Regulation of TGF-β signaling by Smad7. *Acta Biochimica et Biophysica Sinica*, 41 (4), pp. 263–272.

Yanagisawa, H., Sugimoto, M. and Miyashita, T. (2021) Mathematical simulation of tumour angiogenesis: angiopoietin balance is a key factor in vessel growth and regression. *Scientific Reports*, 11 (1), p. 419.

Yao, H., Luo, L., Li, R., Zhao, Y., Zhang, L., Pešić, M., Cai, L. and Li, L. (2024) *New insight into the role of SMAD4 mutation/deficiency in the prognosis and therapeutic resistance of pancreatic ductal adenocarcinomas*. Elsevier B.V.

Yao, Y., Yao, Q., Xue, J., Tian, X., An, Q., Cui, L., Xu, C., Su, H., Yang, L., Feng, Y., Hao, C. and Zhou, T. (2020) Dexamethasone inhibits pancreatic tumor growth in preclinical models: Involvement of activating glucocorticoid receptor. *Toxicology and Applied Pharmacology*, 401, p. 115118.

Yauch, R.L., Gould, S.E., Scales, S.J., Tang, T., Tian, H., Ahn, C.P., Marshall, D., Fu, L., Januario, T., Kallop, D., Nannini-Pepe, M., Kotkow, K., Marsters, J.C., Rubin, L.L. and de Sauvage, F.J. (2008) A paracrine requirement for hedgehog signalling in cancer. *Nature*, 455 (7211), pp. 406–410.

Ye, X., Zheng, X. and Zhu, L. (2025) Knockdown of TBRG4 suppresses the migration, invasion, and epithelial-to-mesenchymal transition of pancreatic cancer cells via TGF-β/smad3 signaling. *Histology and Histopathology*, 40 (8), pp. 1309–1319.

Yoo, J., Ghiassi, M., Jirmanova, L., Balliet, A.G., Hoffman, B., Fornace, A.J., Liebermann, D.A., Böttinger, E.P. and Roberts, A.B. (2003) Transforming Growth Factor-β-induced Apoptosis Is Mediated by Smad-

dependent Expression of GADD45b through p38 Activation. *Journal of Biological Chemistry*, 278 (44), pp. 43001–43007.

Zeisberg, E.M., Potenta, S., Xie, L., Zeisberg, M. and Kalluri, R. (2007) Discovery of Endothelial to Mesenchymal Transition as a Source for Carcinoma-Associated Fibroblasts. *Cancer Research*, 67 (21), pp. 10123–10128.

Zhang, M., Kleber, S., Röhrich, M., Timke, C., Han, N., Tuettenberg, J., Martin-Villalba, A., Debus, J., Peschke, P., Wirkner, U., Lahn, M. and Huber, P.E. (2011) Blockade of TGF-β Signaling by the TGFβR-I Kinase Inhibitor LY2109761 Enhances Radiation Response and Prolongs Survival in Glioblastoma. *Cancer Research* [Post-print], 71 (23), pp. 7155–7167.

Zhang, Q., Yu, N. and Lee, C. (2014) Vicious cycle of TGF-β signaling in tumor progression and metastasis. *American journal of clinical and experimental urology*, 2 (2), pp. 149–55.

Zhang, T., Ren, Y., Yang, P., Wang, J. and Zhou, H. (2022) Cancer-associated fibroblasts in pancreatic ductal adenocarcinoma. *Cell Death & Disease*, 13 (10), p. 897.

Zhao, B. and Chen, Y.-G. (2014) Regulation of TGF- *β* Signal Transduction. *Scientifica*, 2014, pp. 1–9.

Zhou, Q., Xia, S., Guo, F., Hu, F., Wang, Z., Ni, Y., Wei, T., Xiang, H. and Shang, D. (2019) Transforming growth factor-β in pancreatic diseases: Mechanisms and therapeutic potential. *Pharmacological Research*, 142, pp. 58–69.

Zhou, X., Tang, J., Cao, H., Fan, H. and Li, B. (2015) Tissue resident regulatory T cells: novel therapeutic targets for human disease. *Cellular & Molecular Immunology*, 12 (5), pp. 543–552.

Zou, J., Li, C., Jiang, S., Luo, L., Yan, X., Huang, D. and Luo, Z. (2021) AMPK inhibits Smad3-mediated autoinduction of TGF-β1 in gastric cancer cells. *Journal of Cellular and Molecular Medicine*, 25 (6), pp. 2806–2815.

Zudaire, E., Gambardella, L., Kurcz, C. and Vermeren, S. (2011) A Computational Tool for Quantitative Analysis of Vascular Networks. *PLoS ONE*, 6 (11), p. e27385.